MODELING OF RADIAL FLOW DYNAMICS FOR FIXED BED REACTOR

By

ANJANI KUMAR SINGH

Bachelor of Technology

Indian Institute of Technology

Kharagpur, India

1996

Submitted to the Faculty of the
Graduate College of the
Oklahoma State University
In partial fulfillment of
the requirements for
the Degree of
MASTER OF SCIENCE
December, 2005

MODELING OF RADIAL FLOW DYNAMICS FOR

FIXED BED REACTOR

Thesis Approved:

Thesis Advisor, Dr. Karen High

Committee Member, Dr. Martin S. High

Committee Member, Dr. Sundararajan V. Madihally

Dean of the Graduate College, Dr. A. Gordon Emslie

ACKNOWLEDGMENTS

I wish to express my appreciation to my research advisor Dr. Karen High, not only for her continuous support and erudite advice related to project but also for helping me develop a new outlook to this profession. I thank her for her unselfish alacrity to help especially in times of need and for her knowledgeable insight in to day to day modeling of flow distribution. She provided me with unrestricted environment during the period of my stay at Oklahoma State University in which I could not only learn but also develop a professional character. I thank her for making this journey a very pleasant and personally rewarding one.

Many thanks go also to Dr. Martin S High and Dr. Sundararajan V. Madihally for serving on my graduate committee.

My wife and parents provided me with strength and determination to constantly improve myself and achieve my goals. Without them, this would not have been possible. Thanks also goes out to the friends and all that helped in the preparation of the final thesis draft. Thank you all.

TABLE OF CONTENTS

LIST OF TABLES

Table Page

LIST OF FIGURES

NOMENCLATURE

A	Arrhenius pre-exponential factor
AIT	Auto ignition temperature, K
C	Concentration, mol/m^3
CAD	Computer-aided design
CEL	CFX^{TM} expression language
CFD	Computational fluid dynamics
CFX	Computational fluid dynamics software
C_p	Specific heat, KJ/Kg K
D	Diffusion coefficient, m^2/s
E_a	Energy of activation, KJ/mol
EOS	Equation of state
FDP	Flow distribution problem
g	Vertical plane
gm1	Geometry1, uniform bed length RFBR
gm2	Geometry2, reduced bed length with height
gm3	Geometry3, increased bed length with height
h_{tot}	Specific total enthalpy, KJ/Kmole
ΔH_n	Heat of reaction, KJ/ Kmole
K	Boltzmann constant, 1.3807E-23 J/K
k	Reaction rate constant, s^{-1}

MW	Molecular weight, g/mol
NASA	National Aeronautics and Space Administration
N_{jz}	Mass flux due to dispersion in z direction, Kg/m^2
N_{jr}	Mass flux due to dispersion in r direction, Kg/m^2
N_{qa}	Heat flux of component a due to dispersion, KJ/m^2
N_{re}	Reynolds number
N_{sc}	Schmidt number
P	Pressure, Pa
p	Horizontal plane
R	Universal gas constant, 8.314 J/mol-K
RFBR	Radial fixed bed reactor
RTD	Residence time distribution
rxn	Reaction
S_m	Momentum source, $kg/m^2\text{-}s^2$
S_e	Energy source, J/sec
SOLID1	RFBR inlet
SOLID2	Catalyst bed of RFBR
SOLID3	RFBR outlet
t	Time, s
T	Temperature, K
U	Vector of velocity, m/s
u_z	Axial component of velocity, m/s
v_r	Radial component of velocity, m/s

VFBR	Vertical Fixed Bed Reactor
α	Exponential temperature effect, heat capacity
β	Exponential temperature effect
γ	Exponential temperature effect
∇	Del operator
δ	Unit tensor
ε	Void fraction
λ	Thermal conductivity, W/m-K
μ	Viscosity, Kg/m-s
ρ	Density, Kg/m^3
ρ_i	Density of species i, Kg/m^3
σ	Collision diameter, Angstroms

CHAPTER 1

INTRODUCTION

Fixed bed reactors are used for a wide range of industrial processes for gas phase reactions. Currently used vertical fixed bed reactors (VFBRs) offer higher pressure drop than radial fixed bed reactors (RFBRs). RFBRs offer a larger mean cross-sectional area and reduced travel distance as compared to traditional VFBRs [1, 2]. In RFBRs fluid flows both in axial and radial directions. Consequently, the pressure drop in RFBRs is reduced significantly. However research indicates that such geometries introduce flow distribution problem (FDP) [2]. For the FDP to be minimum, the fluid flow should be in the radial direction to ensure fluid is uniformly distributed inside the catalyst bed [3]. Fluid movement in the axial direction, inside the catalyst bed, introduces FDP.

Figure 1-1 presents a radial fixed bed reactor for ammonia synthesis. Fluid moves in the reactor from outside of the cylindrical vessel. The fluid moves inside the catalyst bed in the radial direction and finally axially downward to exit the reactor. The arrangement of the catalyst in the RFBR is to minimize the travel distance of the fluid. For the same amount of catalyst, the travel distance increases for vertical fixed bed reactors (VFBR).

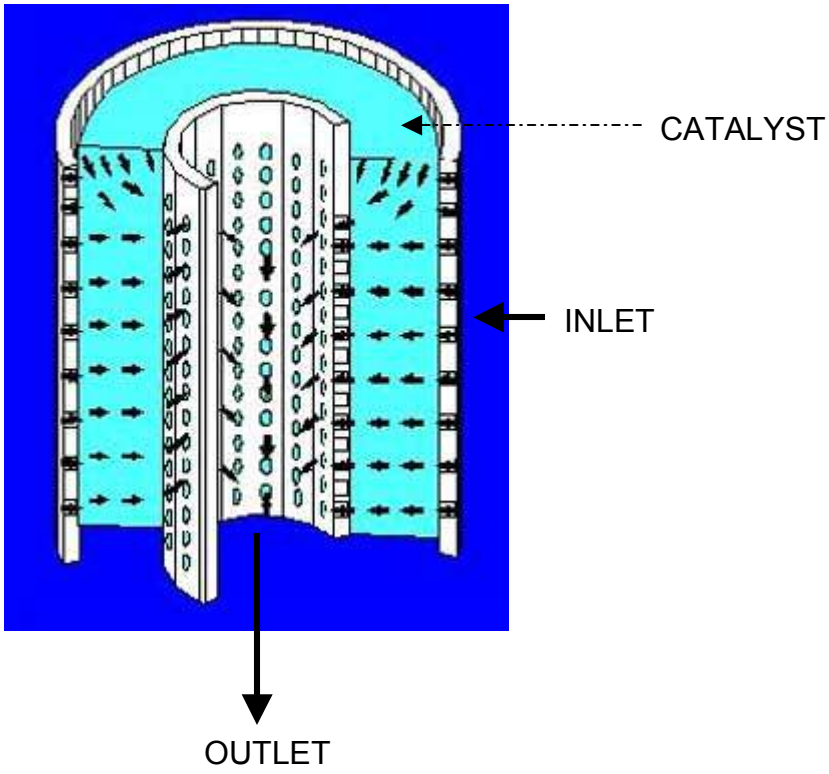

FIGURE 1-1: Casale axial reactor design for ammonia synthesis [39]

The goal of this research is to understand radial flow in fixed bed reactors. The practical goal of the proposed research is to develop a model using the Navier-Stokes equation to analyze the flow distribution in fixed bed reactors for radial flow.

The hypothesis behind the proposed research is that the flow distribution problem in radial flow fixed bed reactors can be controlled by using a tapered geometry (increasing bed depth with bed height). This hypothesis is based on the following observations.

1. Radial flow packed beds offer a larger mean cross-sectional area and reduced travel distance as compared to traditional VFBRs [2].

2. Since pressure drop is directly proportional to bed depth, and by changing the bed depth with height, the least resistance path guides the fluid movement in the radial direction.

Based on these observations the focus of this proposal is the modeling of the radial flow dynamics in radial fixed bed reactors**.** The specific aims are the study of radial flow dynamics as well as to propose improved design to reduce FDP (flow distribution problem).

The intention is to achieve a uniform flow distribution in the catalyst bed, with the flow predominantly in a radial direction. In brief (Figure 1-2), the internal design to be proposed is that flow enters the vessel across the top cross section of the vessel; proceeds downward near the center of the vessel, then radially outward through the bed, and finally exits the reactor in an upward direction.

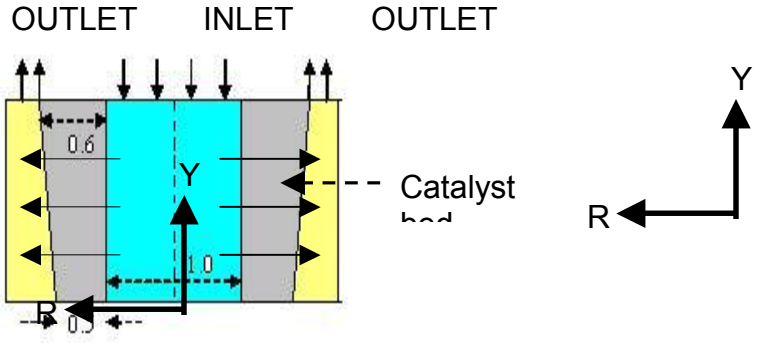

FIGURE1-2: Proposed geometry (gm3, increasing bed length with height of RFBR)

Note: All dimensions are in meter. Arrow indicates fluid movement inside the RFBR.

In the proposed project, the RFBR model will be developed for methanol synthesis. The successful modeling of the present scheme will serve as the basis for development of similar models for other industrially important chemicals. The RFBR can be also used in refineries for hydrodesulphurization, hydrogenation,

hydro cracking and residue hydro conversion. The result will provide valuable input to future computer simulation to assess the technical and economic feasibility of proposed radial flow [6]. Fixed-bed catalytic reactors have been aptly characterized as the workhorses of the process industries. For the economical production of large amounts of product, they are usually the first choice, particularly for gas phase reactions [3].

The standard method to develop a flow profile is to use the Navier-Stokes equation for continuity of component and momentum balance for RFBRs [4]. The proposed method uses the Navier-Stokes equation to develop the model for radial flow. The Navier-Stokes equation is solved in a computational fluid dynamics (CFD) software that is built on numerical integration techniques. CFD is used to model physical systems by using mass, momentum, and chemical species balance equations to mathematically simulate real phenomena inside the system. CFD accomplishes this by subdividing a system into series of finite elements that describe the geometry and by solving the modeling equation differentially at each finite element. The simulation generates realistic information about the temperature, pressure, velocity, and composition at each finite element. For this work the RFBR is divided in to many finite elements and velocity and pressure profiles are found at each element. . The commercial software package used in simulations for this research is CFX^{TM} 5.7.1 [5], (Anysys Canada Limited). The boundary conditions are provided based on actual conditions and transport properties are referred from the data bank available in CFX software

1.1 Rationale

Fixed bed reactors are used for a wide range of industrial processes for gas phase reactions. However research [2] has found that RFBRs geometry introduces flow distribution problem (FDP) [2]. A better alternative as compared to currently used VFBRs is needed. The intention is to achieve a uniform flow distribution in the catalyst bed, with the flow predominantly in a radial direction to minimize flow distribution problem. The poor flow distribution problem contributes to poor product quality and higher pressure drop in the reactor bed.

In some of the reaction systems a major portion of reactor outlet is recycled back (almost 90% as in the case of ethylene oxide reaction) [8]. Therefore a high pressure drop contributes to a major loss of energy for such types of reactions in VFBRs. The larger the bed depths produces more severe problems in maintaining a uniform temperature in the bed. The large temperature variation in the bed contributes to poor product quality and increases the possibility of reaching the auto ignition temperature (AIT) in the bed (due to hot spot generation).

The present research will be able to provide a better alternative to VFBRs. The present research for RFBRs will reduce the FDP [2] as well as maintain uniform catalyst bed temperature. Radial flow in fixed bed reactors promises (i) reduced pressure drop across RFBRs as compared to currently used VFBRs [3] and (ii) uniform flow in radial direction to minimize the FDP. Figure 1-3 demonstrates the experimental results [2] for radial flow. For the most part of the reactor bed, the flow path is both radial and axial. If the bed radius varied in such a manner (as shown in Figure 1-4) to reduce the pressure drop uniformly, the FDP can be reduced.

Figure 1-3 comes from experiments done by Bolton [1]. Fluid moves downward at the center of the vessel and then radially outward to exit from the uniform bed RFBR (gm1, RFBR geometry of uniform bed length with height). In the upper half of the reactor the fluid has both axial and radial component of velocity.

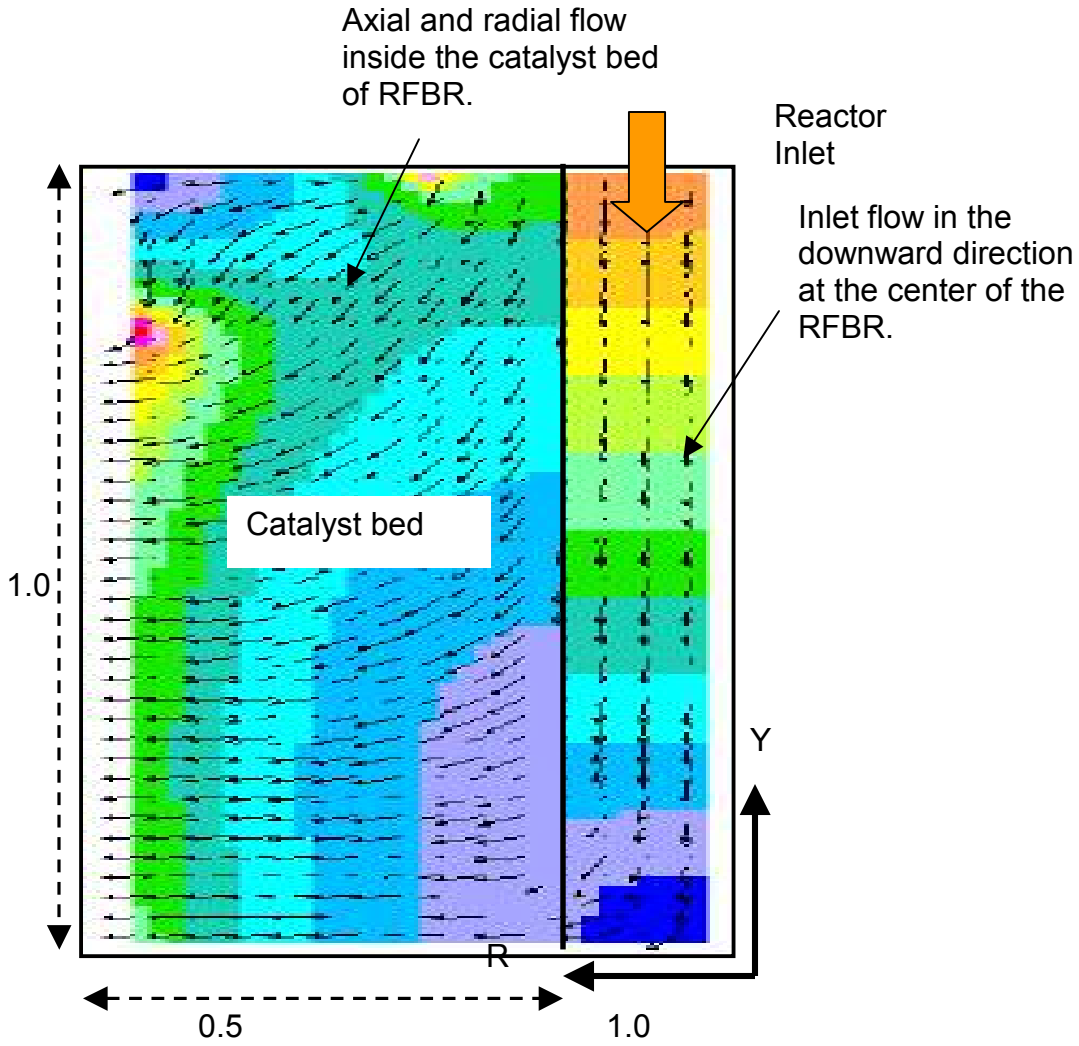

FIGURE1-3: Velocity profile [2]

Note: All dimensions in meter

In uniform bed length of RFBR (gm1), fluid follows the least resistance path. The fluid path is mapped in Figure 1-3 from experimental results. The fluid path deviates from the flow path in the radial direction. At the entrance of reactor the flow distribution problem is evident from the Figure 1-3. This observation is evident from

the experiment conducted [2]. If bed height and radius are increased, higher resistance is offered. The fluid movement will increase towards the radial direction as compared to the axial direction. The arrangement can reduce the axial velocity component. Here the intention is to minimize the axial velocity component to minimize FDP.

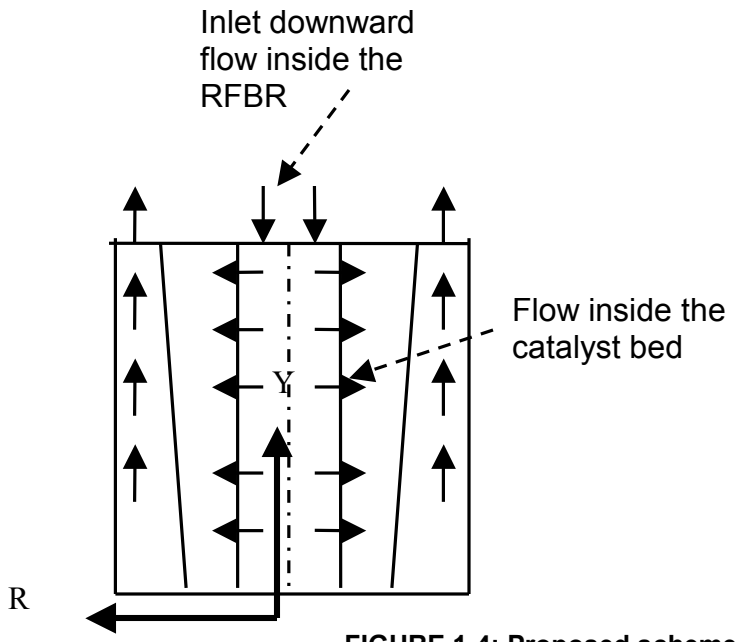

FIGURE 1-4: Proposed scheme

1.2 Goal

In this work, the goal is to improve the flow distribution in RFBRs. The improvement in FDP will improve the reactor performance. The proposed tapered geometry for a fixed bed reactor promises to reduce the FDP. The arrangement for flow in radial direction can improve the energy efficiency of fixed bed reactors. A uniform flow in radial direction also maintains uniform temperature across catalyst bed. This helps in maintaining product quality.

1.3 Objective

The specific objectives are to:

1. Develop a rigorous model for RFBRs that
    - Incorporates pressure gradient.
    - Simulates the velocity map.
    - Improves the flow distribution by optimizing the optimum physical parameters from model solution.
2. Compare the results of the model developed to experiments [2].

1.4 Significance

Presently used vertical fixed bed reactors have disadvantages like high pressure drop, catalyst deactivation, poor product quality and poor heat transfer as well as product formation may be pore diffusion rate limited [3]. The successful modeling of the present RFBR could be the basis for development of similar models that can improve the design and performance of RFBRs. The result will provide valuable input to future computer simulations to assess the technical and economic feasibility of proposed radial flow for specific industrial process such as ethylene oxide production [3]. The power consumption for VFBR and RFBR has been compared for calculating the economic benefit of using RFBRs. The economic advantage is of US $0.48 million per ton of product produced per year. The details are presented in Table 1.1. The calculation was done in Aspen Plus and a uniform pressure drop of 0.4 bar was taken (pressure drop calculation from CFX^{TM}) across the RFBR.

The cost of energy was taken as $0.05 /kw-hr [7]. The production capacity figures were taken from Haldor Topsoe and Dow chemicals web sites [8, 9].

Table 1-1: Power consumption for industrial important chemicals

Reaction		Licensor	Capacity, tons per day	Power, MW (VFBR)	Power, MW (RFBR)
Ammonia	$N_2+3H_2 \rightarrow 2NH_3$	Haldor Topsoe	6000	20	12
Methanol	$CO+2H_2 \rightarrow CH_3OH$	Haldor Topsoe	3000	10	6
Ethylene oxide	$2C_2H_4+O_2 \rightarrow 2C_2H_4O$	Dow Chemicals	1300	12	7.2
Synthesis gas	$CH_4+H_2O \rightarrow CO+H_2$	Haldor Topsoe	12000	30	18

(Note: Calculation done in Aspen^{TM} Plus11.9)

1.5 Thesis organization

To find the best arrangement of catalyst for reducing FDP, a case study approach was used. First results for uniform bed RFBR (gm1) were processed. Then simulation was done in CFX^{TM} for tapered geometry RFBR. For tapered geometry RFBR, gm2 (reducing bed length with height) and gm3 (increasing bed length with height) was first created in Anysys 8.1(a part of CFX^{TM} software) and then simulated to compare the flow distribution in the geometries gm1, gm2 and gm3..

The rest of the thesis is organized as follows:

- Chapter 2 describes the literature review.
- Chapter 3 describes the methodology in detail and further elaborates on the model development in CFX^{TM}.
- Chapter 4 presents and discusses the results from the CFX^{TM} simulation for three geometries gm1, gm2 and gm3.

CHAPTER 2

LITERATURE REVIEW

This chapter reviews the fundamental concepts critical to advanced flow profile modeling for fixed bed reactors. Review of flow profile modeling in packed beds, and numerical methods provide the basis for this work. Once these techniques are reviewed and methods are chosen, the model test conditions are presented.

2.1 Pressure drop in packed bed

The design of process operations involving flow through packed beds is commonly based on the assumption of plug flow; that is, a uniform residence time distribution for all the elements of fluid. The problem associated with radial fixed bed (RFBR) reactors is that of the effect on residence time distribution [10]. The important features [10] of the RFBRs that can affect flow distribution includes (suggested by Heggs, P J):

- Radial dimensions.
- Axial bed length.
- Surface friction factors associated with the inlet.
- Characteristic parameters of the bed packing.

- Flow rate and direction of flow.

The work by Heggs [10] for the modeling of fluid flow distribution in annular packed beds (gas separation and purification) describes in detail the factors described above.

Bird [4] had laid down a guide line to model the flow dynamics of a packed bed. The guide line suggests use of following:

- The equation of continuity
- The equation of momentum
- The component of τ (second order tensor)
- The equation of state
- The equation of viscosity.

2.1.1 Ergun [3] developed the method of pressure drop calculation in fixed bed reactors. It is rationalized on the basis that pressure losses are caused by simultaneous kinetic (inertial) and viscous losses. For the pressure drop calculation in the radial direction, the Ergun equation is used by simply replacing the parameter Z by the radial distance r [3]. This recommendation assumes plug flow and no radial dispersion.

$$\frac{\partial P}{\partial r} = \frac{v_z^2 \rho_f}{d_p}\left(\frac{1-\varepsilon}{\varepsilon^3}\right)\left(1.75 + \frac{150(1-\varepsilon)}{N_{re}}\right) \qquad \textbf{(2-1)}$$

The isotropic loss model in CFX™ calculates pressure drop in porous medium. Isotropic momentum losses are specified using either linear or quadratic

resistance coefficients [5], or by using permeability and a loss coefficient. The linear and quadratic resistance coefficients model is formulated using linear and quadratic resistance coefficients. The permeability and loss coefficient model specifies coefficients for permeability and loss, in the generalized form of Darcy law.

The direction loss model is used in CFX^{TM} to evaluate the resistance loss in specified direction, with flow inhibited in specified direction. The flow inside the RFBR is changes direction with space. For situations like this, CFX^{TM} allows the independent specification of loss for streamwise and transverse direction. For both the streamwise and transverse directions, both types of the loss formulations for the isotropic loss model are available. In many cases, however, the loss coefficients are known only for the streamwise direction, and only the fact that the flow is inhibited in the transverse direction is known. When this occurs, the streamwise coefficient multiplier for the transverse loss model is selected. In this case, the transverse coefficients are taken to be the specified factor times the streamwise coefficients. The transverse multiplier is typically taken to be in the range of 10 to100 [5].

2.1.2 Turbulence and near wall modeling

Turbulence models are used to predict the effects of turbulence in fluid flow without resolving all scales of the smallest turbulent fluctuations. A number of models have been developed that can be used to approximate turbulence based on the Reynolds Averaged Navier-Stokes (RANS) equations. Some have very specific applications, while others can be applied to a wider class of flows

with a reasonable degree of confidence. The models can be classified as either eddy-viscosity or Reynolds stress models. The following turbulence models based on the RANS equations are available in CFX^{TM}.

1. Zero equation model

The Zero equation model in CFX^{TM} provides a good initial guess of velocity for simulations using more advanced turbulence models. It is not used to obtain final results [5].

2. Standard *k*-ε model

One of the most prominent turbulence models, the *k*-ε (*k*-epsilon) model, has been implemented in most general purpose CFD codes and is considered the industry standard model [5]. It has proven to be stable and numerically robust and has a well established regime of predictive capability. For general purpose simulations, the *k*-ε model offers a good compromise in terms of accuracy and robustness [5]. The k-ε model, provide good predictions for many flows of engineering interest, there are applications for which these models may not be suitable. Among these are [5]:

- Flows with boundary layer separation
- Flows with sudden changes in the mean strain rate
- Flows in rotating fluids

3. RNG *k*-ε model

The RNG *k*-ε model is an alternative to the standard *k*-ε model. In general it offers little improvement compared to the standard *k*-ε model [5]. The computational time increases depending on geometry complexity.

4. Reynolds-Stress Models (RSM):

Two-equation turbulence models (*k*-ε and *k*-ω based models) offer good predictions of the characteristics and physics of most flows of industrial relevance. RSM can be used in free shear flow with strong anisotropy like a strong swirl component [5], this includes:

- Flows in rotating fluids.
- Flows with sudden changes in the mean strain rate.
- Flows where the strain fields are complex, and reproduce the anisotropic nature of turbulence itself.
- Flows with strong streamline curvature.

Reynolds stress models have shown superior predictive performance compared to eddy viscosity models in these cases [5]. This is the major justification for Reynolds stress models, which are based on transport equations for the individual components of the Reynolds stress tensor and the dissipation rate. These models are characterized by a higher degree of universality. The penalty for this flexibility is a high degree of complexity in the resulting mathematical system. The increased number of transport equations leads to reduced numerical robustness, requires increased computational effort and often prevents their usage in complex flows [5]. Therefore for simulation in this work k-ε model has been selected as compared to more advanced model. The k-ε model is industry standard for simulation of velocity profile in simple geometry.

2.2 Recent advances

The modeling of fluid-fluid flow distribution in radial packed beds was done by Heggs in 1994 [10]. The work mainly concentrated on flow arrangement with the basic assumption of uniradial flow. The U type flow arrangement shown in Figure 2.1, was found to provide better flow distribution [10]. The U type of arrangement was done as shown in the Figure 2-1. The inlet to reactor is at the center of the vessel and outlet is from outer circumference, in the upward direction. The flow inside the catalyst bed was been assumed to be uniradial in Heggs work.

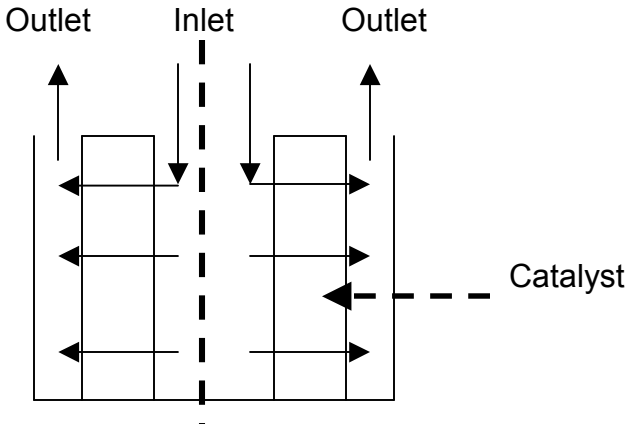

FIGURE 2-1: U type flow

Flow distribution measurements [2] were done in a RFBRs using electrical tomography by Bolton in 2004. Visualization of the flow pattern and distribution inside a radial flow packed bed with lower pressure drop has been accomplished. The findings were presented in Figure 1-3. It can be observed that in the upper half of reactor, the flow distribution is not uniform in the radial direction. This FDP leads to unwanted residence time distributions (RTDs) over and above that occurring due to axial mixing [2]. In practice, the FDP is known to be single most

important variable in attaining optimal operation of RFBRs [10]. Investigation into the effects of FDP with possible change in geometry is need of this study.

2.3 Selected test reactions

The methanol synthesis reaction [11] was selected to test the model of radial flow reactor. The methanol synthesis reaction was chosen because it is a gas phase reaction and most of the industrial reactions using fixed bed reactor are gas phase [3]. All of the data related to reaction kinetics, physical, thermodynamic and transport properties are readily available in literature [12].

Methanol can be produced from synthesis gas which contains H_2, CO, CO_2, water and even small amounts of hydrocarbons [35]. Synthesis gas can be produced, for example by the steam reforming of methane (or other hydrocarbons) or the gasification of biomass. For this project the assumption is made that the starting material is synthesis gas with the following simple composition:

60% H_2, 30% CO and 10% H_2O that can be supplied at any rate required to produce methanol. The overall reaction for producing methanol is:

$$CO + 2\ H_2 \rightarrow CH_3OH$$

The methanol synthesis reaction is exothermic and the equilibrium conversion of methanol decreases with temperature. Figure 2-2 below shows the equilibrium conversion for methanol synthesis against temperature and at various pressures. The pressure range shown in Figure 2-2 is 10, 50 and 80 atm. The temperature ranges from 373.15 K to 773.15 K. The overall conversion decreases with temperature at constant pressure. It can be observed that at 373

K the conversion is 100% but at 473 K the conversion reduces to 50% at constant pressure of 10 atm.

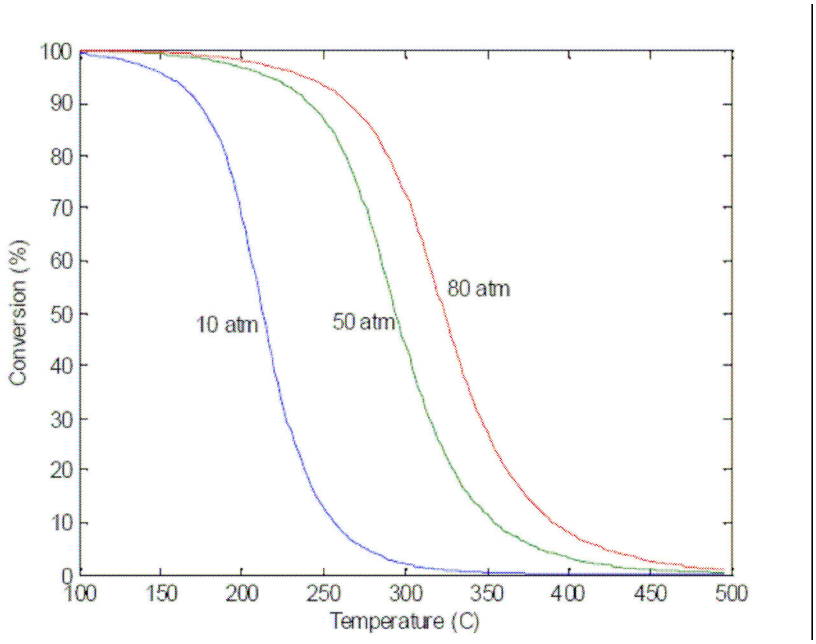

FIGURE 2-2: Equilibrium conversion for methanol synthesis from syngas (60% H_2, 30% CO, 10% H_2O) [25]

. Since the number of moles decreases with the reaction, improved equilibrium conversion is obtained by operation at a high pressure. Modern methanol synthesis reactors operate at temperatures above about 250ºC and at 30-100 atm [25]. The reactors operate in a temperature range of 250 to 270 deg C, above a certain minimum temperature so that reaction rates are high, but below a maximum temperature set by the thermodynamic limits. The reaction can be carried out in tubular reactors packed with catalyst. A common catalyst for this reaction is Cu/ZnO on alumina. Since the reaction is exothermic and high temperatures limit the equilibrium conversion, heat must be removed from the reactor system to obtain an acceptable final conversion. This is most easily done

by using several reactors in series with inter-stage cooling to decrease the temperature of the gases to the minimum operating temperature.

2.4 Numerical solution methods

The model developed in this work will involve very complex kinetics, requiring numerical methods. Analytical solutions for partial differential equations are possible for only the simplest cases and are not possible for highly non-linear systems with complex kinetics [32]. Since the model being developed includes second order partial derivatives in at least two dimensions as well as potentially non-linear terms, analytical solutions are not possible. Generalized numerical solution methods will be required.

Many numerical programs are available for the solution of partial differential equations, with most methods designed for specific solutions. For solution of model equations under a wide range of assumptions, a much more generalized code must be implemented. PDECOL™ [39] is a widely used publicly available set of routines for the solution of a wide range of partial differential equations. PDECOL™ was originally developed as a generalized tool capable of handling a very wide range of coupled partial differential equations in three spatial dimensions and one time dimension. Because of its generality, PDECOL™ has been used for the solution of partial differential equations ranging from the very simple to highly coupled nonlinear magneto-hydrodynamic problems.

PDECOL™, though very general, is limited to systems that do not contain cross derivatives. Cross derivatives are of the generalized form:

$$\frac{\partial C}{\partial x \partial y} \qquad \textbf{(2-2)}$$

and are not features of this work. Using finite difference techniques and the method of lines [39], PDECOL™ converts the partial differential equations into coupled first order ordinary differential equation (ODE). Subsequent solution is completed using traditional finite difference methods and techniques.

2.4.1 Finite difference

Finite difference methods approximate partial differential equation derivatives by dividing the area of interest into an evenly spaced system of grid points and application of Taylor series expansions to approximate the solution at each grid point. This method of approximation is by far the most commonly used and extensively covered in numerical methods texts. An extraordinary amount of research and development in numerical approximation has led to the development of many methods based on finite difference principles. Methods include Euler, Runge-Kutta, Adams-Moulton, Gears, etc; each with many different forms and variations. For the purpose of this document, discussion will be limited to the Adams-Moulton, since it is available with the PDECOL™ algorithm.

2.4.2 Method of lines

One of the most common methods used for solving second order ordinary differential equations or partial differential equations is the method of lines (MOL). Using a transformation of variables solution, the method of lines converts second order or higher partial differential equations into coupled first order

ordinary differential equations. Once the equations have been reduced and the system Jacobian generated, integration is completed using an appropriate integration routine. PDECOL™ implements a variable order Adams-Moulton method for equation solution.

2.4.3 Adams-Moulton

The Adams-Moulton methods use backward finite difference techniques to approximate the solution of ordinary differential equations (Hornbeck 1975). The simplest Adams-Moulton method incorporates an iterative solution approach that includes the point being predicted. This first order Adams-Moulton formula:

$$y_{i+1} = y_i + hf(t_{i+1}, y_{i+1}) \qquad \textbf{(2-3)}$$

is commonly referred to as the backward difference Euler formula. Higher order Adams-Moulton methods are more typically employed. The high order methods take into account previously computed solutions and provide solutions of much higher accuracy.

PDECOL™ uses a variable order Adams-Moulton method [39] for equation integration. Adams-Moulton methods, due to the backward difference techniques, offer very high accuracy at the expense of iteration time. It should be noted that integration with Adams-Moulton techniques, though slow, offer an actual error that is an order of magnitude lower than techniques using forward difference techniques such as Gears method. The Adams-Moulton method is used throughout all phases of solution due to its stability and accuracy.

2.4.4 Summary

The present chapter for literature review describes different models that are at present used for modeling of flow distribution in fixed bed reactor. The K-ε model in CFX^{TM} is widely used in the industry. The model description is followed by recent work performed by various researchers. Two important researches done on radial flow is presented in this chapter. First, the work done by Heggs [10], who suggested U type of flow for RFBR. The second work done by Bolton [1], that presents experimental results for flow distribution in RFBR. The literature review for methanol synthesis reaction is also presented here with the equilibrium conversion chart. Finally the numerical solution described for finding solution for reaction inside the catalyst bed.

CHAPTER 3

METHODOLOGY

This chapter is divided into four sections which are organized to follow the logical flow and development of flow profile models. The model development starts with the designation and review of generic bed reactor conditions and geometry [13]. Formulation and application of model assumptions along with the equations are presented. Finally, support equations for physical property calculations are presented along with degree of freedom analysis to determine if the system is completely defined and ready for solution.

3.1 Generic radial flow reactor model

Design, operation, and troubleshooting of fixed bed reactors for gas phase reactions require understanding of heterogeneous catalysis, the laws of thermodynamics, reaction kinetics, and transport properties together with the associated empirical coefficients essential for quantitative work [14].

The most widely accepted and rational approach for the complex two dimensional problem is to apply familiar continuity equations for both momentum and component transport [15]. Because of the high mass velocities required for heat transfer [16], the temperature gradient between the catalyst and the fluid is generally negligible. The actual mechanism for heat transport is quite complex,

involving conduction in solid catalyst, convection in the fluid, and radiation between phases [18].

3.2 Model assumptions

Simplified assumptions were implemented to minimize computational time and decrease overall complexity [19]. An analytical solution of the most complex reactors that takes into account all the features of turbulent reacting flow is not possible [17]. Numerical approximation of complex equations can be time consuming and in many cases is not currently feasible. Therefore for cylindrical coordinates the equation were obtained with the following assumptions [4, 20-23].

- The fluid is Newtonian.
- The flow is steady and fully developed.
- The temperature is constant.
- Slip on the wall is zero.
- The flow is only in the radial and the axial directions.
- The edge effect is negligible.

3.3 Geometry configuration

This section discusses about the geometry creation for CFX^{TM} simulation. Three geometries are created one for uniform bed length RFBR and other two for tapered geometry (increasing and decreasing bed length with height) RFBR. Depending on bed geometry flow distribution was be studied at various planes

that divides the catalyst bed into small sections. Three geometry of reactor selected for simulation are shown in Figure 3-1 to 3-3.

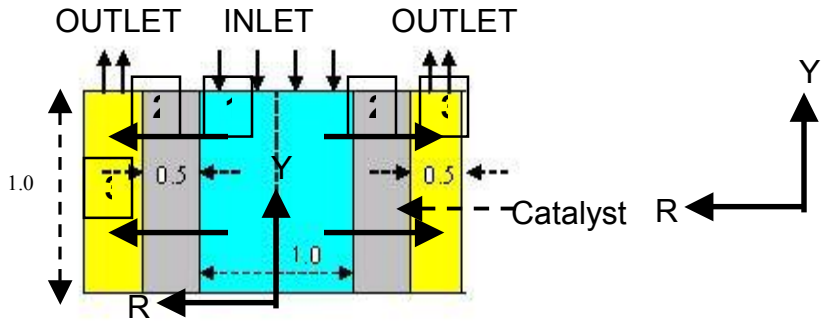

FIGURE 3-1: Uniform bed length RFBR, gm1

Note: All dimensions are in meter. Arrow (➔) indicates fluid flow direction. Regions are indicated by numbers in square.

Geometry1 (or gm1) was created to study the velocity and pressure profiles in a uniform bed RFBR. The simulated velocity profile will also be compared with the experimental results [2]. The fluid moves downward at the center, then radially outward towards the outer circumference and then finally in an upward direction to exit the RFBR. The RFBR was divided into three regions to apply different flow model to different region. The reactor inlet is represented Region 1. Region 1 (or SOLID1) is a cylindrical vessel that is the inlet to the RFBR. Region 2 represents the catalyst bed (or SOLID2) of the RFBR. The velocity profile inside the catalyst bed was studied in this work. Region 3 (or SOLID3) represents the reactor outlet. The Region 2 is filled with the catalyst, Region 1 and 3 are cylindrical vessel without any catalyst inside and designed for inlet and outlet of the RFBR. The fluid movement changes flow direction from inlet to the outlet. In the RFBR inlet fluid moves downward while fluid exit in the axial direction at the reactor outlet.

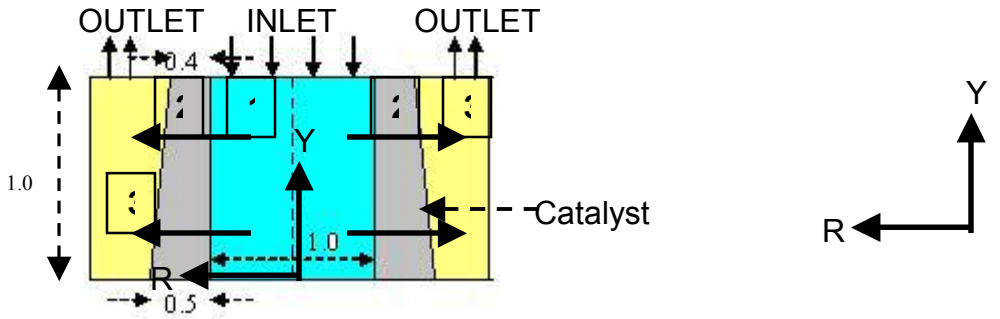

FIGURE 3-2: Reducing bed length with height of RFBR, gm2

Note: All dimensions are in meter. Arrow indicates fluid flow direction. Regions are indicated by numbers in square.

Geometry2 (or gm2, Figure 3-2) designed to study the velocity profile in tapered geometry of the RFBR. The regions numbered in Figure 3-2 represent same regions as it represents for Geometry1 (gm1) in Figure 3-1.The fluid movement path is similar to that fluid movement as in gm1 of the RFBR. The generated velocity profile will be compared with the simulated velocity profile of gm1 to study improvement in flow distribution.

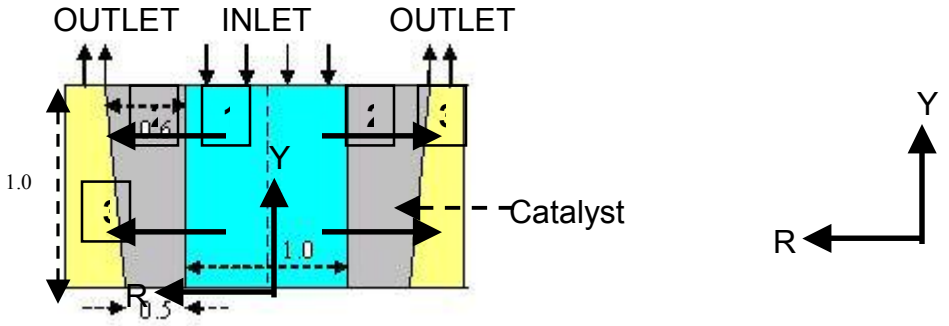

FIGURE3-3: **Increase in bed length with height, gm3**

Note: All dimensions are in meter. Arrow indicates fluid flow direction.

Geometry3 (or gm3) was created to compare the improvement in velocity profile compared to the velocity profile of geometry gm1 and geometry gm2. The regions numbered in Figure 3-3 represent the same regions as it represented for

Geometry1 (or gm1) in Figure 3-1. The fluid movement direction is similar to that in geometry gm1 and geometry gm2 of the RFBR.

3.4 Model selection for modeling flow in different regions of geometries of the RFBR

3.4.1 Region 1 and 3 (or SOLID1 and SOLID3)

The fluid flow in region 1 and 3 (Figure 3-1, 3-2 and 3-3) is turbulent (Reynolds number is of the order 10^4). In principle, the Navier-Stokes equations describe both laminar and turbulent flows. Therefore Navier-Stokes equation can be used to map the velocity profile in region 1 and 3. However, turbulent flows at realistic Reynolds number span a large range of turbulent length and time scales. The direct numerical solution needs smaller than the smallest finite volume mesh which can be practically used in numerical analysis [5]. The direct numerical simulation (DNS) of these flows would require computing power which is many orders of magnitude higher than is available in the near future. The k-ε model will be used to map velocity in region 1 and region 3. The k-ε model is widely used, as it offers good compromise between numerical effort and computational accuracy. For flow in turbulent region, the k-ε model modifies the Navier-Stokes equation after statistical analysis. The details are available in CFX^{TM} solver model theory help files [5].

3.4.2 Region 2 (or SOLID2)

Region 2 (Figure 3-1, 3-2 and 3-3) is filled with catalyst pellets. The region 2 geometry is too complex to resolve with a grid. The flow inside the catalyst bed is modeled as flow in porous media. The model recommended in CFX^{TM} for flow

in porous media is the Darcy model. The Darcy model is a generalization of both the Navier-Stokes equations and Darcy's law commonly used for flow in porous region [5]. Since the model retains both advection (fluid movement) and diffusion term, it can be used for flow in complex fluid path where such effects are important. The details are available in CFX^{TM} solver model theory help files.

The component balance for methanol synthesis reaction is presented in Table 3-1 [3]. The inlet and outlet flow for forced convection and dispersion has been considered. The flow model was first solved for no reaction and then the velocity correction was applied for reaction inside the RFBR. The symbols descriptions are presented in next page.

3.5 Component balance [3]

Table 3-1: Component balance

Component	In	out
Axial flow (forced convection)	$C_j u_z 2\pi r \Delta r\, \Delta t\|_z$	$C_j u_z 2\pi r \Delta r\, \Delta t\|_{z+\Delta z}$
Radial flow (forced convection)	$C_j v_r 2\pi r \Delta z\, \Delta t\|_r$	$C_j v_r 2\pi r \Delta z\, \Delta t\|_{r+\Delta r}$
Axial dispersion (dispersion in z direction)	$\varepsilon N_{jz}\, 2\pi r\, \Delta r\, \Delta t\|_z$	$\varepsilon N_{jz}\, 2\pi r\, \Delta r\, \Delta t\|_{z+\Delta z}$
Radial dispersion (dispersion in r direction)	$\varepsilon N_{jr}\, 2\pi r \Delta z\, \Delta t\|_r$	$\varepsilon N_{jr}\, 2\pi r \Delta z\, \Delta t\|_{r+\Delta r}$
Reaction	$\rho_b \sum \nu_{jn} R_n 2\pi r\, \Delta r\, \Delta z\, \Delta t$	
Accumulation	$\varepsilon\, C_j\, 2\pi r \Delta r\, \Delta z\|_{t+\Delta t} -$ $\varepsilon\, C_j\, 2\pi r \Delta r\, \Delta z\|_t$	

Where,

C_j	Concentration of j component, mol/m^3
u_z	Axial component of velocity, m/s
v_r	Radial component of velocity, m/s
ε	Void fraction
N_{jz}	Mass flux due to dispersion in z direction, Kg/m^2
N_{jr}	Mass flux due to dispersion in r direction, Kg/m^2
r	Radial distance, m
z	Axial distance, m
t	Time, s
ρ_b	Bulk density, Kg/m^3
R_n	Reaction inside the catalyst bed
D	Diffusion coefficient, m^2/s
θ	Angular distance, rad
υ	Stoichiometric coefficient

$$N_{jZ} = D_Z \left[\frac{\partial C_j}{\partial Z} \right]_{r,t} \quad \textbf{(3-1)}$$

and $$N_{jr} = D_r \left[\frac{\partial C_j}{\partial r} \right]_{z,t} \quad \textbf{(3-2)}$$

On simplification the terms in Table 3-1 can be represented in equation 3-3 [3].

$$\varepsilon \left[\frac{\partial C_j}{\partial t} \right]_{z,t} + \left[\frac{\partial (C_j u_z)}{\partial z} \right]_{t,r} + \left[\frac{\partial (C_j v_r)}{\partial r} \right]_{t,z} - \varepsilon D_a \left[\frac{\partial^2 C_j}{\partial z^2} \right]_{t,r} - \varepsilon D_r \left[\frac{\partial^2 C_j}{\partial r^2} + \frac{1}{r} \frac{\partial C_j}{\partial r} \right]_{t,z}$$

$$= \rho_b \sum_1^n v_{jn} R_n \quad \textbf{(3-3)}$$

where all the variables are defined above.

3.6 Momentum balance

r component [3]

$$\rho \left(\frac{\partial v_r}{\partial t} + v_r \frac{\partial v_r}{\partial r} + u_z \frac{\partial v_r}{\partial z} \right) = -\frac{\partial p}{\partial r} + \mu \left(\frac{\partial}{\partial r} \left(\frac{1}{r} \frac{\partial r v_r}{\partial r} \right) + \frac{1}{r^2} \frac{\partial^2 v_r}{\partial \theta^2} + \frac{\partial^2 v_r}{\partial z^2} \right) \quad \textbf{(3-4)}$$

z component [3]

$$\rho\left(\frac{\partial u_z}{\partial t}+v_r\frac{\partial u_z}{\partial r}\right)=-\frac{\partial p}{\partial z}+\mu\left(\frac{1}{r}\frac{\partial}{\partial r}\left(r\frac{\partial u_z}{\partial r}\right)+\frac{1}{r^2}\frac{\partial^2 u_z}{\partial \theta^2}+\frac{\partial^2 u_z}{\partial z^2}\right) \quad \textbf{(3-5)}$$

where all the variables have been defined in the previous page.

3.7 Boundary conditions

The boundary conditions of a simulation supply information about what occurs at the boundary (surface) of the geometry. The Table 3-2 provides the details of input used in each simulation. For all simulations, the isothermal condition was assumed. The reactor inlet velocity fixed at 25 m/sec and pressure at reactor outlet was fixed at 19.0 bar. The boundary conditions and feed composition taken for methanol synthesis reaction [25] are shown in Table 3-2, Table 3-3 and Table 3-4 respectivelly.

Table 3-2: Boundary condition for no reaction inside the catalyst bed (for gm1) [25]

Boundary Name	Boundary Type	Value	Temperature	X	Y	Z
Velocity	Inlet	25 m/sec	518.15K	0	1.0	0<Z<0.5
Pressure	Outlet	19.0 bar	518.15K	0	1.0	1.0<Z<1.5

Note: For geometry gm2 and gm3 of reactor, the value of Z will change (0.4 for gm2 and 0.6 for gm3) [25].

Table 3-3: Boundary condition for reaction inside the catalyst bed (for gm1) [25]

Boundary Name	Boundary Type	Value	Temperature	X	Y	Z
Velocity	Inlet	25 m/sec	518.15K	0	1.0	0<Z<0.5
Pressure	Outlet	19.0 bar	518.15K	0	1.0	1.0<Z<1.5
H_2: CO	Inlet	2.5:1	518.15K	0	1.0	0<Z<0.5

Note: Depending on geometry of reactor, the value of Z will change (0.4 for gm2 and 0.6 for gm3).

Table 3-4: Feed composition at inlet of RFBR [25]

Component	H_2	CO	H_2O
Volume %	64.24	25.71	10.0

3.8 Heat capacity calculations

The average heat capacities are determined using the cubic form of the heat capacity equation

$$C_{pi} = \alpha_i + \beta_i T + \gamma_i T^2 + \delta_i T^3 \quad \textbf{(3-6)}$$

where α, β, γ, and δ are coefficients for equation (3-6).

Coefficient values for above equation are widely published in the literature and available from sources like Perry's Chemical Engineer's Handbook [34] or commercial simulation engines like HYSYS™ or ASPEN™.

3.9 Enthalpy of reaction calculations

In order to accurately account for non-isothermal variations in the reaction rate and system energy, the heat capacity equations must be used to calculate the heat of reaction. Heat capacity coefficient terms for all components are used to solve the following equations [33]:

$$\Delta\alpha = \frac{d}{a}\alpha_d + \frac{c}{a}\alpha_c + \frac{b}{a}\alpha_b + \alpha_a \quad \textbf{(3-7)}$$

$$\Delta\beta = \frac{d}{a}\beta_d + \frac{c}{a}\beta_c + \frac{b}{a}\beta_b + \beta \quad \textbf{(3-8)}$$

$$\Delta\gamma = \frac{d}{a}\gamma_d + \frac{c}{a}\gamma_c + \frac{b}{a}\gamma_b + \gamma_a \quad \textbf{(3-9)}$$

$$\Delta\delta = \frac{d}{a}\delta_d + \frac{c}{a}\delta_c + \frac{b}{a}\delta_b + \delta_a \qquad \textbf{(3-10)}$$

Where a, b, c and d are stoichiometric coefficients and α, β, γ, and δ are coefficient for equation (3-6).

The above equations are of the form (reactants – products) and care should be taken to insure that the stoichiometric coefficients are properly entered in the equation 3-7 to 3-10. Values calculated from equations 3-7 to 3-10 were used to solve the overall heat of reaction equation:

$$\Delta H_R(T) = \Delta H_R^{\circ}(T_R) + \Delta\alpha(T - T_R) + \frac{\Delta\beta}{2}(T^2 - T_R^2) + \frac{\Delta\gamma}{3}(T^3 - T_R^3) + \frac{\Delta\delta}{4}(T^3 - T_R^3) \qquad \textbf{(3-11)}$$

where H_R is the heat of reaction at temperature T, and T_R is the reference temperature.

The above equation is the numerical integration for the heat of reaction from the reference temperature to the current system temperature.

3.10 Complete definition of system

To insure the complete definition of the generic fixed bed reactor, an analysis is done to determine the number of equations required. For the generic case, the above mentioned phenomena and the following items must be accounted for to ensure accurate model solutions:

- Species material balances for all components.
- Reaction expressions for each reaction present.
- Overall momentum equations.

- Overall energy balances.

For the developed model equations to be properly defined and solvable, the number of unknowns is determined by following equation

$$N_{cc} - N_{rxn} + N_{vel} + N_{heat} = N_{eq} \quad \textbf{(3-12)}$$

Where N_{cc} is the number of equations from component balance, N_{rxn} is the number of different reaction, N_{vel} is the number of equations from momentum balance and N_{heat} is the number of equations from heat balance. N_{eq} is number of equations available. For the case of one reaction, three chemical species and z and r momentum, five equations are required for complete definition and solution. Test systems consisting of one reaction and three chemical species, provide the reaction equation and stoichiometric relations required to begin solution. Determination of the remaining equations requires assumptions on the basic mass, velocity and energy equations. Solution of the developed model and description of the model test reactions are detailed in Chapter 4.

3.11 Methanol synthesis reaction

The methanol synthesis reaction selected for this was invented by Pinto Alwyn (Stockton-on-Tees, GB2), patent: 4309359 [29, 35]. The reaction condition and catalyst details are as follows:

Reaction condition: Temperature 518.15K (range: 463-543K)

Pressure 20 bar (range: 10-150atm)

Catalyst details: [30]

Composition: Copper, Zinc oxide, and Alumina containing catalyst

Size: 0.3 E-2 m

Work load: 10 mol / liter hour

Density: 1120 Kg/m^3

Diffusivity: 0.007cm^2/sec

Main reaction (r_1) and side reactions (r_2 and r_3) [35] are as follows:

$$CO + 2H_2 \rightarrow CH_3OH \qquad \Delta H_1\text{=-90.6 KJ / gmol} \qquad r_1$$

$$CO_2 + H_2 \Leftrightarrow CO + H_2O \qquad \Delta H_2\text{=41.2 KJ / gmol} \qquad r_2$$

$$CO_2 + 3H_2 \Leftrightarrow CH_3OH + H_2O \qquad \Delta H_3\text{=-49.6 KJ / gmol} \qquad r_3$$

Rate expressions [36] are as follows:

$$r_1 = \frac{k^*_w K^*_{OH(1)} \left(P_{CO} P_{H_2O} / P^{0.5}{}_{H_2}\right)\left(1 - P_{H_2} P_{CO2} / k_w P_{CO} P_{H_2O}\right)(C^T s_1)^2 S_c \rho_b}{\left(1 + K^*_{CH_3O(1)}\left(P_{CH3OH} / P^{0.5}{}_{H_2}\right) + K^*_{HCOO(1)} P_{CO_2} P^{0.5}{}_{H_2} + K^*_{OH(1)}\left(P_{H_2O} / P^{0.5}{}_{H_2}\right)\right)^2}$$

$$r_2 = \frac{k_D K^*_{CH_3O(2)} \left(P_{CH3OH} / P^{0.5}{}_{H_2}\right)\left(1 - P^2{}_{H_2} P_{CO} / k_D P_{CH_3OH}\right) C^T{}_{s2} C^T{}_{s_{1a}} S2a \rho_b}{\left(1 + K^*_{CH_3O(2)}\left(P_{CH3OH} / P^{0.5}{}_{H_2}\right) + K^*_{OH(2)}\left(P_{H_2O} / P^{0.5}{}_{H_2}\right)\right)\left(1 + K^{0.5}{}_{H(2a)} P^{0.5}{}_{H_2}\right)}$$

$$r_3 = \frac{k_R K^*_{CH_3O(1)} \left(P_{CH3OH} / P^{0.5}{}_{H_2}\right)\left(1 - P^3{}_{H2} P_{CO2} / k_R P_{CH3OH} P_{H_2O}\right) C^T{}_{s_1} C^T{}_{s_{1a}} S_c \rho_b}{\left(1 + K^*_{CH_3O(1)}\left(P_{CH3OH} / P^{0.5}{}_{H_2}\right) + K^*_{HCOO(1)} P_{CO_2} P^{0.5}{}_{H_2} + K^*_{OH(1)}\left(P_{H_2O} / P^{0.5}{}_{H_2}\right)\right)\left(1 + K^{0.5}{}_{H(1a)} P^{0.5}{}_{H_2}\right)}$$

The H_2 to CO ratio is usually greater than stoichiometric because this enables the rate of synthesis reaction to be greater [29, 32] to increase CH_3OH synthesis. The parameters value are presented in Table 3-5 and Table 3-6 and P_i represents partial pressure and subscripts denotes respective components.

Table 3-5: Parameter values for methanol synthesis reaction

Parameter	Value	Unit	Parameter	Value	Unit
C^I_{S1}	7.5E-6	mol m^{-2}	Sc	102	m^2g^{-1}
C^T_{S1a}	1.5E-5	mol m^{-2}	ρ_b	1300	Kgm^{-1}
C^T_{S2}	7.5E-6	mol m^{-2}	R	8.314	J $mol^{-1}K^{-1}$
C^T_{S2a}	1.5E-5	mol m^{-2}	T	518.15	K

Table 3-6: Parameter values for methanol synthesis reaction [36]

Parameter	Value	Unit	Parameter	Value	Unit
k_R	31813.7	$m^2(mol\ s)^{-1}$	$K^*_{HCOO(1)}$	0.18902	$bar^{-1.5}$
k_w	86502.8	$m^2(mol\ s)^{-1}$	$K_{H(1a)}$	0.59799	bar^{-1}
k_D	2732.26	$m^2(mol\ s)^{-1}$	$K_{H(2a)}$	425.41	bar^{-1}
$K^*_{CH3O(1)}$	0.68135	$bar^{-0.5}$	$K^*_{CH3O(2)}$	3836.6	$bar^{-0.5}$
$K^*_{OH(1)}$	0.49241	$bar^{-0.5}$	$K^*_{OH(2)}$	3836.6	$bar^{-0.5}$

3.12 CFX^{TM} solver models

In this section, the CFX^{TM} model selected for the simulation is discussed. The developed model is described and is divided primarily in to four sections.

- CFX^{TM} model development.
- Model selection for simulation.
- Boundary condition.
- Model initialization.

First, an overview of CFX^{TM} model development and presentation of the overall model flow chart is shown in Figure 3-4 and discussed in this section.

- Generation of geometries gm1 (uniform bed RFBR), gm2 (reducing bed depth with height of RFBR), and gm3 (increasing bed depth with height of RFBR), in Ansys^{TM} 8.1 workbench (part of CFX^{TM}). Geometry2 (gm2) created in CFX^{TM} is shown in Figure 3-4. SOLID 1 represents reactor inlet, SOLID2 represents catalyst bed and SOLID3 represents the outlet of reactor. The reactor inlet is at the center of vessel (SOLID1) and outlet is from SOLID3 (in the upward direction). The catalyst bed is tapered (reducing bed length with height) for gm2. The tapered geometry helps in guiding the flow in radial direction. This reduces the velocity in the axial direction.

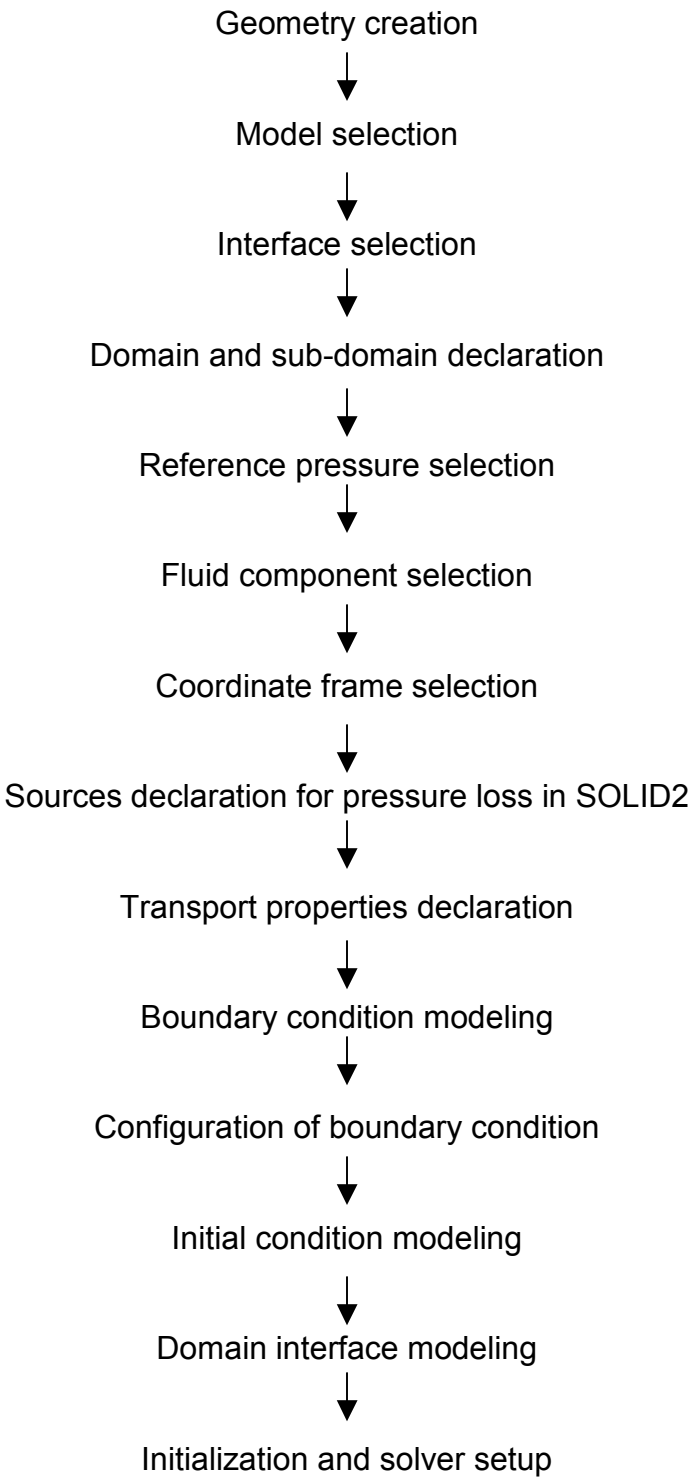

FIGURE 3-4: Flow diagram for solver setup in CFX™

Each step description is detailed in this section.

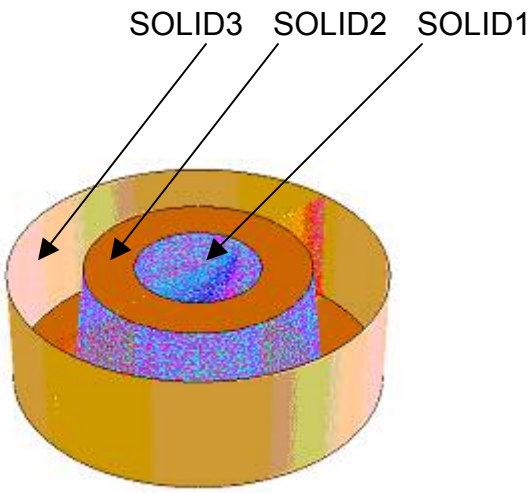

FIGURE 3-5: Geometry2 (gm2), generated in CFX

- Generation of mesh in CFX™

The mesh generation is accomplished after the geometry creation. The steps size, mesh type and volume mesh is generated at this level in Anysys™ 8.1 of CFX™.

- The following models selected for simulation as solution strategy and discussed in detail in section 3.14 of this chapter.
  - Radial partitioning for finite element.
  - Darcy model for flow inside the catalyst bed.
  - Isotropic loss model for pressure drop calculation in catalyst bed.
  - Direction loss model for flow in transverse direction inside the RFBR.
  - k-ε model for turbulence and near wall modeling.
  - Fluid- fluid interface for connection type.
- Post-Processing - To extract and display data, post-processing suite has been used in CFX™. With visualization capabilities, CFX™-post provides

insight into flow field behavior with features such as iso-surfaces, slices, vectors, surface plots and streamlines.

For modeling the flow dynamics, CFX^{TM} is one of the most cost effective and the least time consuming tool. All the above features available in CFX^{TM} help in testing the model developed. However CFX^{TM} has some limitations too. It cannot simulate the methanol synthesis reaction. Majority of the reactions available in the CFX^{TM} in- built library are combustion reactions. Once a mesh is created then it is just a black box. The solution can be known by varying the outside parameter and boundary condition. Therefore only certain aspects of CFX^{TM} are useful for modeling.

3.13 Domains and subdomains

Regions of fluid flow and heat transfer in CFX^{TM}-5 are called Domains. The fluid domain is a region of fluid flow, while a solid domain is a region occupied by a conducting solid in which volumetric sources of energy are specified. The domain in this work requires three specifications.

- The region defining the flow or conducting solid. A domain is formed from one or more 3D primitives that constrain the region occupied by the fluid and conducting solids.
- The physical nature of the flow. This determines the modeling of specific features. In this work pressure drop calculation is considered.
- The properties of the materials in the region.

The present model is defined in a single domain and the domain is defined by 3D primitives.

For this work the domain consists of:

Inlet, catalyst and outlet labeled in Figure 3-6, are part of the domain. And each one is considered separately in the sub-domain. The fluid enters through the inlet (SOLID 1) , passes through catalyst bed (SOLID 2) and finally exit the reactor from outlet (SOLID 3). The regions are labeled in Figure 3-6.

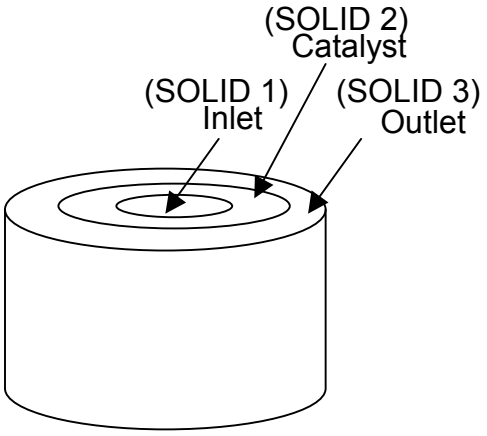

FIGURE 3-6: Domain description for CFX model

Subdomains are regions of fluid flow and heat transfer in a domain in which volumetric sources of mass, momentum, energy, turbulence, additional variables, mass fractions and radiation can be specified. They have been used to model flow resistance for this work. Subdomain regions are defined in the same way as domains that are from 3D primitives. A 3D primitive used for a subdomain must also be contained in the parent domain.

For this work subdomain was defined separately for

- Inlet fluid flow to the cylindrical vessel (SOLID1).
- Fluid movement inside the catalyst (SOLID2).
- Fluid movement outside of catalyst to the reactor outlet (SOLID3).

3.14 Physical models

Physical models were selected to setup the simulation. The physical models defined the type of simulation that was performed for this work. In this work the physical models selected are detailed below.

3.14.1 Steady state flows

The time dependence of the flow characteristics can be specified as either steady state or transient. In this work the steady state model was assumed. The assumption was made that the fluid flow is fully developed. Sometimes simulations which ware run in the steady state mode had difficulty converging, no matter what action was taken regarding mesh quality and time step size, the solution did not converge. This could be an indication of transient behavior. If a steady state calculation was run and oscillatory behavior of the residual plots was seen then test was done to observe a transient effect by reducing or increasing the time step size by a known factor. If the period of oscillation of the residual plot changed by changing the time step size, then the phenomenon was most likely a numerical effect. If the period stays the same, then it was probably a transient effect [5].

3.14.2 Turbulence model

Turbulence models are used to predict the effects of turbulence in fluid flow without resolving all scales of the smallest turbulence fluctuation [37]. A number of models have been developed that can be used to approximate turbulence based on the Reynolds Averaged Navier-Stokes (RANS) equations.

Some have very specific applications, while others can be applied to a wider class of flows with a reasonable degree of confidence. The models can be classified as either eddy-viscosity or Reynolds stress models. The following turbulence models based on the RANS equations are available in CFX^{TM}-5 that has been selected for simulation in this work.

- The k-ε model

One of the most prominent turbulence models, the *k*-ε (*k*-epsilon) model, has been implemented in most general purpose CFD codes and is considered to be the industry standard model. It has proven to be stable and numerically robust and has a well established regime of predictive capability. For general purpose simulations, the *k*-ε model offers a good compromise in terms of accuracy and robustness [5]. Within CFX^{TM}-5, the *k*-ε turbulence model uses the scalable wall-function approach to improve robustness and accuracy when the near-wall mesh is very fine. The scalable wall functions allow solution on arbitrarily fine near wall grids, which is a significant improvement over standard wall functions [5].

While standard two-equation models, such as the *k*-ε model, provide good predictions for many flows of engineering interest, there are applications for which these models may not be suitable. In this work the simulation did not encounter any of the conditions described but here the condition are mentioned for academic interest. Among these are [5]:

- Flows with boundary layer separation.
- Flows with sudden changes in the mean strain rate.
- Flows in rotating fluids.

3.15 Reference pressure

In CFX^{TM}-5 a reference pressure has to be specified for simulation. The reference pressure is specified on the general options tab panel of the domains form, but is a property of the entire simulation so all domains must use the same value. Each time a new domain is created or applied for a change to an existing domain, the reference pressure in that domain is applied to all domains.

All relative pressure specifications set in CFX^{TM}-5 are measured relative to this reference pressure value. The reference pressure will affect the value of every other pressure set in the simulation.

The reference pressure is used to avoid problems with round-off errors. These can occur when the dynamic pressure change in a fluid, which is what drives the flow, are small compared to the absolute pressure level.

3.16 Multicomponent fluid

The fluid in the present work contains four components and its properties are calculated from those of the constituent components. The components was assumed to be mixed at the molecular level and the properties of the fluid are dependent on the proportion of its components [5]. The components exist in fixed mass fractions (fixed composition mixture). For variable composition mixtures, the proportions of each component present may vary in space or time. This may be caused by the conversion of one component to another through a chemical reaction, such as combustion, driven by diffusion or caused by specifying different proportions at different boundaries or in the initial conditions. In this work both cases of fixed and variable mixture composition was considered. There are

no reaction (fixed composition mixture) and reaction (variable composition mixture).

3.17 Coordinate frame

In addition to being the default coordinate frame in CFX^{TM}-Pre, the CFX^{TM}-Solver always computes solutions in the global Cartesian coordinate frame. This coordinate frame's origin is located at (0 0 0) and has the Cartesian basis vectors (1 0 0), (0 1 0) and (0 0 1). Unless specified otherwise all material properties, boundary conditions, source terms and initial conditions are calculated in the global coordinate frame. If CFX^{TM} expression language (CEL) is being used, the built-in variables x, y and z (global) can be used to refer to the three directions of the global coordinate frame.

3.17.1 Cylindrical coordinate frame

The cylindrical coordinate frame was selected for this work because the variables are r and theta (Th) in CFX^{TM} expression language (CEL) expressions, where r and theta are defined in the local coordinate frame as:

$r = (X^2+Y^2)^{0.5}$ and theta = Atan (Y/X)

Cylindrical frames are setup the same way as cartesian frames in CFX^{TM}-Pre. In addition, the CFX^{TM}-Solver performs transformations on cartesian vectors and coordinates as if the cylindrical frame were a cartesian frame. In this work the calculation are presented in the cylindrical coordinate frame. The transformation from Cartesian coordinate frame was done by solver itself. The relation between Cartesian and Cylindrical coordinate frame below.

So, for cylindrical coordinate frames:

- R → Cartesian axis 1 (X)
- Th → Cartesian axis 2 (Y)
- Z → Cartesian axis 3 (Z)

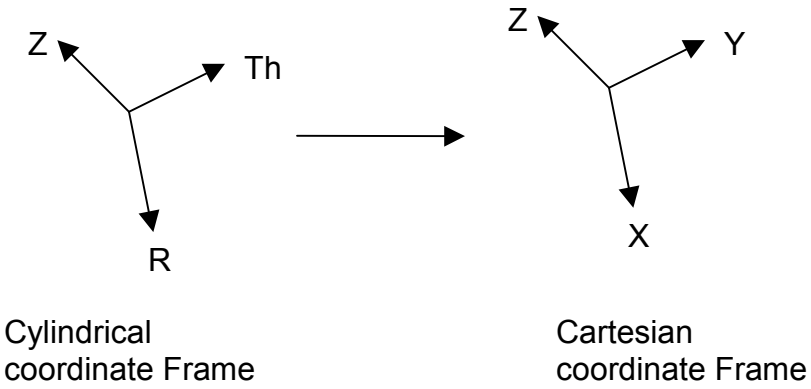

FIGURE 3-7: Coordinate frame

In this case, the three coordinate axes (R, Th, and Z) exactly correspond to a set of Cartesian coordinate axes (X, Y, Z).

3.18 Sources

Sources are optional terms which are attached to most equations, so as to model additional or specialized physical processes. They are specified either as point sources, within a volume defined by a subdomain, as momentum, heat and mass in particles and as radiation sources on boundaries. In point sources or volumes defined by a subdomain, sources of energy, momentum, resistance, mass, turbulence, radiation, components and additional variables can be created.

Within subdomains, the same equations of fluid flow are solved as for domains. Subdomains are useful for modeling fluid resistances and sources of

heat generation, where the resolution of the flow field is not required to the same scale as the rest of the fluid domain.

In this present case the source is identified in the subdomain named as catalyst. Catalyst bed acts as a source of pressure loss.

The source taken in consideration for this work are described below

3.18.1 Isotropic loss model

Isotropic momentum losses can be specified using either linear or quadratic resistance coefficients, or by using permeability and a loss coefficient. This model is appropriate for isotropic porous regions [5].

3.18.2 Permeability and Loss Coefficient

This model specifies coefficients for permeability and loss, in the generalized form of Darcy's Law [5].

$$S_i = -\frac{\mu}{K_{perm}} U_i - K_{loss} \frac{\rho}{2} |U| U_i \qquad \textbf{(3-13)}$$

Where S_i is a momentum source term, K_{perm} is the permeability coefficient (for the viscous loss), K_{loss} is the resistance loss coefficient (for the inertial loss) and U is the velocity.

Note that the velocity determined by the code (and assumed by the model) is the superficial fluid velocity. In a porous region, the true fluid velocity of the fluid is larger because of the flow volume reduction. Sometimes a loss model is formulated in terms of true velocity rather than superficial velocity. In this case, the specified coefficients must be adjusted accordingly: the permeability must be

multiplied by the porosity, and the loss coefficient must be divided by the square of the porosity.

3.18.3 Linear and quadratic resistance coefficients

An isotropic momentum source has been formulated using linear and quadratic coefficients resistance coefficients C_{R1} and C_{R2}. These coefficients are related to the permeability and loss coefficients (mentioned before) as follows:

$$C_{R1} = \mu / K_{perm} \qquad [5]$$

$$C_{R2} = K_{loss} * \rho / 2 \qquad [5]$$

where C_{R1} and C_{R2} are constant, μ is dynamic viscosity in mPoise, K_{perm} is the permeability coefficient (for the viscous loss), K_{loss} is the resistance loss coefficient (for the inertial loss).

3.18.4 Directional Loss Model

For present applications, a certain resistance loss was specified in a direction, with flow inhibited in the transverse direction. This was the case when the model had to take care of the effect of flow straightening devices such as honeycombs, porous plates, and turning vanes without modeling the details of the flow around the obstacles [5]. For situations like this, CFX^{TM}-5 allows the independent specification of loss for the stream wise and transverse directions.

For both the stream wise and transverse directions, both types of the loss formulations available for the isotropic loss model are available. In many cases, however, the loss coefficients are known only for the stream wise direction, and only that the flow that is inhibited in the transverse direction is known. In the

present work this occurs, therefore the stream wise coefficient multiplier for the transverse loss model was selected. In this case, the transverse coefficients were taken to be the specified factor times the stream wise coefficients. (If the stream wise loss includes permeability, the implied transverse permeability is divided, not multiplied, by this factor). The transverse multiplier is typically taken to be about 10-100 [5]. In some cases, the option of only inhibiting the transverse flow without having any stream wise loss is also available. In this case, the 'Zero Loss' option may be selected for the stream wise loss. Of course, if this is chosen, the 'stream wise coefficient multiplier' is not appropriate for the transverse loss, because it will result in zero transverse loss. In all cases, the directional loss model requires the stream wise direction to be specified. It may be described in either Cartesian or Cylindrical coordinates. In the present work, the direction of flow is specified, and the CFX^{TM} automatically chooses the streamline coefficient depending on location.

3.19 Material properties

The materials editor in CFX^{TM}-Pre is used to create and modify material properties for both pure substances and mixtures. Pure substances can be solids, liquids or gases. Liquids or gases can be used in fluid domains and solids can be used for either conjugate heat transfer models or particle tracking. In the present work the gas properties were required for CH_3OH, CO, H_2 and H_2O.

3.20 Equation of state

Equations of state can be modeled in four different ways in CFX^{TM}-5:

- By directly setting density
- By using the built in ideal gas equation
- By using the built in Redlich Kwong equation
- By reading properties from a CFX™ software package.

All properties except density and specific heat capacity can be modeled using any valid expressions containing CFX™-5 System Variables. For the present work, the properties were directly read from tables available in CFX™.

3.21 Molar mass

For all pure substances CFX™-5 requires that the Molar Mass (relative molecular mass) is provided.

For the ideal gas or the Redlich Kwong equation of state, it is essential to set the correct molar mass since it is always used by the CFX™-Solver. When density is directly specified using option=value, the molar mass is only used in certain situations:

- When the fluid is involved in a chemical reaction
- When species transfer occurs for a multiphase-multicomponent simulation

In other cases it is not essential to specify an accurate molar mass. Therefore in the present work this value was not set.

3.22 Transport properties

3.22.1 Dynamic viscosity

For fixed and variable composition mixture, the dynamic viscosity is determined by a mass fraction weighted arithmetic average. For calculation of

dynamic viscosity in this work, the Sutherland's formula is used, that is available in CFX^{TM} software.

Sutherland's formula:

This approximation for viscosity is valid for dilute gases and was obtained from the kinetic theory by Sutherland. In this case viscosity only varies with temperature as:

$$\frac{\mu}{\mu_0} = \frac{T_{ref} + S}{T + S}\left(\frac{T}{T_{ref}}\right)^n \qquad \textbf{(3-14)}$$

[5]

where μ_0 is the reference molecular viscosity, *S* is the Sutherland constant and is a characteristic of the gas, T_{ref} is 273.0 K, and n is the temperature exponent, usually set to 1.5 for most gases.

Rigid non interacting sphere model [37]

This model is based on elementary kinetic theory and is valid for gases using user supplied equations of state or either of the built in equation of state models (Ideal Gas, Redlich Kwong) [5]:

$$\mu = 26.69\frac{\sqrt{wT}}{\sigma^2} \qquad \textbf{(3-6)}$$

where μ is dynamic viscosity in mP, *w* is the molecular weight in g/mol and *T* is temperature in Kelvin and σ is the collision diameter, in Angstroms, and is calculated using

$$\sigma = 80.1\ (V_c)^{1/3} \qquad \textbf{(3-7)}$$

where V_c is the critical molar volume in cm^3/mol.

3.23 Boundary condition modeling

The equations relating to fluid flow can be closed (numerically) by the specification of conditions on the external boundaries of a domain. It is the boundary conditions that produce different solutions for a given geometry and set of physical models. Hence boundary conditions determine to a large extent the characteristics of the solution obtained. Therefore, it is important to set boundary conditions that accurately reflect the real situation to obtain accurate results.

- A “Fluid Boundary” is simply an external surface of the fluid domain excluding surfaces where a solid domain meets the edge of the fluid domain.
- A “Solid Boundary” is where a solid domain meets the edge of the fluid domain.
- A “Fluid-Solid Interface” is the interface between a solid domain and the region of the fluid domain in which fluid flows.
- A “Solid-Solid Interface” is the interface between two different solid domains.

The type of boundary conditions that can be set depends upon what sort of boundary or interface the boundary condition is placed on. The following boundary condition types are available in CFX^{TM}-5:

Fluid Boundaries

A “Fluid Boundary” is simply an external surface of a Fluid Domain.

- Inlet - fluid is constrained to flow into the domain only.
- Outlet - fluid is constrained to flow out of the domain only.

- Opening - fluid can simultaneously flow both in and out of the domain. This is not available for domains with more than one fluid present.
- Wall - impenetrable boundary to fluid flow.
- Symmetry plane - a plane of both geometric and flow symmetry.

3.23.1 Configurations of boundary conditions

The inlet boundary condition is based on inlet velocity of the fluid and the outlet boundary condition is based on static exit pressure of the fluid. The inlet total pressure is an implicit result of the prediction and is based on actual reaction condition.

The magnitude of the resultant normal velocity at the boundary is specified to be 2 meter/sec. The value that is specified is transferred from the fluid domain normal to each element face on that boundary during the execution of the CFX^{TM}-Solver. This option is especially useful for non-planar Inlet boundaries, i.e. curved surfaces.

3.23.2 Turbulence

Reasonable values of either the turbulence intensity, or k and ε at an inlet boundary have to be set. Several options exist for the specification of turbulence quantities at inlets. However, unless there is no given value of the turbulence levels in simulation (in which case recommended option is the Medium Intensity = 5%), a well chosen values of turbulence intensities and length scales may also be taken. Nominal turbulence intensities range from 1% to 5% but depend on specific application. The default turbulence intensity value of 0.037 (i.e. 3.7%) [5]

is sufficient for nominal turbulence through a circular inlet, and is a good estimate in the absence of experimental data. The allowable range of turbulence intensity specification for an Inlet boundary is from 0.001 to 0.1 (i.e. 0.1% to 10%), corresponding to very low and very high levels of turbulence in the flow respectively [5].

3.23.3 Medium turbulence intensity

This defines 5% intensity and a viscosity ratio equal to 10. This is the recommended option if there is no information available about the inlet turbulence. Therefore turbulence intensity of 5% has been chosen for this work [5].

3.23.4 Heat transfer

The Inlet specification for the energy equation requires a value for the fluid temperature. The fluid temperature was set at 518.15 K for this work.

3.23.5 Static temperature

A fixed static (thermodynamic) temperature was specified at the inlet. For present model it was specified at 518.15 K. The present value of temperature was selected as it is condition of feed for reaction to happen. The reaction condition is isothermal and it was assumed that minor change in temperature would not affect the velocity profile for this work. The temperature varies in the range of 515 K to 525 K. Therefore the average temperature of 518.5K was selected.

3.23.6 Wall

Walls are solid (impermeable) boundaries to fluid flow. Walls allow the permeation of heat and additional variables into and out of the domain through the setting of flux and fixed value conditions at wall boundaries.

Walls are the default boundary condition in CFX™-Pre for fluid-world and solid-world regions; any of these regions that are not part of an existing boundary condition will remain in a default wall boundary when the definition file is written.

3.23.7 Wall influence on flow

There are three options for the influence of a Wall boundary on the flow, namely:

- No slip
- Free slip
- Rotating walls

3.23.8 Profile boundary conditions

It is possible to specify a boundary condition based on the interpolated values from a data file. This is useful to use the results of a previous simulation or experimental results as a boundary condition for the current simulation. CFX™-Pre will generate CFX™ expression language (CEL) expressions that refer to the imported data, using interpolation functions. This data is automatically generated when creating a boundary condition using the 'Profile' method. The method is integral part of CFX™ software package.

3.24 Initial condition modeling

Initial values for all solved variables need to be set before the solution can begin. For a steady-state calculation, the initial variable values serve to give the CFX™-solver a flow field from which to start its calculations. Convergence is more rapidly achieved if sensible initial values are provided. However, care has to be taken for converged results that should not be affected by the initialization.

3.24.1 Setting the initial condition

In CFX™-Pre, each solved variable has to be set to either the automatic or automatic with value initialization options. Only solved (or principle) variables are initialized; if an initial field is required for other variables, it is derived from the solved variable initial fields. Other option to choose to set initial conditions on a per-domain basis (set on the Initialization tab for the domain when the enable initial conditions toggle on the basic settings form), or globally (selecting define → Initialization from the main menu bar) is checked. Global initialization options apply to all domains in the simulation.

3.25 Domain interface modeling

Domain Interfaces provide a way of connecting meshes or domains together. There are four types of Domain Interfaces:

- Fluid-fluid interfaces are be used to simply connect matching or non-matching meshes together or allow a change in reference frame between two mesh regions.

- Fluid-solid interfaces are required at the bounding region between a fluid domain and a solid domain, but are often generated automatically.
- Solid-solid interfaces are required at the bounding region between two solid domains, but are often generated automatically.
- Periodic interfaces are used to model periodicity in a simulation. The mesh on these interfaces can be matching or non-matching.

3.26 Initialization

The initialization process of a simulation provides a numerical basis from which calculations proceeds. With bad initial values for calculation to proceed from, convergence can be greatly slowed down or make solution unachievable and in certain case produce incorrect solution. For all simulations, the auto-initiate (with values) function was used. Also, in some instances it was advantageous to calculate a cold flow (no reaction occurring) to generate initial conditions for a simulation with reaction occurring.

3.27 Solver setup

The solver setup of a simulation defines values used by CFX^{TM}-5 solver manager to calculate results. Several important values set in this section include: step size, the advection scheme, mesh adaptation and transient file output information. Selection of these parameters can influence both the output and performance of solver.

Information about number and step size are the first input parameters. The target residuals and advection scheme help to set the level of accuracy of

simulation. The target residuals are calculated from deference of solution variables from one step to the next. The level of convergence set for all simulations was 10^{-4} for maximum residual of a variable. The advection scheme increases the accuracy of simulation by increasing the accuracy of differentiation. Two level of differentiation are available in CFX™ 5.7, first order and high resolution (second order).

The final information needed in the solver is about output files and mesh adaptation. These data tell solver how often and what solution data to write to the output file. Mesh adaptation is used to refine the mesh in areas with high gradients to increase accuracy and aid in convergence.

For simplicity, the flow diagram for solver setup is presented in page 32. Each term used in the flow diagram has already been defined in this chapter. The steps followed may not be sequenced as shown in the flow diagram.

This chapter gives details of the model selected for simulation in CFX™. The RFBR (radial fixed bed reactor) was divided in to three regions, namely inlet, outlet and the catalyst bed. For inlet and outlet the K-ε model was selected and for the catalyst bed Darcy model was selected. The boundary condition was taken from actual reaction condition [25]. After creating the geometry and proper model selection the simulation was run in CFX™-Pre. The simulation results are presented in the Chapter 4.

CHAPTER 4

RESULTS

This chapter focuses on the results obtained from simulation for three different geometries discussed in Chapter 3 (Section 3.3). The analysis performed included an evaluation of the bed geometry, and the sensitivity to reaction. The model equations were implemented on the gas phase methanol synthesis reaction under isothermal conditions to evaluate limitations and feasibility. Results were compared to experimental data when available. Finally, the model is used to evaluate the velocity profile in radial fixed bed reactor (RFBR) to study the flow distribution problem (FDP).

4.1.1 Velocity profile for uniform bed of RFBR (radial fixed bed reactor)

In the case of the uniform bed RFBR (gm1) flow has both axial and radial components. The SOLID2 of the RFBR has been divided in to eleven horizontal (plane p) and vertical (plane g) planes to study the velocity profiles. The SOLID2 is divided into eleven horizontal and vertical planes to make the profiles simple to study and compare the results with the experiment conducted by Bolton [1]. In this study a comparison has been done between velocity profiles in adjacent planes. In each plane the radial and axial velocity components have been found. The radial velocity is presented in p plane (horizontal) while the axial velocity is presented in g plane (vertical plane).

The simulation results presented in the next section is of geometry of uniform bed length (gm1). Only the simulation results of the axial velocity component are presented in this Chapter. The rest of the simulation results have been added to Appendix D for simplicity of data presentation in this chapter. The CFX^{TM} simulated velocity profile for uniform bed RFBR is presented in Figure 4-1. The velocity profile shown inside the SOLID1 represents the velocity profiles in the inlet of the RFBR. The velocity at the inlet boundary can be observed to be 25 m/sec. The velocity slowly decreases with a decrease in height of the RFBR. The velocity profile inside the catalyst bed is shown in SOLID2. The exact value of velocity with position is presented in Table 4-1, that was obtained through an excel file generated in CFX^{TM}. From the profile shown in Figure 4-1, the velocity can be observed to be in the range of 0 to 12.0 m/sec.

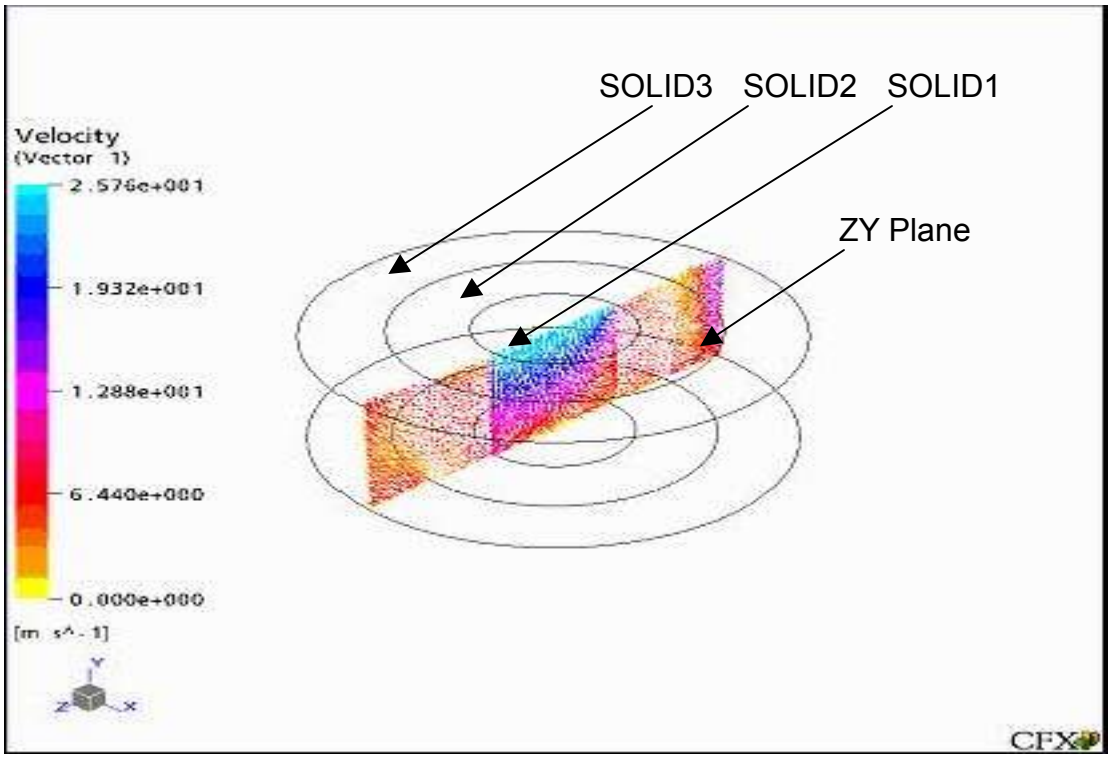

FIGURE4-1: **CFX simulated velocity map of model reactor for gm1 (RFBR of uniform bed)**

The fluid moves into the innermost cylinder (SOLID1) from top (Figure 4-1). The SOLID2 represents the catalyst bed of the RFBR. The SOLID3 represents outlet from the RFBR. For the study of velocity profile, the SOLID2 (flow inside the catalyst bed) has been divided into eleven horizontal (plane p) and eleven vertical planes (plane g). The planes have been represented in Figure 4-2

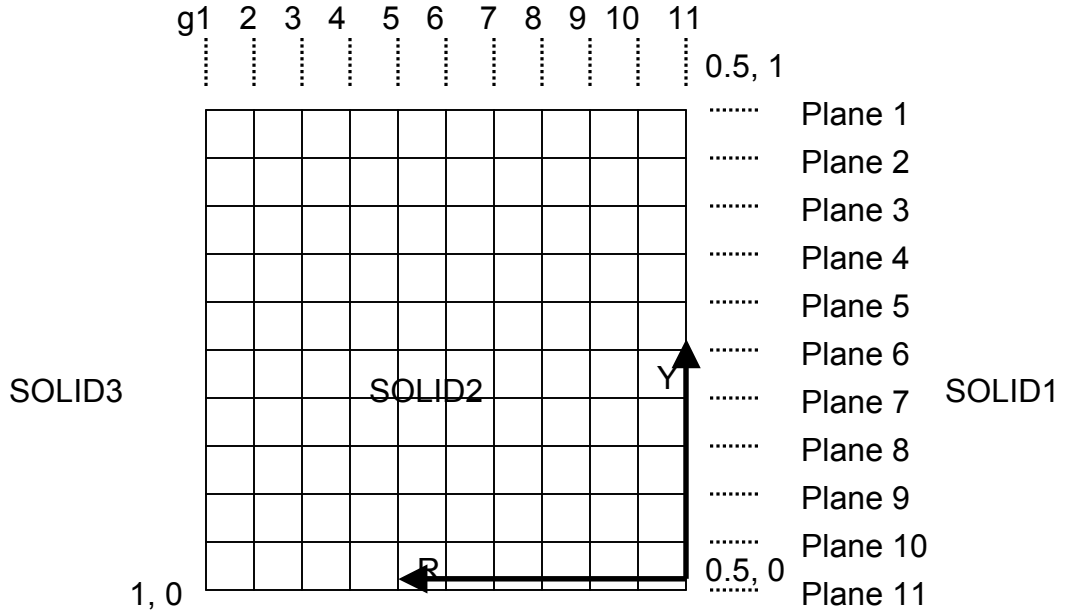

FIGURE4-2: SOLID2 regions divided in eleven horizontal and vertical planes

The SOLID2 dimensions are; inside diameter of 0.5 m, outside diameter of 1.0 m and height of 1.0 m. The distance between each plane (g1 to g2 and p1 to p2) is 0.05 m. Plane g1 represents the interface plane between SOLID2 and SOLID3. And plane g11 represents interface plane between SOLID 1 and SOLID2 (Figure 4-1, 4-2). Plane 11 (or p11) is at the bottom of SOLID2. And plane 1 (p1) is at the top SOLID2. The Table 4.1 represents the axial component of the velocity inside the catalyst bed.

The axial velocity profile of gm1 (uniform bed RFBR) is shown in Table 4-1. At the cross section of the vertical plane g1 and horizontal planes p1 to p11 velocity ranges from 1.28 to 7.23 m/sec. The axial velocity component increases in the down ward direction in the plane g10 while it increases in the upward direction for the plane G1. For planes g2 to g9 axial velocity component first increases and then decreases.

Table 4-1: Axial velocity component for uniform bed of RFBR (m/s)

Plane	g1	g2	g3	g4	g5	g6	g7	g8	g9	g10
p1-2	7.23	0.74	-0.62	-0.26	-0.30	0.39	-0.52	-0.46	1.27	1.80
p2-3	3.66	3.10	2.25	2.29	1.25	1.50	1.24	2.49	2.10	2.63
p3-4	3.62	3.31	2.95	2.73	2.32	2.68	2.82	2.80	3.12	3.56
p4-5	3.23	3.12	3.07	3.05	3.10	3.22	3.00	3.32	3.64	3.83
p5-6	3.19	2.96	3.05	3.02	3.16	3.34	3.62	3.69	3.93	4.12
p6-7	2.86	2.86	2.83	2.96	2.59	3.20	3.64	3.83	4.29	4.52
p7-8	2.45	2.63	2.67	2.66	2.59	3.19	3.39	3.68	4.28	4.64
p8-9	2.33	2.01	1.81	1.87	2.22	2.47	3.31	3.74	4.25	4.97
p9-10	1.62	1.50	1.14	1.22	1.35	2.12	2.39	2.90	4.49	5.53
p10-11	1.28	-0.38	-0.46	-0.40	-0.21	-1.57	-0.52	0.59	2.49	5.62

Note: p1-2 represents space between plane 1 and plane2

Plane 1 (at the top of catalyst bed, SOLID2), plane 2, and plane 6 to plane 11 have wide variations in radial and axial velocity component (see Table D-1 for radial velocity component). The axial velocity component in plane 1 is as high as 7.23 m/sec. The average axial velocity from plane 2 to plane 10 is 3.68 m/sec. While the average radial velocity from plane gm1 to gm11 is 4.73 m/sec.

The numerical solution (Appendix D) matches closely with the simulated results observed in CFX^{TM}. The average radial velocity is 4.74 m/sec while the average axial velocity is 3.63 m/sec. Also wide variations in axial and radial velocity are observed in plane 1, plane 2 and plane 6 to plane 10. The maximum variation in velocity of the order of 6.5 m/sec is observed in plane 1, plane 9 and plane 10.

The numerical solution found for the methanol synthesis reaction. The axial velocity component as well as the radial velocity component reduces, depending on amount of conversion. The reason is that velocity profile depends on continuity equation and pressure drop inside the bed. The mass is conserved but conversion volume reduces (one mole of CO and two mole of H_2 produces one mole of CH_3OH) and therefore both component of velocity reduces. The average radial velocity is found to be 4.84 m/sec while the average axial velocity is 3.78 m/sec.

The velocity profile is presented in the Figure 4-4. The vertical planes are indicated by g1, g2 …g10 and horizontal planes are indicated by p1, p2 …p10. The distance at the catalyst inlet is indicated by zero in the x axis. The vertical plane gm1 indicates the exit axial velocity at each plane from the catalyst bed. The exit velocity at plane p1-2 is 7.23 m/sec and at plane p10-11 is 1.28 m/sec. Similarly the vertical plane g10 indicates inlet velocity to the catalyst bed at each horizontal plane. The inlet velocity at plane p1-2 is 1.80 m/sec and at the plane p10-11 is 5.62 m/sec. Similarly each vertical plane indicates the axial velocity component inside the catalyst bed with reference to horizontal planes. It can be

inferred from the chart in Figure 4-3 that the axial velocity component first increases and then decreases for plane g2 to g9. For vertical plane g1 axial velocity component continuously increases from 1.28 m/sec to 7.23 m/sec with height. For vertical plane G-10 the axial velocity component reduces from 5.62 m/sec to 1.80 m/sec with height.

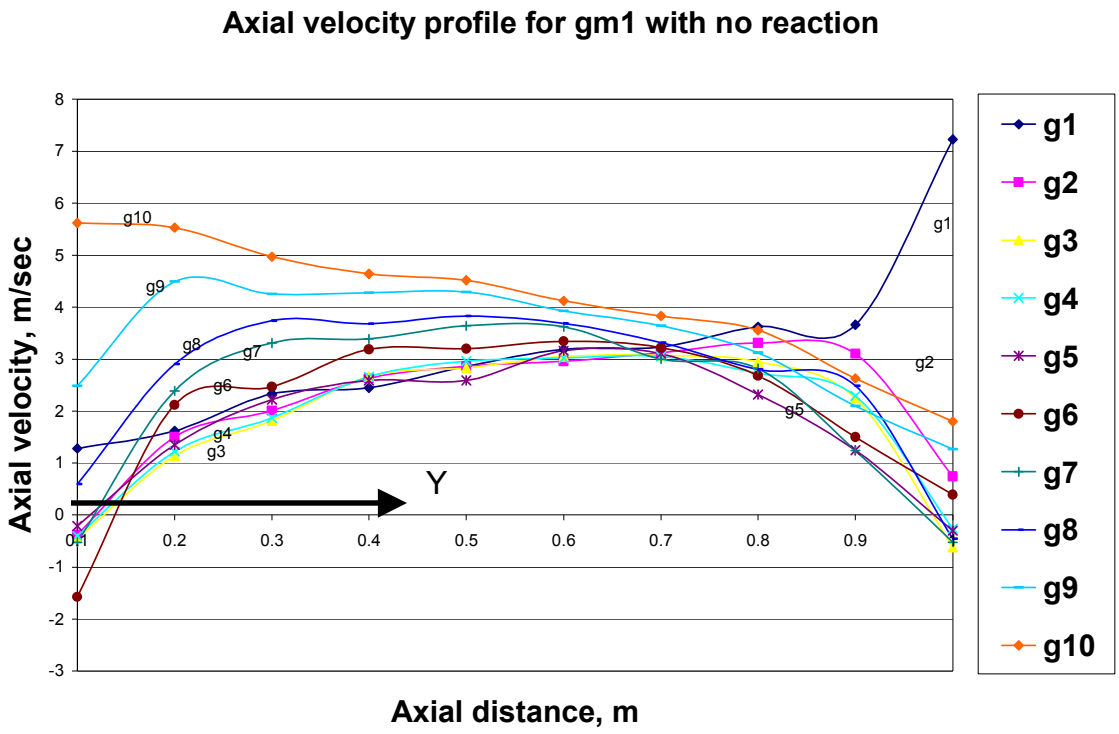

FIGURE 4-3: Axial velocity profile, CFX solution for gm1 with no reaction

Note: Points are connected by line to indicate the plane to which points correspond. The velocity should be read only at the cross section of plane, not in between.g1, g2 ..g10, theses are vertical planes at a fixed radial distance. The axial distance is represented by horizontal Y axis.

From the velocity profile it can be referred that flow distribution problem is higher on plane g1 at the outlet and plane g10 at the inlet. Further the FDP for rest of the planes is almost same.

4.1.2 Velocity profile for reduced bed length with height of RFBR (gm2)

The CFX™ simulated velocity profile for reduced bed length with height for RFBR is presented in Figure 4-4. The velocity profile shown inside the SOLID1 represents the velocity profiles in the inlet of the RFBR. The velocity at the inlet boundary can be observed to be 25 m/sec. The velocity slowly decreases with decrease in height of the RFBR. The velocity profile inside the catalyst bed is shown in SOLID2. The exact value of velocity with position is presented in Table 4-2, that was obtained through excel file generated in CFX™. From the profile shown in Figure 4-4, the velocity can be observed to be in the range of 0 to 12.0 m/sec.

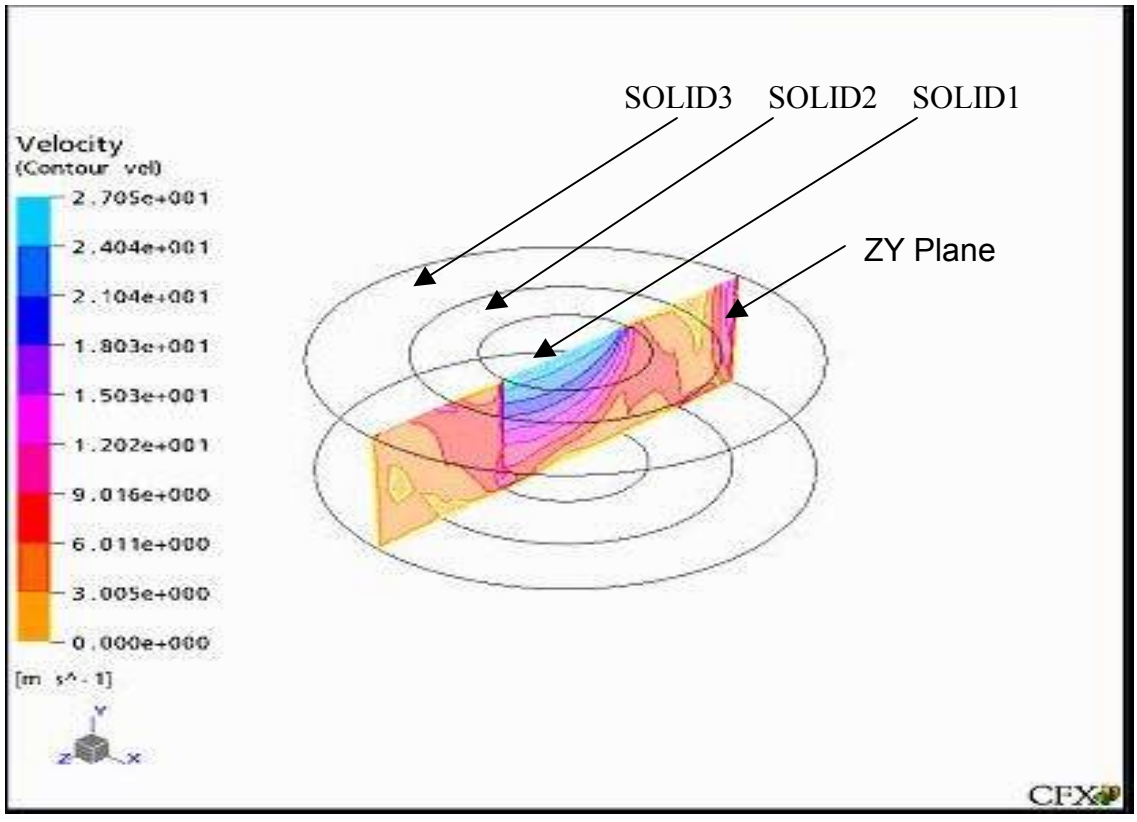

FIGURE 4-4: **CFX simulated velocity map for reduced bed length with height for RFBR (gm2)**

The fluid moves into the innermost cylinder (SOLID1) from top (Figure 4-4). The SOLID2 represents the catalyst bed of the RFBR. The SOLID3 represents outlet from the RFBR. For the study of velocity profile, the SOLID2 (flow inside the catalyst bed) has been divided into eleven horizontal (plane p) and eleven vertical planes (plane g, Figure 4-5).

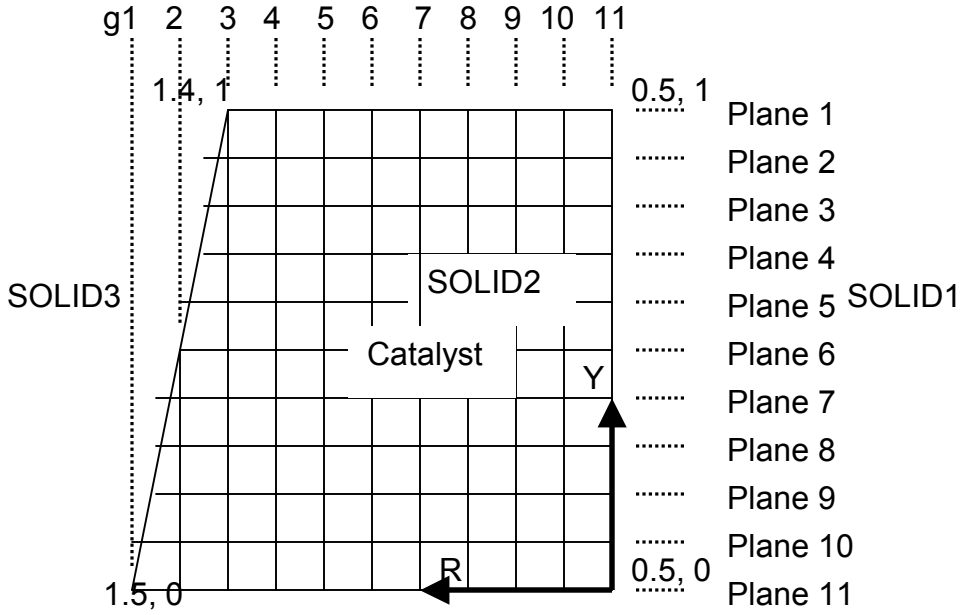

FIGURE 4-5: SOLID2 region divided in eleven horizontal and vertical planes for gm2 (reduced bed length with height of RFBR)

The SOLID2 dimensions are; inside diameter of 0.5 m, outside diameter of 1.0 m at the bottom and 0.9 m at the top, and height of 1.0 m. The distance between each plane is 0.05 m. Plane g1 represents the interface plane between SOLID2 and SOLID3. And plane g11 represents interface plane between SOLID 1 and SOLID2 in Figure 4-5. Plane 11 (p11) is at the bottom of SOLID1, SOLID2 and SOLID3. And plane 1 (p1) is at the top SOLID1, SOLID2 and SOLID3. The Table 4.2 represents the axial component of the velocity inside the catalyst bed.

Table 4-2: Axial velocity component for reduced bed length with height of RFBR (gm2)

Plane	g1	g2	g3	g4	g5	g6	g7	g8	g9	g10
p1-2	x	x	3.60	2.92	0.34	0.04	1.06	0.61	1.62	2.64
p2-3	x	4.45	4.45	3.26	2.87	2.20	2.10	2.52	2.25	3.18
p3-4	x	3.95	3.68	3.62	3.46	3.26	2.96	3.33	3.38	3.52
p4-5	x	3.54	3.56	3.51	3.58	3.56	3.60	3.62	4.00	4.32
p5-6	x	3.39	3.45	3.46	3.54	3.72	3.92	4.08	4.26	4.36
p6-7	2.84	2.94	3.02	3.13	3.28	3.65	3.70	4.10	4.46	4.46
p7-8	2.49	2.82	2.75	2.62	2.90	3.42	3.68	3.95	4.30	4.69
p8-9	2.29	2.20	1.95	2.19	2.13	3.17	3.22	3.33	4.21	4.93
p9-10	1.93	1.71	1.43	1.81	1.49	1.32	2.21	3.04	4.41	5.21
p10-11	1.17	0.00	0.00	0.04	1.19	-0.80	0.46	0.54	2.83	4.36

Note: 'x' represents locations not considered for study due to change in catalyst bed dimensions (no catalyst is available at these locations). All dimensions are in m/sec

The average radial velocity is 4.84 m/sec while the average axial velocity is 2.99 m/sec. There is no major change in the radial velocity but the axial velocity reduced from 3.78 m/sec to 2.99 m/sec as compared to the velocity profile of gm1. The range of radial velocity is on average is between 6 and 3 m/sec, while the axial velocity, is in the range of 1 to 3 m/sec.

The numerical solution observed has a similar solution as observed in CFX^{TM} simulation. The average axial velocity observed is 2.90 m/sec while the average radial velocity observed is 4.87 m/sec. Here it can be observed that the radial velocity is same as for gm1. While average axial velocity has come down from 3.63 to 2.90 m/sec (axial velocity reduced by 20%). The chart of velocity profile is presented in the Figure 4-6. The vertical planes are indicated by g1, g2 …g10 and horizontal planes are indicated by p1, p2 …p10. The vertical plane g1

indicates the exit axial velocity at each plane from the catalyst bed. The exit velocity at plane p1-2 is 3.60m/sec and at plane p10-11 is 1.17 m/sec. Similarly the vertical plane g10 indicates inlet velocity to the catalyst bed at each horizontal plane. The inlet velocity at plane p1-2 is 2.60 m/sec and at the plane p10-11 is 4.36 m/sec. Similarly each vertical plane indicates the axial velocity component inside the catalyst bed with reference to horizontal planes. It can be inferred from the Figure 4-6 that the axial velocity component first increases and then decreases for plane g2 to g9. For vertical plane g1 axial velocity component continuously increases from 1.17 m/sec to 2.84 m/sec with height. For the vertical plane g10 the axial velocity component reduces from 5.21 m/sec to 2.64 m/sec with increase in height of the catalyst bed.

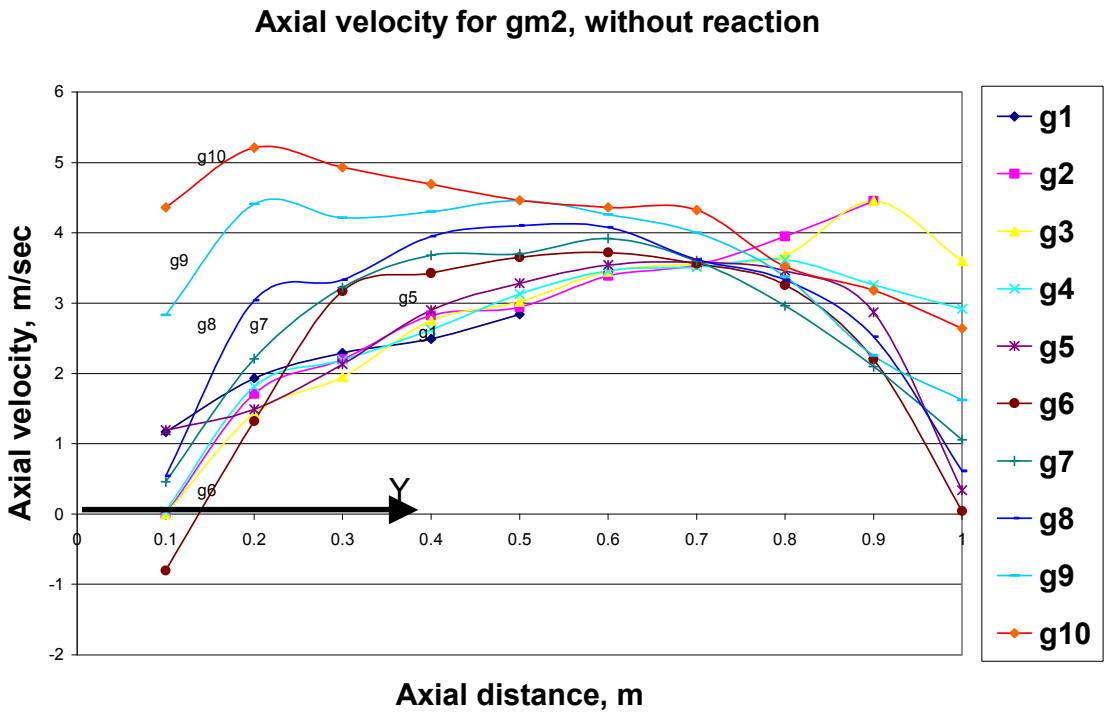

FIGURE 4-6: Axial velocity profile for gm2 from CFX simulation

4.1.3 Velocity profile for increased bed length with height of RFBR (gm3)

The CFX™ simulated velocity profile for increased bed length with height for RFBR is presented in Figure 4-7. The velocity profile shown inside the SOLID1 represents the velocity profiles in the inlet of the RFBR. The velocity at the inlet boundary can be observed to be 25 m/sec. The velocity slowly decreases with decrease in height of the RFBR. The velocity profile inside the catalyst bed is shown in SOLID2. The exact value of velocity with position is presented in Table 4-3, that was obtained through excel file generated in CFX™. From the profile shown in Figure 4-7, the velocity can be observed to be in the range of 0 to 12.0 m/sec inside the catalyst bed.

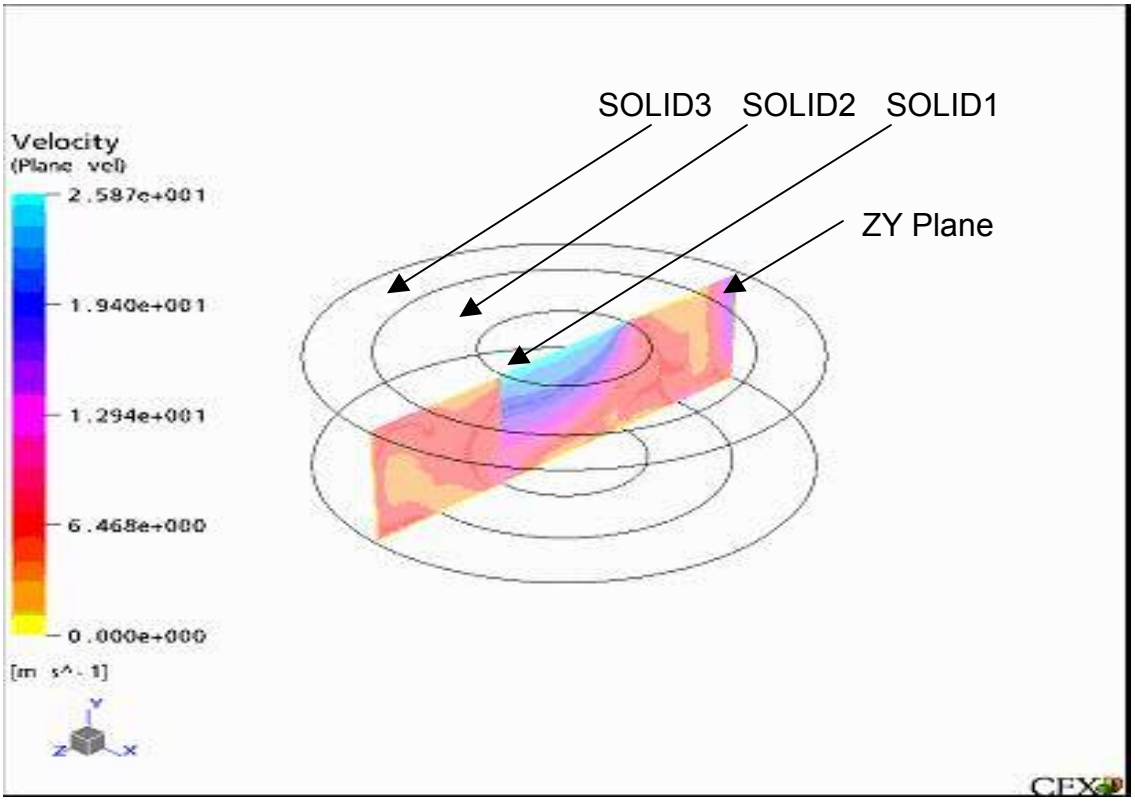

FIGURE4-7: CFX™ simulated velocity map of model reactor for increased bed length with height of RFBR, gm3

The fluid moves into the innermost cylinder (SOLID1) from the top (Figure 4-7). The SOLID2 represents the catalyst bed of the RFBR. SOLID3 represents outlet from the RFBR. For the study of velocity profile, SOLID2 (flow inside the catalyst bed) has been divided into eleven horizontal (plane p) and thirteen vertical planes (plane g). The planes have been shown in Figure 4-8.

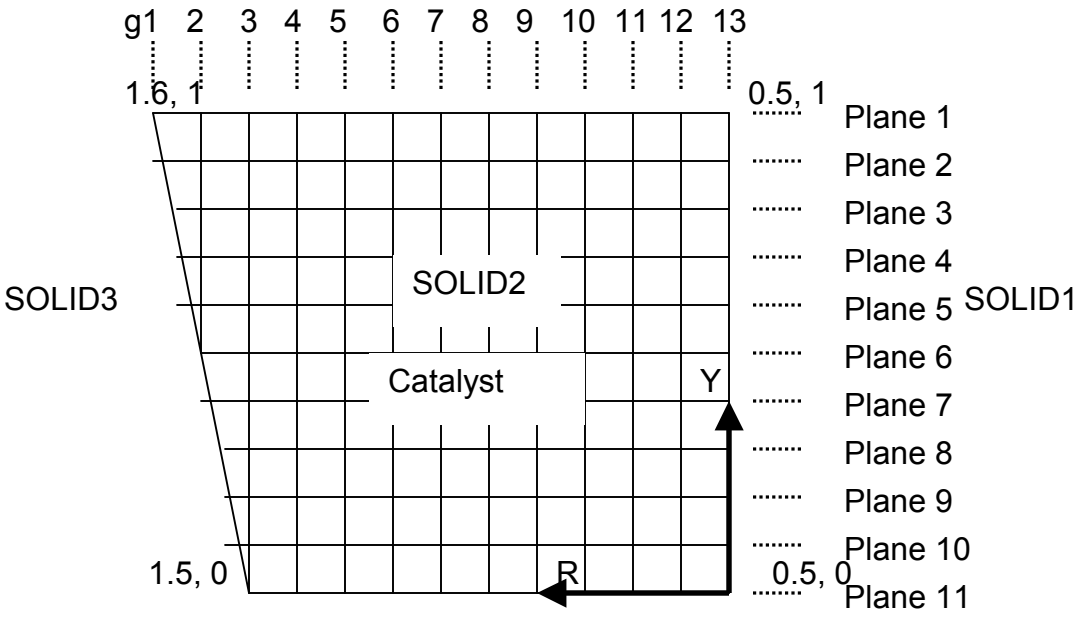

FIGURE 4-8: SOLID2 regions divided in eleven horizontal and thirteen vertical planes for gm3

SOLID2 dimensions are; inside diameter of 0.5 m, outside diameter of 1.0 m at the bottom and 1.1 m at the top, and height of 1.0 m. The distance between each plane (g1 to g2 and p1 to p2) is 0.05 m. Plane g1 represents the interface plane between SOLID2 and SOLID3. And plane g11 represents the interface plane between SOLID 1 and SOLID2 in Figure 4-7. Plane 11 (p11) is at the bottom of SOLID2. And plane 1 (p1) is at the top SOLID2.The Table 4.3 represents the axial component of the velocity inside the catalyst bed.

Table 4-3: Axial velocity component for increased bed length with height of RFBR (gm3)

	g1	g2	g3	g4	g5	g6	g7	g8	g9	g10	g11	g12
p1-2	6.60	2.64	-0.39	-0.32	-0.48	-0.21	-0.27	-0.37	-0.29	0.61	0.09	1.31
p2-3	3.22	3.43	1.41	0.91	1.42	0.86	0.92	0.92	1.29	1.31	1.90	2.90
p3-4	3.18	3.00	2.74	2.45	2.29	1.70	2.17	1.94	2.13	2.63	2.84	3.20
p4-5	2.91	2.85	2.74	2.56	2.50	2.44	2.60	2.80	3.12	3.10	3.74	3.86
p5-6	2.83	2.82	2.70	2.63	2.63	2.67	2.93	2.96	3.17	3.37	3.69	4.06
p6-7	x	2.75	2.60	2.46	2.54	2.63	2.82	3.18	3.62	3.78	4.27	4.25
p7-8	x	2.44	2.22	2.19	2.31	2.34	2.56	3.04	3.30	3.97	4.24	4.67
p8-9	x	2.03	2.03	2.10	1.96	1.95	2.13	2.32	2.83	3.47	4.11	4.81
p9-10	x	1.95	1.37	1.20	1.10	-0.23	1.14	1.74	2.45	3.55	4.79	5.47
p10-11	x	1.15	0.31	0.07	0.08	0.51	-0.33	-0.46	-0.55	-0.53	1.98	5.46

Note: 'x' represents locations not considered for study due to change in catalyst bed dimensions (no catalyst is available at these locations, see Figure 4-3). All dimensions are in m/sec.

The average radial and axial velocity was observed to be 4.52 and 2.27 m/sec respectively. The radial velocity came down by 6 % (as compared to that of Geometry1) while the axial velocity came down from 3.84 to 2.27 m/sec (an improvement of 40%). The 6% drop in radial velocity and 40% drop in axial velocity helps in reducing the pressure drop inside the bed. The variation in velocity profile also reduces as compared to that of Geometry1 and Geometry2 of RFBR. Also the velocity profile from plane 2 to plane 7 is almost uniform. The improvement may also be observed from Figure 4-9. The improvement in axial velocity as compared to that of Geometry2 is from 2.90 to 2.27 m/sec (an improvement of 21%).

The velocity profile is presented in the Figure 4-9. The vertical planes are indicated by g1, g2 …g12 and horizontal planes are indicated by p1, p2 …p10. The vertical plane g1 indicates the exit axial velocity at each horizontal plane (p1 to p11) from the catalyst bed. The exit velocity at plane p1-2 is 6.60 m/sec and at plane p10-11 is 1.15 m/sec. Similarly the vertical plane g12 indicates inlet velocity to the catalyst bed at each horizontal plane (p1 to p11). The inlet velocity at plane p1-2 is 1.31 m/sec and at the plane p10-11 is 5.46 m/sec. Similarly each vertical plane indicates the axial velocity component inside the catalyst bed with reference to horizontal planes. It can be inferred from the Figure 4-9 that the axial velocity component first increases and then decreases for plane g2 to g11. For vertical plane g1 axial velocity component continuously increases from 2.83 m/sec to 6.60 m/sec with height. This observation indicates that flow distribution is uniform for plane g2 to g11. At the inlet to the catalyst bed and at the outlet of catalyst bed the flow has wide variation in velocity. For vertical plane g12 the axial velocity component reduces from 5.36 m/sec to 1.31 m/sec with height. Such wide variations in velocity are not observed for planes g2 to g11.

The average radial and axial velocity is 4.86 and 2.90 m/sec respectively. Here there is no major change in radial velocity as compared with the simulated results of Geometry1. While axial velocity came down from 3.78 to 2.90 m/sec (axial velocity came down by 23%). Also the variation in velocity has come down. These observations in the catalyst bed for tapered geometry would help in maintaining better flow distribution as compared to that of g1and g2.

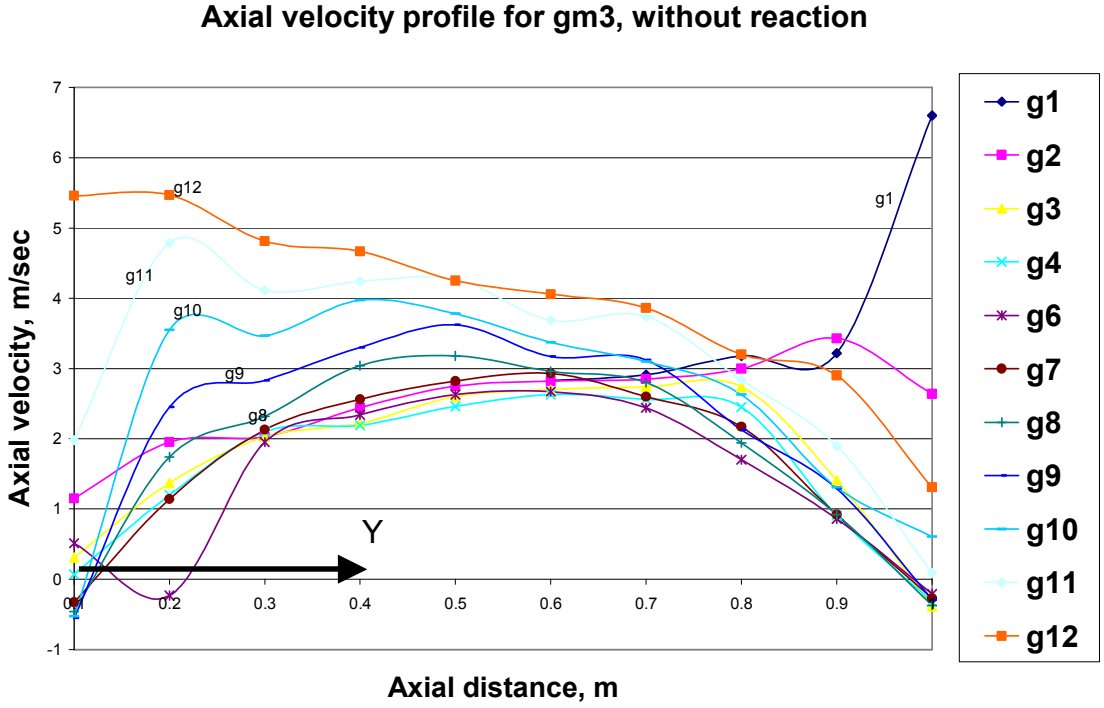

FIGURE 4-9: Axial velocity profile for increased bed length with height (gm3) without reaction

The axial velocity component is presented in Table 4-4. For plane g2 to g6 velocity first increases and then decreases with increase in height. The trend is similar to results obtained from simulation done in CFX^{TM} for gm1. For plane g1 the velocity reduces with increase in height while for g7 it reduces with height. Similar trend can be observed from simulation results for gm1.

Table 4-4: Axial velocity profile for gm1 from experiment done [2]

Plane	g1	g2	g3	g4	g5	g6	g7
p1-2	0.020	0.013	0.015	0.010	0.007	0.005	0.007
p2-3	0.009	0.010	0.009	0.008	0.010	0.018	0.022
p3-4	0.017	0.011	0.009	0.013	0.014	0.015	0.033
p4-5	0.022	0.022	0.033	0.025	0.033	0.040	0.033
p5-6	0.012	0.020	0.050	0.033	0.022	0.040	0.033
p6-7	0.036	0.022	0.050	-0.025	-0.067	-0.067	-0.067
p7-8	0.036	0.017	0.007	0.007	0.014	0.014	0.014

Note: All dimensions are in m/sec

The results are summarized below:

- Based on results of three geometries gm1, gm2 and gm3; the axial velocity value presented in Table: 4-1 through 4-3. The experimental value of axial velocity component is presented in Table 4-4.
- The results of this work indicate that axial velocity component decreased by 40% for gm3 and 20% for gm2 and this shows a better flow distribution for geometry gm3 as compared to that of gm1 and gm2.
- For the methanol synthesis reaction, both the average axial and radial velocity component reduces by same proportion depending on conversion amount. Results are presented in Appendix D, for gm1 in Table D-4, D-5, for gm2 in Table D-9, D-10 and for gm3 in Table D-13,D-14.
- The changes in the velocity component are not directly comparable because there are no experimental results available for the methanol synthesis reaction. The experimental value of the velocity component of gm1 is available for water as fluid. Therefore trend of the velocity can be compared not the numerical value. The trend of the velocity component for both the methanol synthesis component and water matches for gm1.
- gm1 represents the experimental geometry, therefore the velocity profile for gm1 compared with the experimental results.
- The changes in velocity component for no reaction compared with the experimental results from Bolton (2004). The distribution of velocity profile (for gm1) is similar for experimental and simulated results.

- The change in the velocity profile in between geometries gm1, gm2 and gm3, is mainly due to the change in geometry, this changes the least resistance path.
- The numerical solution for gm3 shows a marked decrease in axial velocity. The result observed to be same for conditions when reaction proceeds and when there is no reaction in the catalyst bed. The axial velocity decreased to 2.27 m/sec from 3.84 m/sec (decreased by 40%). While the radial velocity decreased only by 6%. This decrease in axial velocity component indicates that fluid flow reduces by 40% in axial direction. The FDP (flow distribution problem) to be minimum, ideally the axial velocity component should be zero [2].

The Chapter 4 presents the simulation results for geometry gm1, gm2 and gm3. The axial velocity component is presented in this chapter. The radial velocity component for three geometries with and without reaction is presented in Appendix D. The flow distribution profile is presented in different planes. The axial velocity component measures the flow distribution at various planes. The planes have been identified for flow distribution problem for gm1. The flow profile for tapered geometry compared with flow profile for gm1. The experimental flow profile for RFBR also compared with gm1. Finally a marked improvement of 40% observed for flow distribution for gm3.

CHAPTER 5

CONCLUSIONS AND RECOMMENDATIONS

5.1 An outline of the contributions of this work

This work has made four important contributions.

First, this work has documented the mechanism for flow distribution problems in a RFBR (radial fixed bed reactor) and reasons considered why despite the other variables (catalyst size, void fraction, reaction condition) available to manipulate flow distribution in a RFBR, the bed length of catalyst is the most important variable. This work has used CFX^{TM} to simulate the velocity profiles. The velocity profiles were evaluated using CFD and numerical methods.

Second, this work has proposed a new approach for designing a RFBR model suitable for solving flow distribution problem (FDP). This approach compares the flow distribution profiles by varying different variables and proposes the tapered geometry RFBR for reducing flow distribution problem.

Third, this work has proposed a method for simulation of velocity profiles for designing the best RFBR for minimum FDP. This method specifies how to model the velocity profiles in different region of the RFBR. The models selected in this work to simulate velocity profiles are the k-ε (k epsilon) for flow near the wall and the Darcy model for flow inside the catalyst bed.

Fourth, this work has included a comprehensive example of an application of the proposed methodology. This work has used a methanol synthesis reaction to model the flow distribution. This example has also included evaluation of suitable model designs. Using the demonstration of flow distribution with different geometry it will be easier to implement the proposed model in the industry.

5.2 Advantages and disadvantages of the proposed model

Modeling flow distribution is a very difficult problem because the flow inside the RFBR passes through different flow regions. In addition, it is difficult to find a good model for simulating for flow in varying Reynolds number ranges. Hence, the suitability of different models for simulating flow profiles is often unknown a priori. This work has proposed an efficient model for simulating flow profiles and evaluating flow profiles for the RFBR. Although other such models for simulation of flow profiles are available in CFX^{TM}, the model selected in this work is a compromise between accuracy and time taken for simulation. The approach of modeling flow distribution in this work is the first attempt to minimize flow distribution in a RFBR. This approach allows:

- Potential use of a mathematical model whose application to model flow distribution has been discussed in the literature to date.
- Making the problem of modeling flow distribution by representing different regions of the RFBR as a separate model component.
- Searching through large libraries of very diverse mathematical models, which is extremely important in this case when the selection of the modeled regions is hard to determine a priori.

Even for the cases when the applicable model design is approximately known, the proposed method can be used for refining the design further. Although this proposed approach for model selection is so universal, its practical application may seem difficult because of the requirement of different models for different regions and for flow in a range of Reynolds number. However, creation of libraries of models is a straight forward task as long as modeling of flow profiles in different flow regions is concerned.

This work is also the first to propose to minimize the flow distribution in a RFBR. Unlike conventional approaches for modeling flow distribution, the approach in this work assumes realistic conditions for different regions in the RFBR. This new approach also has clear advantage over other methods for estimating flow distribution in the RFBR.

One issue that remains unresolved in this study and is recommended as the first step in future studies is the inclusion of experimental results for reactions. There is no experimental result available for any reaction in the RFBR. The reason for the inclusion of reaction is that the simulated results of CFX^{TM} needs experimental results to validate the claim. The current issue of FDP (flow distribution problem) was studied for three different geometries. The FDP and simulated results are discussed in the following sections.

This work focused on geometry of RFBR. There are no experimental results available for validating the results of CFX^{TM} simulation. Therefore further experiments need to be conducted to verify the advantage of using a tapered geometry RFBR.

It is recommended that the present approach of finding the velocity should using CFD technique be used as an alternative to actual experiments conducted for similar geometry and fluid. The experimental results would help in validating the results of CFX^{TM} simulation. The model in the present work then can be used for scale up and improvement in flow distribution by changing the geometry. The bed geometry can be made more suitable to reduce the flow distribution by changing the slope or bed dimension.

The methods of quantifying velocity profile using CFD presented in this paper can all be useful in modeling radial fixed bed reactor. Calculation of velocity profiles was particularly useful for this work since the decrease in axial velocity component directly affects the performance of reactor. The velocity profiles information should be used with correlated data from previous work for uniform bed (gm1) reactor. Velocity profiles for reaction is particularly useful for visualization of region with good mixing but should not be relied upon as a stand alone test. The final configuration of geometry (gm3) is most promising, even though this geometry may have problem while filling the catalyst in reactor bed. This geometry (gm3) will work well for systems where flow path has been kept as modeled for the simulation. Flow distribution problem is the single most important parameter for optimum operation of RFBR [10]. Therefore an improvement in flow distribution in RFBR promises to improve the performance of RFBR. Use of RFBR saves the operation cost by 30% (Table 1-1). An improvement in flow distribution will certainly lead to further reduction in operating cost. There is

further scope of study for quantifying the advantages of using RFBR of increased bed length with height (or gm3).

5.3 Future work

In addition to validating the simulation results, there are at least three directions for future work that will improve the method for designing optimal RFBR for minimizing flow distribution problem. The first direction is automation of proposed method for flow distribution modeling for different geometries. In this work first geometries were created and then flow profile was simulated. In automation, a suitable geometry may be designed for a flow distribution. The second direction is extending this approach to cases where no experimental results are available. This would require testing the models for that experimental result are available and then improving it for scale up. The third direction is the inclusion of the calculation for cost saving for improving flow distribution in a RFBR.

Other questions posed to the next researcher are:

1. Is it possible to automatically find a value of the velocity for the percentage change in slope of bed geometry?
2. How does one identify rules which will guide in choosing bed geometry for scale up?
3. How can successful rules from simulation be validated without performing experiments?

In conclusion the present study puts forward a new methodology namely introduction of tapered geometry for reducing flow distribution problem. CFX^{TM}

proves to be a versatile technology for use in finding the velocity components and lays foundation for further research in this field.

5.4 The impact of this work

Advances in computer hardware allow creation of very large mathematical models with a great number of parameters, massively parallel processing and great deal of stability in numerical solution. These models can often imitate very complex phenomena. The flow pattern in the regions is very complex and this work presents the guide lines to model such a phenomena. However, in many cases, simpler models have a clear advantage over the complex ones. This is the case when:

- The type of reaction has very simple kinetics and all the parameters are available from literature.
- A similar model is available from literature.
- The model has to operate in real time using a limited amount of computing resources.

All these three conditions apply to the models designated to model flow distribution in different regions of the RFBR. To perform the task of identifying faults in modeling, the flow profile was compared with the experimental results available from Bolton, G. T.

5.5 Applications

The current work can be utilized in various fields and can be directly applied to the following:

1. Detecting relation between velocity profile and bed geometry.
2. Provide a linguistic guidance and training framework for design engineers.
3. Autonomous development of decision rule base for slope of bed geometry.
4. Model monitoring by finding cause and effect relations in flow distribution problem and bed geometry.
5. Finding input-output rules which define which define bed geometry design and tuning from results of CFX™ simulation.
6. For level of protection analysis and safety system design for uncertain flow distribution.

The current work coupled with fast simulation technologies such as CFX™ will prove effective for above areas where solution is required in short period of time.

BIBLIOGRAPHY

(In order of appearance)

1. Bolton, G.T., Hooper, C. W., Mann. R., *Flow distribution measurement in a radial flow fixed bed reactor using electrical resistance tomography, http://www.itoms.com/pdfs/ISCRE17.pdf, Jan 21,2005.*

2. Bolton, G.T., Hooper, C.W., Mann, R., Stitt, E.H., *Flow distribution and velocity measurement in a radial flow fixed bed reactor using electrical resistance tomography.* Chemical Engineering Science, 2004. **v59** (n 10): p. 1989-1997.

3. Rase, H.F., *Fixed Bed Reactor Design and Diagnostics*. 1990, Stonehamm MA, Butterworths Publishers.

4. Bird, R.B., Warren, E. S., Edwin, N. L., *Transport Phenomena*. Second Ed. 2002, Singapore: John Wiley & Sons.

5. Anysys, *CFX solver model, CFX 5.7, Printbook (help),* 2004, Anysys Canada Ltd.

6. Klingman, K.J., Lee, H., *Model for catalytic reactions in packed beds based on alternating flow model.* Chemical Engineering Science, 1988. **v 43** (n 8): p. 1795-1800.

7. Kartraice, D.H., *Cost of energy, http://www.newton.dep.anl.gov/newton/askasci/1995/eng/ENGM27.HTM, Jan 16, 2005*..

8. Dow, C., *Production capacity, http://www.the-innovation-group.com/ChemProfiles/Ethylene%20Oxide.htm, Jan 16, 2005*. 2005.

9. Haldor, T., *Production capacity, http://www.haldortopsoe.com/site.nsf/all/CHAP-6CHJCD?OpenDocument, Jan 16, 2005*.

10. Heggs, P.J., Ellis, D.I., *The modeling of fluid flow distribution in annular packed beds, gas separation and purification*. 1994.

11. Zhou. L., G., S., Imbihl. R., *Low pressure methanol oxidation over a Cu(110) surface under stationary conditions: (I) reaction kinetics.* Journal of Catalysis, 2005. **v230** (n 12): p. 166-172.

12. NIST, *NIST chemistry web book,http://webbook.nist.gov/chemistry/fluid/, Jan 17, 2005*.

13. Sungwon, H., Robin, Smith., *Heterogeneous catalytic reactor design with optimum temperature profile.* Chemical Engineering Science, 2004. **v59**: p. 4229-4243.

14. Rajesh, G., Bhagat, B.R., *Reactive flow in porous media.* Journal of Applied Mechanics, 2000. **v67** (n 4): p. 749-757.

15. Mann, R.S., Djamarani, K., *Experimental fixed-bed reactor dynamics for SO_2 oxidation.* Chemical Engineering Research & Design, 1986. **v10** (n9): p. 445-454.

16. Segall, N.L., MacGregor, J. F., Wright, J. D. *Accounting for radial gradients in the modelling of packed bed tubular reactors*. 1983: McMaster Univ, Dep of Chemical Engineering, Hamilton, Ont, Canada.

17. Nauman, E.B., *Chemical Reactor Design*. 1987, Troy, New York: John Wiley & Sons.

18. Specchia, V., Baldi, G., Sicardi, S., *Heat transfer in packed bed reactors with one phase flow.* Chemical Engineering Communications, 1980. **v4** (n2-3): p 361-380.

19. Treybal, R.E., *Mass Transfer Operations*. Third Ed. 1981, Singapore: McGraw-Hill.

20. Himmelblau, D.M., *Basic Principles and Calculations in Chemical Engineering*. 1996, Upper Saddle River, NJ, Prentice Hall International Series.

21. Genkin, V.S., Gribanov, A.V., Mamontov, G.V., *Prospective designs of radial reactors.* Chemical and Petroleum Engineering, 1989. **v25** (n1-2): p. 9-10.

22. Gunn, D.J., *Axial and radial dispersion in fixed beds.* Chemical Engineering Science, 1987. **v42** (n2): p. 363-373.

23. Gunn, D.J., Ahmad,M. M., *Radial heat transfer to fixed beds of particles.* Chemical Engineering Science, 1987. **v42** (n9).

24. Vortmeyer, D., Schuster, J., *Evaluation of steady flow profiles in rectangular and circular packed beds by a variational method.* Chemical Engineering Science, 1983. **v38** (n10): p. 1691-1699.

25. Pinto; Alwyn (Stockton-on-Tees, G., *Energy process in methanol synthesis*, in *http://www.freepatentsonline.com/4309359.html, Jan 23,*

2005, U.S. Patent, Editor. 1982, Imperial Chemical Industries Limited (London, GB2): UK.

26. Wade, R.E., *Fixed bed reactor modeling and kinetics evaluation*, MS Thesis in *Chemical Engineering*. 1999, Oklahoma State University: Stillwater.

27. Hicks, R.E., *Pressure drop in packed bed of spheres*, ed. I.a.E.C. Fundamentals. **v9**. 1970. 55-502.

28. Hicks, R.E., *The effect of viscous forces on heat and mass transfer in system with turbulence promoters and in packed beds.* Chemical Engineering Science, 1968. **v23**: p. 1201-1210.

29. Froment, G.F., Bischoff, K. B., *Chemical Reactor Analysis and Design*. 1979: John Wiley & Sons.

30. Hill, N., *Fixed bed catalytic reactors, http://jbrwww.che.wisc.edu/~jbraw/chemreacfun/ch7/slides-masswrxn.pdf, Jan 23, 2004*. Nob Hill Publishing.

31. Himmelblau, D.M., Bischoff, K. B., *Process analysis and simulation: deterministic systems*. 1968: John Wiley & Sons.

32. Octave, L., *Chemical Reaction Engineering*. Third Ed. 1999, New York: John Wiley and Sons.

33. Fogler, S.H., *Elements of Chemical Reaction Engineering*. 1992, Upper Saddle River, NJ: Prentice-Hall Inc.

34. Perry, R.H., *Perry's Chemical Engineers Handbook*. Sixth Ed. 1984, NewYork: McGraw-Hill Book Company.

35. Pinto; Alwyn, G., *Energy process in methanol synthesis*, in *http://www.freepatentsonline.com/4309359.html*, U. Patent, Editor. 1982, Imperial Chemical Industries Limited (London, GB2): UK.

36. Ashish, V.P., *A radial microfluidic processor, http://www.lehigh.edu/~asp2/docs/Pattekar-Kothare-JPS.pdf, Mar 16, 2005.*, in *Power Sources*, Elsevier.

37. Andrade, J.S., Costa, M. S., *Inertial effects on fluid flow through disordered porous media, http://polymer.bu.edu/hes/articles/acams99.pdf, Jan 17, 2005*. 1999.

38. Jorge, L.M., Jorge R. M., *Evaluation of heat transfer in a catalytic fixed bed reactor at high temperatures.* Brazilian Journal of Chemical Engineering, 1999. **v 16** (n4): p. 407-420.

39. Das, K.S., Mohan, R., *Numerical study of the influence of horizontal tube banks on the hydrodynamics of a dense gas-solid bubbling fluidized bed.* International Journal of Chemical Reactor Engineering, 2003. **v1** (A26): p. 1-12.

40. www.casale.ch/ammonia, Jan 21, 2005.

APPENDIX A

CFX™ SIMULATION DETAILS

This guide line shows geometry creation and meshing for a radial fixed bed reactor (Geometry1, gm1). Geometry1 (gm1) consists of three solids as described below

- Solid1 – represents inner part of reactor where fluid moves in and is free of catalyst.
- Solid2 – represents that part of reactor where bed is filled with catalyst bed.
- Solid3 – represent the region where fluid moves out of the bed and is free of catalyst.

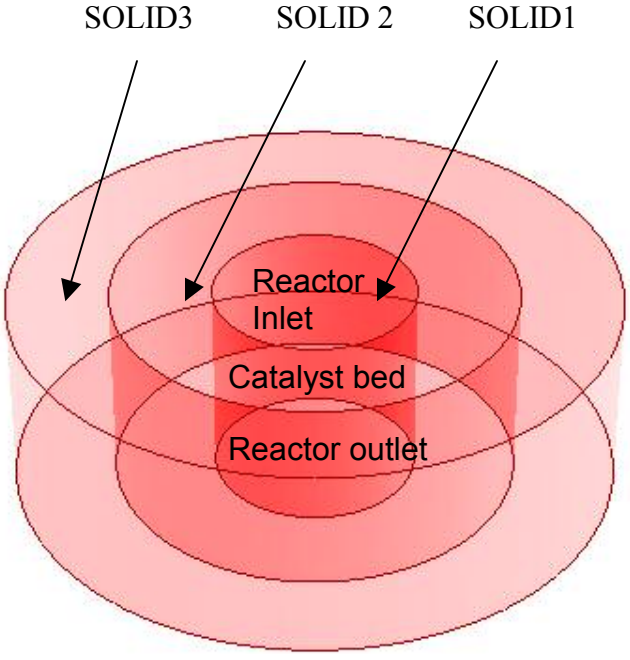

FIGURE A-1: Uniform bed RFBR, gm1

Solid1 is first created with mesh in ANYSYS 8.1™. And then Solid2 and Solid3 are created with mesh. The procedure is described below.

The following geometry and meshing features are used

- Basic geometry creation using Revolve operation; and
- Basic meshing operations

CFX™ mesh

In order to create a mesh using CFX™-Mesh, the steps are as follows.

- Create the Geometry.
- Define Regions.
- Define the Mesh Attributes.
- Create the Surface Mesh (this is optional).
- Create the Volume Mesh.

The geometry can be created either in ANSYS Workbench or by importing it from a CAD package. The geometry for this work has been created in ANSYS Workbench 8.1. The guidelines below will refer to ANSYS Workbench 8.1 only.

Creating the project

The first step for any new case is to create the project.

- Open ANSYS Workbench. On Windows, this can be done by going to the Start Menu>Programs section and selecting ANSYS 8.1>ANSYS Workbench.
- Start a new project from scratch by selecting Empty Project from the new section of the Start window in the middle of the ANSYS Workbench window.

- The next setting is to tell ANSYS Workbench where the project files has to be created. Select File>Save, and save the project as solid1gm1.wbdb in the working directory of CFX™. Then Design Modeler can be opened in order to start creating the solid.
- At the left side of the Project Page, click on Design Modeler (DM), new geometry (under Create Design Modeler Geometry).
- In the popup window, select meter as the desired length unit.

Creating the Solid1

- Click on XY plane in the tree view towards the top left of the screen.
- Click on the sketching tab (underneath the tree view) to work on the sketch.
- Before starting to create your sketch, it helps to set up a grid of lines on the plane in which the sketch will be drawn. The presence of the grid allows the precise positioning of points (when snap is enabled).
- Click on settings (in the sketching tab) to open the settings toolbox.
- Click on grid and turn on show in 2D and snap.
- Click on major grid spacing and set it to 1.
- Click on minor-steps per major and set it to 10.
- Select the draw toolbox from the sketching tab.
- Click on polyline and then create the shape shown below:

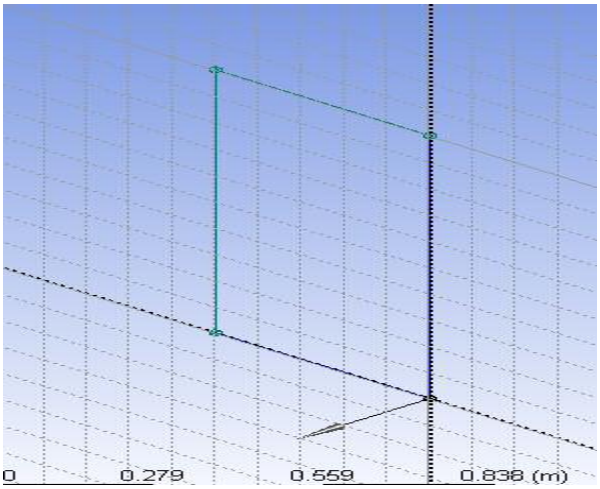

FIGURE A-2: Solid1gm1, sketch1

- To close the polyline after selecting the last point, click with the right mouse button to bring up a menu and choose closed end.

Now the main body of the geometry1 solid1 will be created by revolving the new sketch around the Y-axis.

- Select revolve from the 3D features toolbar. This toolbar is located above the model view.
- Details of the revolve operation are shown in the details view at the bottom left of the window. Leave the name of the revolve as the default, revolve1.
- The base object is the name of the sketch to be revolved. It defaults to the sketch that has been just created, sketch1, so this setting does not need to be changed.
- The axis for the rotation does not have a default setting. in the model view, click on the grid line which runs along the Y-axis and then click on apply in the details view. The text next to axis should now change to

selected. If instead it changes to not selected with a yellow background, click on the text not selected and then try selecting the axis again in the model view, remembering to press apply in the details view after it has been selected.

- Leave Operation set to add material.
- The sketch needs to be revolved by a full 360 degrees, so change angle from 30 degrees to 360 degrees. Leave the other settings as default.
- To activate the revolve operation; click on generate. This can be selected from the menu.
- After generation, the solid should look like as shown below. Save it as solid1gm1.agdb.

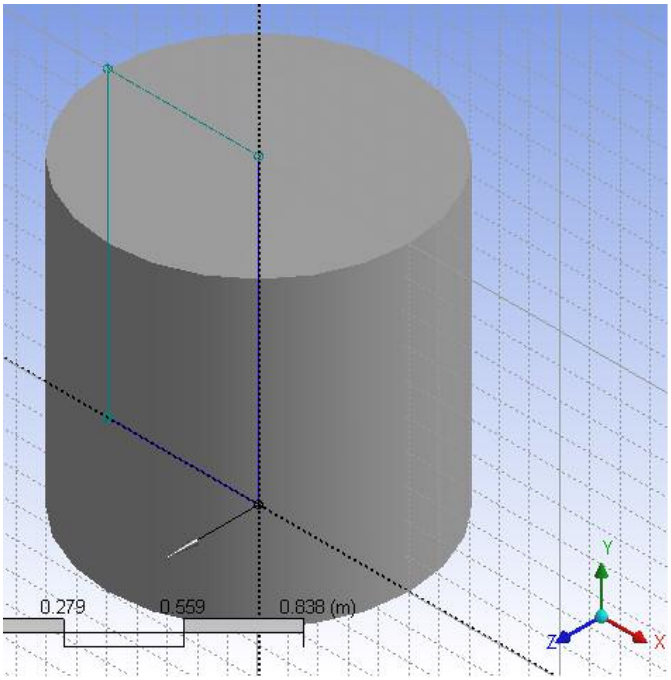

FIGURE A-3: Solid1gm1

Mesh generation

In order to set up the mesh, move out of Design Modeler and into CFX™-Mesh.

At the top of the ANSYS Workbench window, there are two tabs: geometry1 (Project) and geometry1 (Design Modeler). Click on solid1gm1 (project) to return to the project page. In the left-hand column, near the top, click on generate CFX™ mesh.

Setting up the regions

The first step is to define some regions on the geometry. Composite 2D regions are created from the solid faces (primitive 2D Regions) of the geometry. They can be used in CFX™-Pre to assign boundary conditions, such as inlets and outlets, to the problem. Regions are also used to attach two different solids through interface.

Create the Composite 2D Region for the reactor inlet:

- Right-click over regions in the tree view.
- Select insert>composite 2d region
- A new object, composite 2d region 1, is inserted under regions in the tree view. In the details view, there will be two buttons, apply and cancel, next to location, and this means that you are ready to select the face from the model view.

- In the model view, click on the circular face at the top of the solid which is at the position with the highest value of the Y-coordinate. This will turn green to show that it has been selected.
- Click on apply in the details view.
- Change the name of the region to inlets1gm1: right-click over the name, select rename and then type over the existing name.

Similarly create outlet from Geometry1. Rename it outlets1gm1.

Setting up the mesh

- Click on default body spacing in the tree view, which is contained in mesh>spacing.
- In the details view, change maximum spacing to 0.05 m.
- Press enter on the keyboard to set this value.

The remaining settings will be left as their default.

Generating the surface mesh

- Click on the plus sign next to preview in the tree view to open it up.
- Right-click over default preview group and select generate this surface mesh. The default preview group always contains all faces in the geometry, so the mesh will be generated everywhere.
- Similarly generate volume mesh by right clicking on mesh in tree view.
- Save all the highlighted files and exit out of Anysys.8.1™.
- Mesh file will be unnamed in working directory. Rename it to meshs1gm1.gtm.
- The generated surface mesh will look like as shown in figure below.

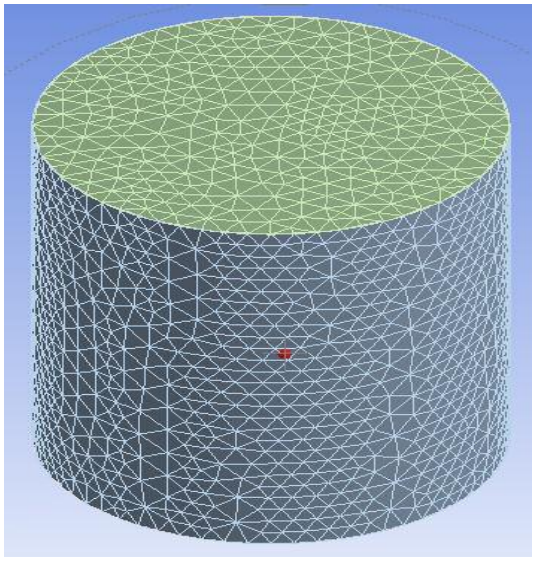

FIGURE A-4: Solid1gm1 surface mesh

Similarly create two more solids and generate its mesh. The details of geometry are described in Chapter 3. Caution should be taken while naming default 2D region while mesh creation. For solid2 the face touching solid1 will be named as inlets2gm1 and face touching solid3 will be named as outlets2gm1. Similarly for solid3 the face touching with solid2 will be named as inlets3gm1 and outlet to top of solid will be named as outlets3gm1.

Finally geometry1 with inlet and outlet will be represented as shown in following section.

After creating all the three solids for geometry1 ANYSYS 8.1^{TM} is closed and CFX^{TM}5.7 for windows is opened. Set the working directory as CFX^{TM}/working directory and click CFX^{TM}-Pre.

Defining the new simulation in CFX^{TM}-Pre

This section describes the step-by-step definition of the flow physics in CFX^{TM}-Pre.

Creating a new simulation

Start CFX™-Pre and create a new simulation named geometry1 using the General Mode.

Importing the meshes

The geometry1 is comprised of three distinct parts:

- Solid1 – Inlet section of reactor
- Solid2 – Reaction section (Filled with catalyst pellets)
- Solid3 – Outlet section of reactor

Next you will import a generic inlet / outlet section and the catalyst housing section from already generated files in ANYSYS ™ 8.1.

Inlet section – Solid1

The first mesh that will be imported is the Solid1gm1 mesh for the reactor inlet, created in ANYSYS™8.1, named as Solid1gm1.gtm. This mesh was created using units of meter.

- Click the mesh tab to access the mesh workspace.
- Click import mesh
- In the mesh workspace, on the definition panel, set:
    - Mesh format to CFX™5 GTM file
    - File to Solid1gm1.gtm
- Click apply to import the mesh while leaving the import mesh panel open.

Similarly import mesh for Solid2gm1 and Solid3gm1.

Caution: After importing the last mesh (Solid3gm1) do not click apply button. Just click OK. Otherwise the same mesh will be imported twice.

After importing all the three solids for geometry1 the mesh will appear like as shown in next page.

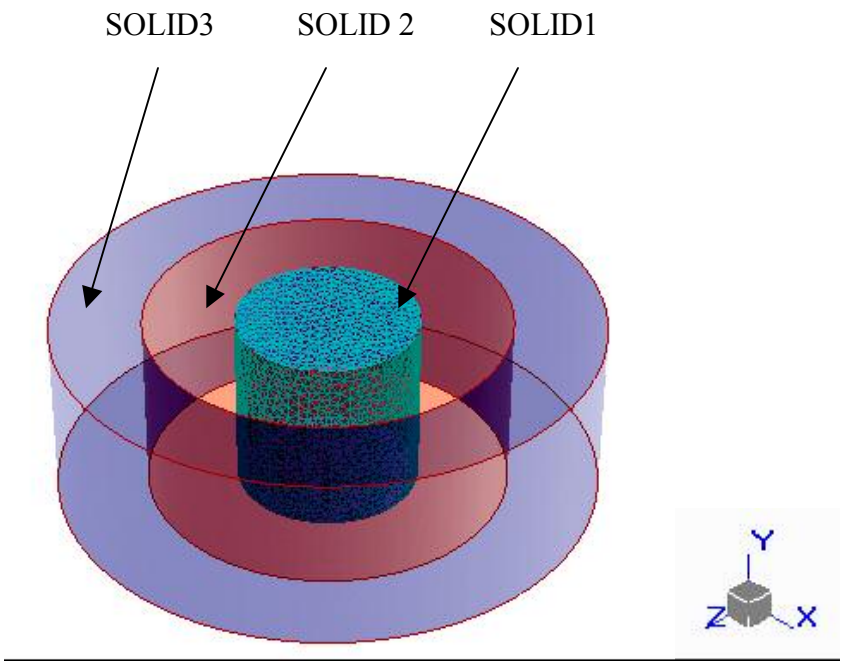

FIGURE A-5: Imported mesh of solids in CFX-Pre

Creating a union region

Three separate assemblies now exist, but since there is no relative motion between each assembly it is needed to create a single domain. This can be done by simply using all three assemblies in the domain location list or, as in this case, by using the region editor to create a union of the three assemblies.

- Click the regions tab in the CFX™-Pre workspace.
- Click create new object.
- Set name to RadReactor1.
- Set combination to union.
- Set dimension to 3D; this will show the existing 3D regions in the regions list.

- Hold down the <Ctrl> key and select the regions assembly, assembly 2 and assembly 3.
- Click ok to create the new region.

Creating the Domain

For this simulation an isothermal heat transfer model has been used and turbulent flow has been assumed.

- Click the physics tab.
- Click domain on the main toolbar.
- Set name to RadReact1 and then click OK.
- On the general options panel:
    - Set location to RadReactor1.
    - Set domain type to fluid domain.
    - Set Fluids List to air ideal gas (for simplicity).or CO and H_2 for this work.
    - Set cord frame to cord 0.
    - Set reference pressure to 1 atm.
    - Under buoyancy, set option to non buoyant.
    - Under domain motion, set option to stationary.
- Click the fluid models tab, then:
    - Under heat transfer model, set option to isothermal and fluid temperature to 518.15 K.
    - Under turbulence model, set option to k-epsilon.
    - Leave turbulent wall functions set to scalable.

- Under reaction or combustion model and thermal radiation model, leave option set to none.
- Click OK to create the domain.

Creating the Subdomain

The catalyst-coated honeycomb structure will be modeled using a subdomain with a directional source of resistance.

For quadratic resistances, the pressure drop is modeled using:

$$\frac{\partial p}{\partial x_i} = -K_Q \mid U \mid U_i$$

Where K_Q is the quadratic resistance coefficient, U_i is the local velocity in the i direction, and $\frac{\partial p}{\partial x_i}$ is the pressure drop gradient in the i direction.

- Click subdomain from the main toolbar.
- Set name to catalyst, leave domain set to RadReact1 and then click OK.
- On the basic settings panel, expand the regions list by clicking, and set location to B1 P3 2 (assembly2). This is the entire catalyst housing section.
- Click the sources tab. The Sources panel lets to setup sources of momentum, resistance and mass for the subdomain (other sources are available for different problem physics).
- On the Sources panel:
  - Turn on sources, momentum source/porous loss, and directional loss model.

- Under stream wise direction, set: option to Cartesian components X component to 1, Y component to 1, and Z component to 1 (for loss in any direction).
- Under stream wise loss, set option to linear and quadratic coefficients.
- Turn on quadratic coefficient and then set quadratic coefficient to 650 kg m^-4 (The figure depends on bed structure. For this work this figure has been taken from similar model used in CFXTM for an example on catalytic converter).
- Click OK to create the subdomain.

Creating boundary conditions

Inlet boundary condition

On the Basic Settings panel, set:

- Boundary type to inlet
- Location to Inlets1gm1

On the boundary details panel:

- Under mass and momentum, set option to normal speed and normal speed to 25 m s^-1.
- Leave turbulence set to medium (intensity = 5%).
- Click OK to create the boundary condition

Outlet boundary condition

- Create an outlet boundary named outlet.

- On the Basic Settings panel, set:
    - Boundary type to outlet
    - Location to outlets3gm1
- On the Boundary Details panel:
    - Under mass and momentum, set option to static pressure (not average static pressure) and relative pressure to 0 Pa
- Click OK to create the boundary condition.
- The remaining surfaces are automatically grouped into the default no slip wall boundary condition.

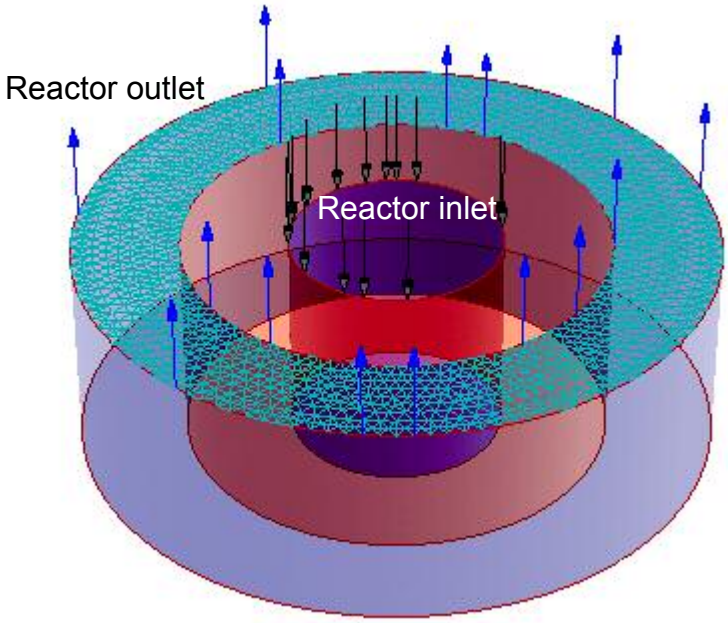

FIGURE A-6: Geometry1 (gm1) with inlet and outlet flow

Creating the domain interfaces

Domain interfaces are used to define the connecting boundaries between meshes where the faces do not match or when a frame change occurs. Meshes are ‘glued’ together using the General Grid Interface (GGI) functionality of CFX^{TM}-5. Different types of GGI connections can be made. In this case you require a simple Fluid-Fluid Static connection (no Frame Change). Other options allow changing reference frame across the interface or creating a periodic boundary with dissimilar meshes on each periodic face.

Two Interfaces are required, one to connect the inlet to the catalyst housing and one to connect the outlet to the catalyst housing.

Inlet to catalyst housing Interface

- Click Domain Interface.
- Set Name to Inlet Side.
- On the basic settings panel, set:
    - Interface Type to Fluid Fluid
    - Under Side 1, set Domain (Filter) to -- All Domains.
    - Region List 1 to outlets1gm1
    - Under Side 2, set Domain (Filter) to -- All Domains --.
    - Region List 2 to inlets2gm1
    - Frame change to none
    - Pitch change to automatic
- Click OK to create the interface.

Outlet of catalyst housing interface

- Create a second domain interface named Outlet Side.
- On the Basic Settings panel, set:
    - Interface type to fluid fluid
    - Under side 1, set domain (filter) to -- all domains --.
    - Region List 1 to outlets2gm1
    - Under side 2, set domain (filter) to -- all domains --.
    - Region list 2 to inlets3gm1
    - Frame change to none
    - Pitch change to automatic
    - Click OK to create the interface.

Setting initial values

- Click global initialization

A sensible guess for the initial velocity is to set it to the expected velocity through the catalyst housing. As the inlet velocity is 25 (m s^-1) and the cross sectional area of the inlet and housing are known, conservation of mass can be applied to obtain an approximate velocity of 2 (m s^-1) through the housing.

- Under Cartesian velocity components, set:
- Option to automatic with value
    - U to 2 m s^-1
    - V to 2 m s^-1
    - W to 2 m s^-1

- Turn on turbulence eddy dissipation and leave option set to automatic
- Click OK to set the initialization details.

Setting solver control

- Click solver control
- Assuming velocities of 25 (m s^-1) in the inlet and outlet pipes, and 2 (m s^-1) in the catalyst housing, an approximate fluid residence time of 0.1 (s) can be calculated. A sensible time step of 0.04 (s) (1/4 to 1/2 of the fluid residence time) will be applied.
- Under advection scheme, leave option set to high resolution.
- Under convergence control, set timescale control to physical timescale and physical timescale to 0.04 s.
- Leave all other settings at their default values.
- For the convergence criteria, an RMS value of at least 1e-05 is usually required for adequate convergence, but the default value is sufficient for demonstration purposes.
- Click OK to set the solver control parameters.

Writing the solver (.def) file

- Click write solver (.def) file
- Leave operation set to start solver manager.
- Turn on report summary of interface connections.
- Click OK.

Obtaining a solution

When CFX^{TM}-Pre has shut down and the CFX^{TM}-solver manager has started, you can obtain a solution to the CFD problem by following the instructions below:

In the solver manager, at the time of defining run, check the box ‘show advance controls’, then in solver tab tick ‘detailed memory overrides’ and enter a memory multiplier of 1.5. Repeat the same exercise on partition tab also.

If above exercise not done then run may fail with error message ‘insufficient memory allocated’.

- Click start run
- When finished click OK
- Click post process results
- When the start CFX^{TM}-post dialog box appears, turn on shut down solver manager then click OK.

Viewing the results

When CFX^{TM}-Post opens, create a YZ plane through X = 0 and color the plane by pressure. The pressure falls steadily throughout the main body of the catalytic housing.

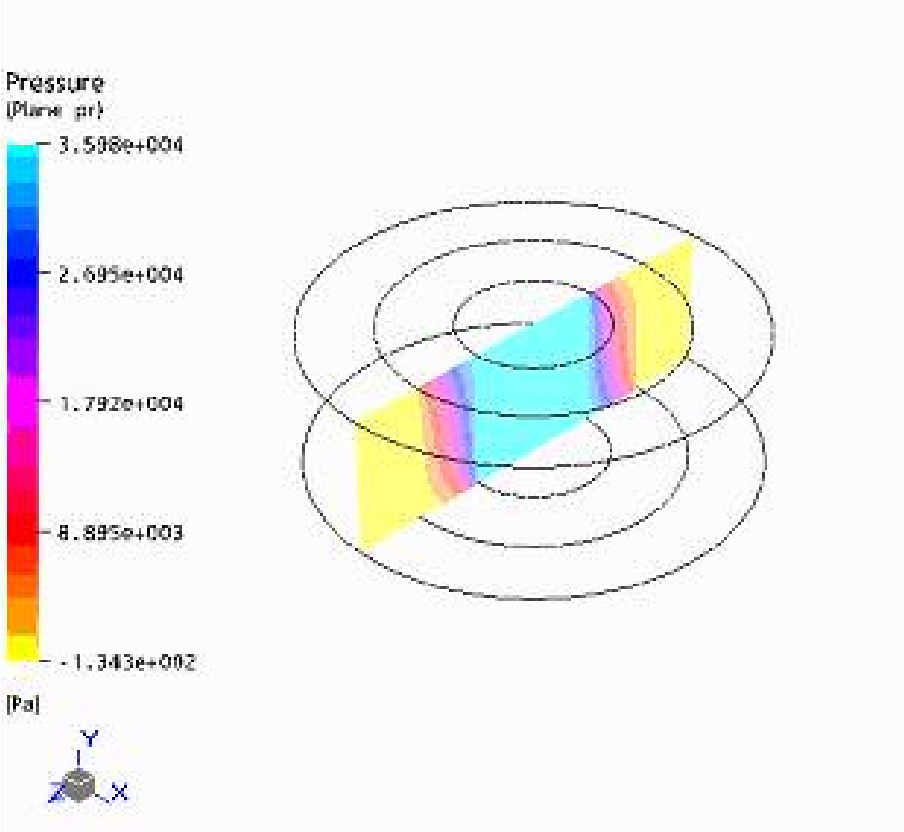

FIGURE A-7: Pressure profile in ZY plane at X=0 for gm1

- Make the YZ plane invisible.
- Create a contour plot, using the plane for the location, pressure as the variable and 30 as the # of contours. Contour plot shown in next page.
- Disable the draw faces toggle on the render panel.
- Create a vector plot with the same plane for location and variable set to velocity. On the symbol panel, set symbol size to 0.3 and turn on normalize symbol.

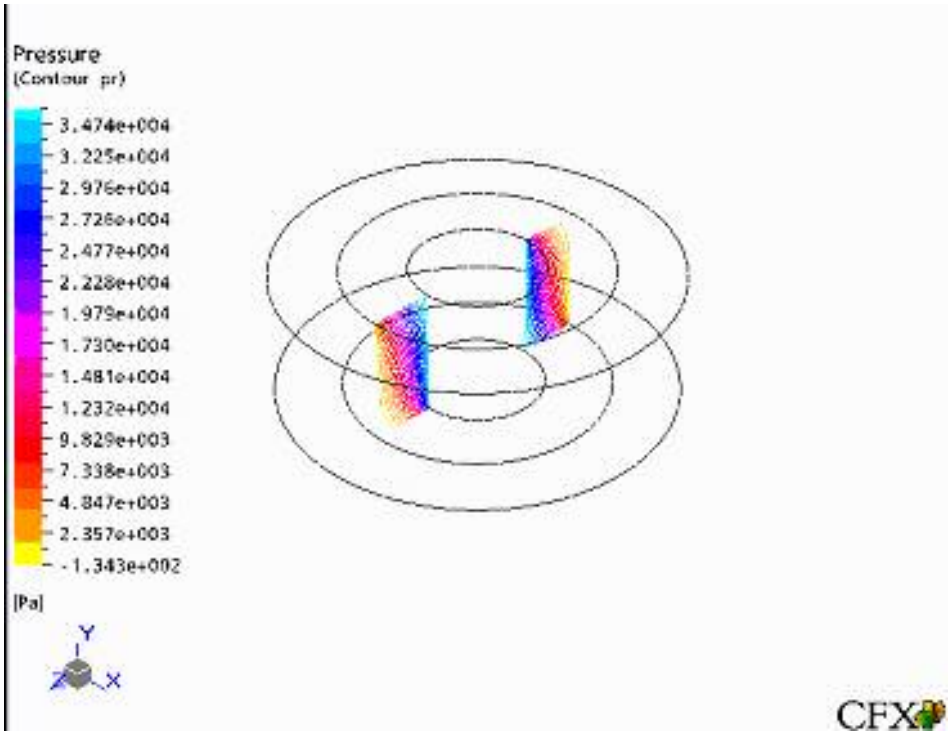

FIGURE A-8: Contour plot for pressure profile for gm1

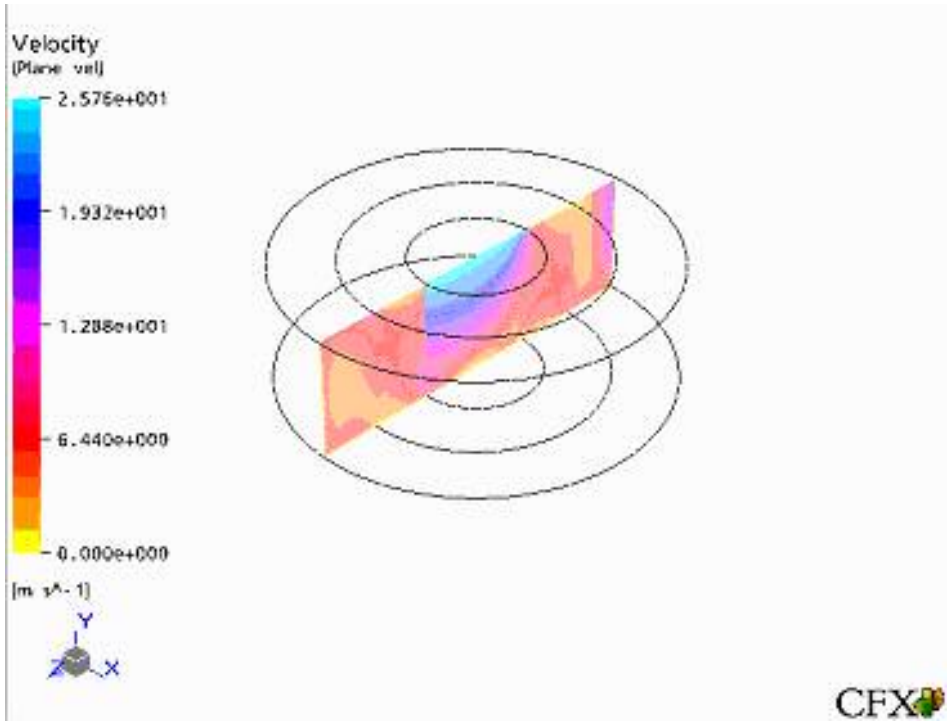

FIGURE A-9: Vector plot for velocity for gm1

Creating a polyline

- First, make the vector and contour plots invisible.
- Click create polyline from the main toolbar and accept the default name.
- On the Geometry panel:
    - Set method to boundary intersection.
    - Set boundary list to RadReact1 default, inlet and outlet.
    - Set intersect with to plane1
- Click the color tab and choose a bright constant color for the polyline.
- Click the render tab and increase the line width to 3 (the units are pixels).
- Click apply.

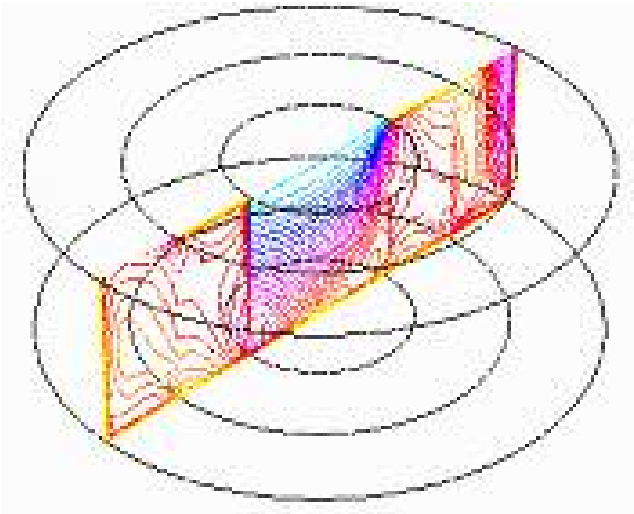

FIGURE A-10: Polyline on YZ plane at X=0

Creating a chart

- Click Create chart from the main toolbar and accept the default name.

- In the charts workspace, on the chart panel
- Set title to pressure drop through a catalytic converter.
- Turn off use data for axis labels.
- Set X axis to Z
- Set Y axis to Pressure
- Click the chart line 1 tab in the chart editor.
- Set line name to pressure drop.
- Set locator to polyline1.
- Set X Axis to Z (to plot the z-coordinate values along the x axis of the graph).
- Set Y axis to pressure (to plot pressure values along the y axis of the graph).
- Expand the appearance frame and set symbols to rectangle.
- Click apply to create the chart line.

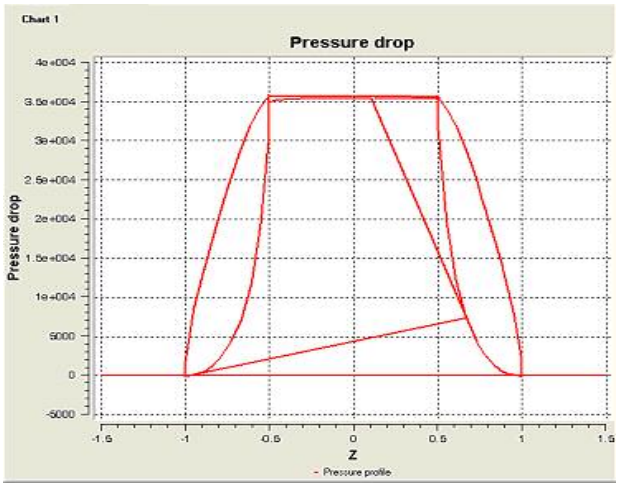

FIGURE A-11: Pressure drop profile for gm1

Exporting data

- From the main menu select file > export.

The export dialog box appears. Ensure that export geometry information is turned on. This will cause X, Y, and Z to be sent to the output file.

- In the Select Variable(s) list, select pressure.
- Set Locators to polyline 1.
- Click the formatting tab.
- Set precision to 3.
- Click Save to export the selected results.

The file export. at will be written to the current working directory. This file can be opened in any text editor. It can be used to plot charts on other software.

- When finished, close CFX™-Post.

APPENDIX-B

NUMERICAL METHOD

The numerical method selected for solution of second order partial differential equation is method of lines. The method of lines is a general technique for solving partial differential equations (PDEs) by typically using finite difference relationships for the spatial derivatives and ordinary differential equation for time derivative. This solution approach can be solved either using ODE solver package using POLYMATH or partial differential equation using PDECOL^{TM}. The software package selected for solution of PDEs is PDECOL^{TM}.

The developed computer code is described and algorithm description is divided in to four sections:

- PDECOL^{TM} description,
- Code flow and main routine,
- Boundary condition,
- Equation definition and kinetics, and
- Physical property calculations.

We begin with an overview of the PDECOL^{TM} code and presentation of the overall model flow chart.

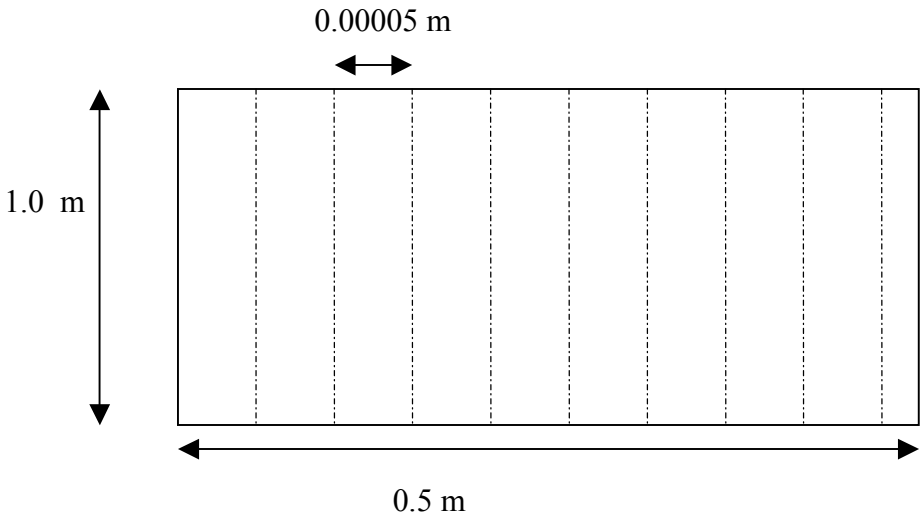

FIGURE B-1: Schematic diagram for numerical solution

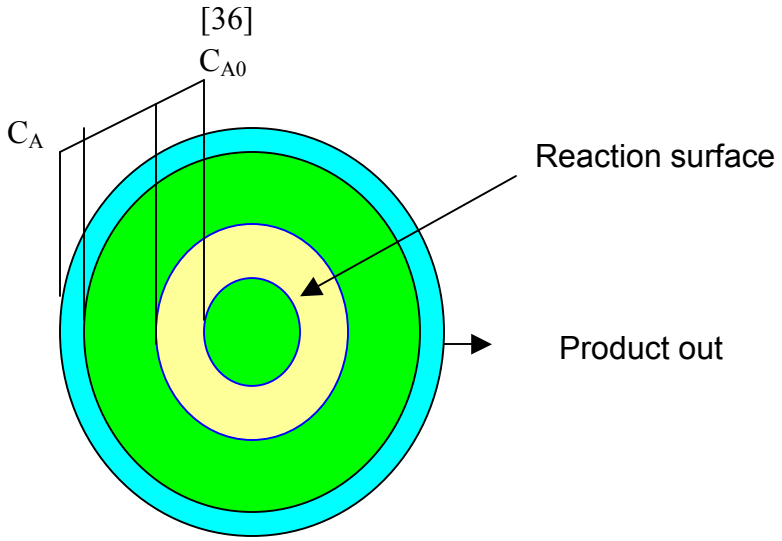

FIGURE B-2: Schematic diagram of concentration profile

[36]

B-1 PDECOL™ code

The package implements finite element collocation methods based on piecewise polynomials for the spatial discretization techniques. PDECOL™ is unique because of its flexibility both in the class of problems it addresses and in the variety of methods it provides for use in the solution process. High order methods (as well as low order ones) are readily available for use in both the spatial and time discretization procedures. The time integration methods used feature automatic time step size and integration formula order selection so as to efficiently solve the problem at hand. PDECOL™ is designed to solve the general system of NDPE non linear partial differential equations at most second order on the interval.

The software package PDECOL™ is based on method of lines and uses finite difference collocation procedure for discretization of spatial variable r and z. The collocation procedure reduces the PDE system to semidiscrete system that only depends on r variable [39].

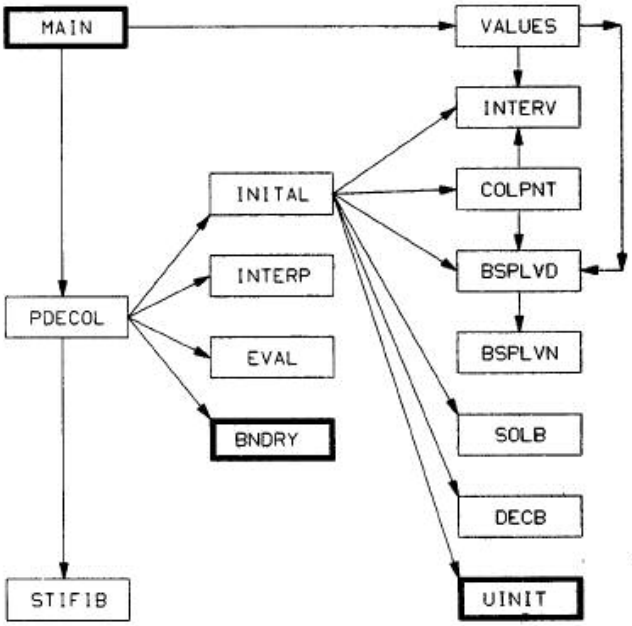

FIGURE B-3: Algorithm for PDECOL™ numerical solution

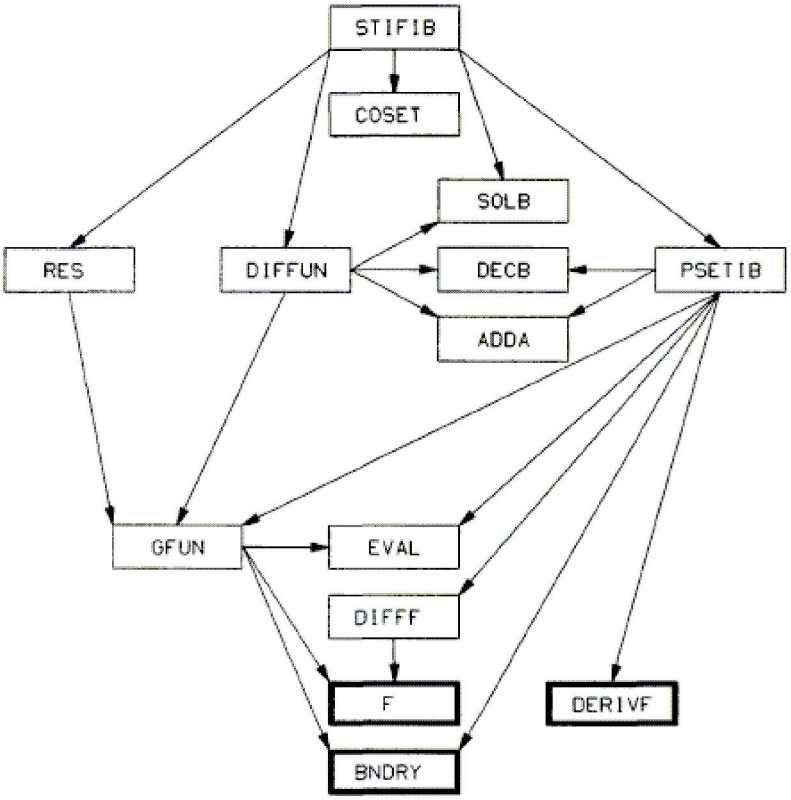

FIGURE B-4: Subroutines application flow diagram

[36]

The software package PDECOL™ is discussed below to find the numerical solution.

Component balance

$$\varepsilon\left[\frac{\partial C_j}{\partial t}\right]_{z,t}+\left[\frac{\partial(C_j u_z)}{\partial z}\right]_{t,r}+\left[\frac{\partial(C_j v_r)}{\partial r}\right]_{t,z}-\varepsilon D_a\left[\frac{\partial^2 C_j}{\partial z^2}\right]_{t,r}-\varepsilon D_r\left[\frac{\partial^2 C_j}{\partial r^2}+\frac{1}{r}\frac{\partial C_j}{\partial r}\right]_{t,z}$$

$$=\rho_b\sum_1^n v_{jn}R_n$$

Boundary condition (Fluid flow without reaction):

At r=r1 and z=0; u_z=0

At r=r_2 for all z, C_A=C_{A0}

Boundary condition (Fluid flow with reaction):

At r=r1 and z=0; u_z=0

At r=r_2 for all z, C_A=C_{b0}

Component	H_2	CO	H_2O
Volume %	64.24	25.71	10.0

APPENDIX C

Additional CFX™ results

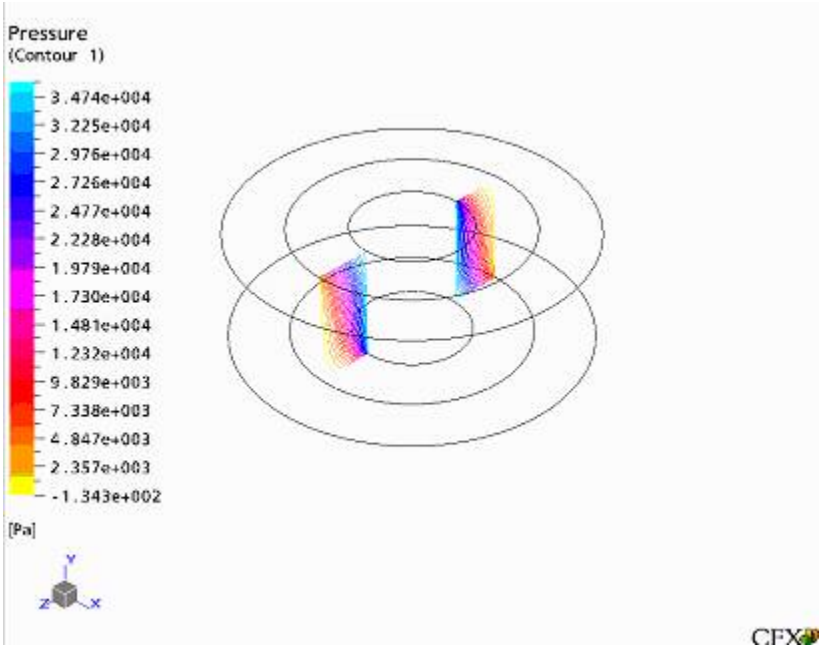

FIGURE C-1: Pressure profile for gm1

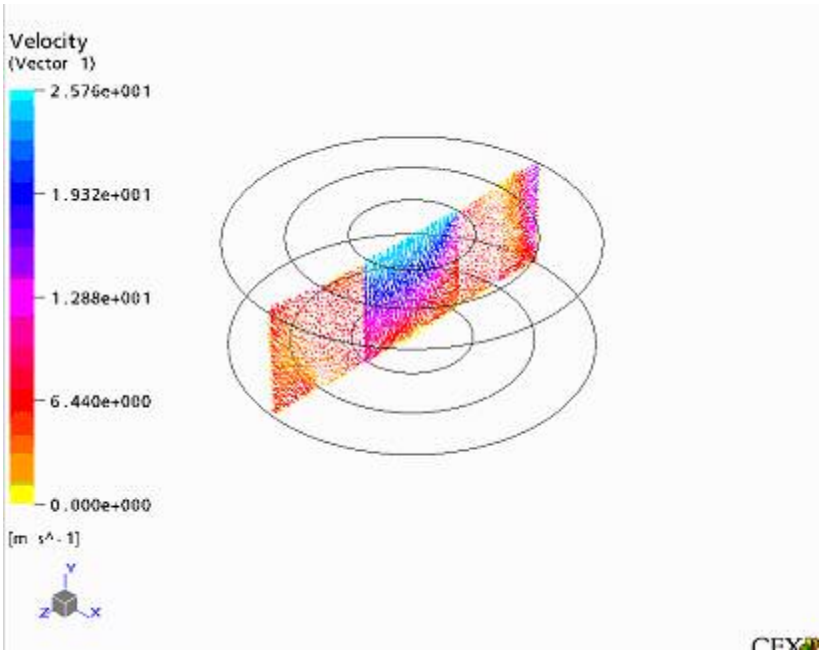

FIGURE C-2: Velocity profile for gm2

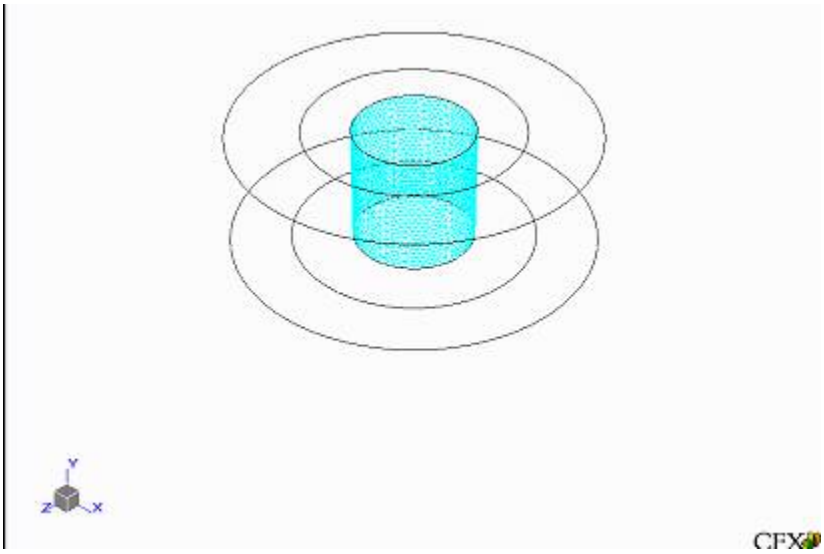

FIGURE C-3: Wire frame for gm2

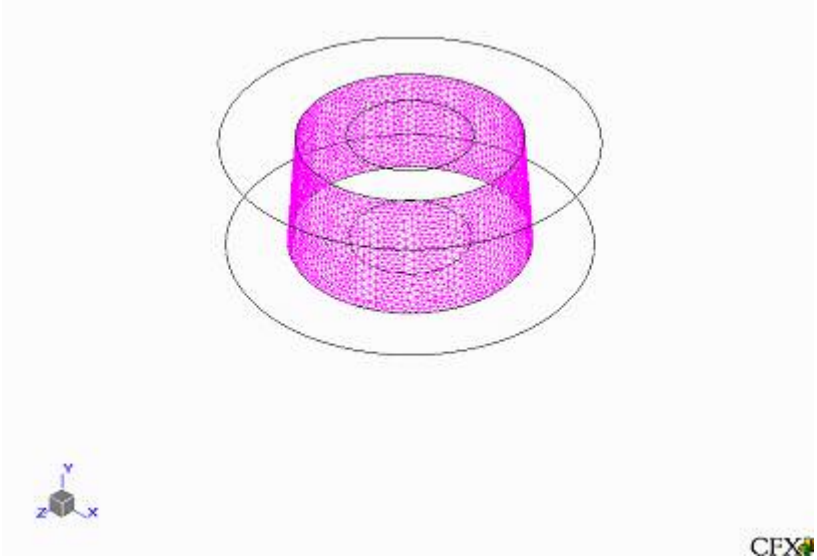

FIGURE C-4: Catalyst bed for gm2

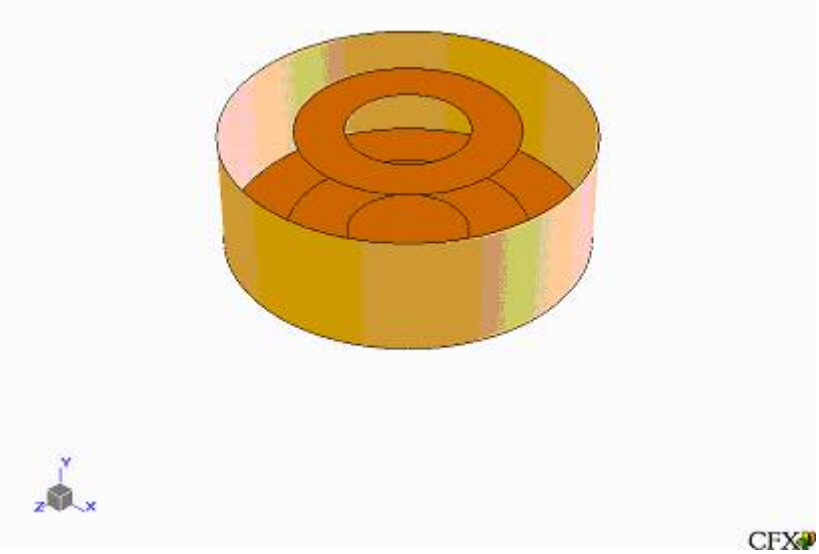

FIGURE C-5: Inlet and Outlet for gm2

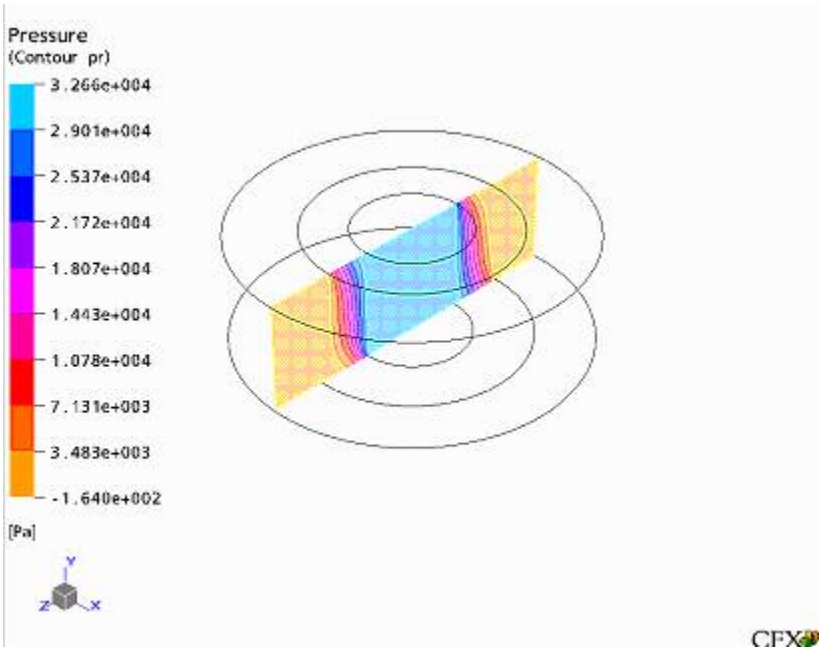

FIGURE C-6: Pressure profile for geometry gm2

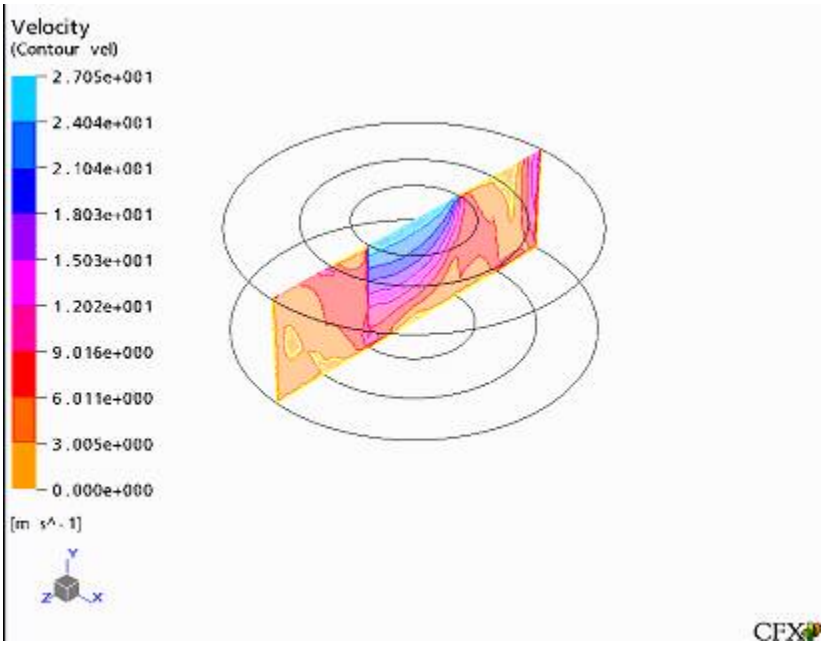

FIGURE C-7: Velocity profile for gm2

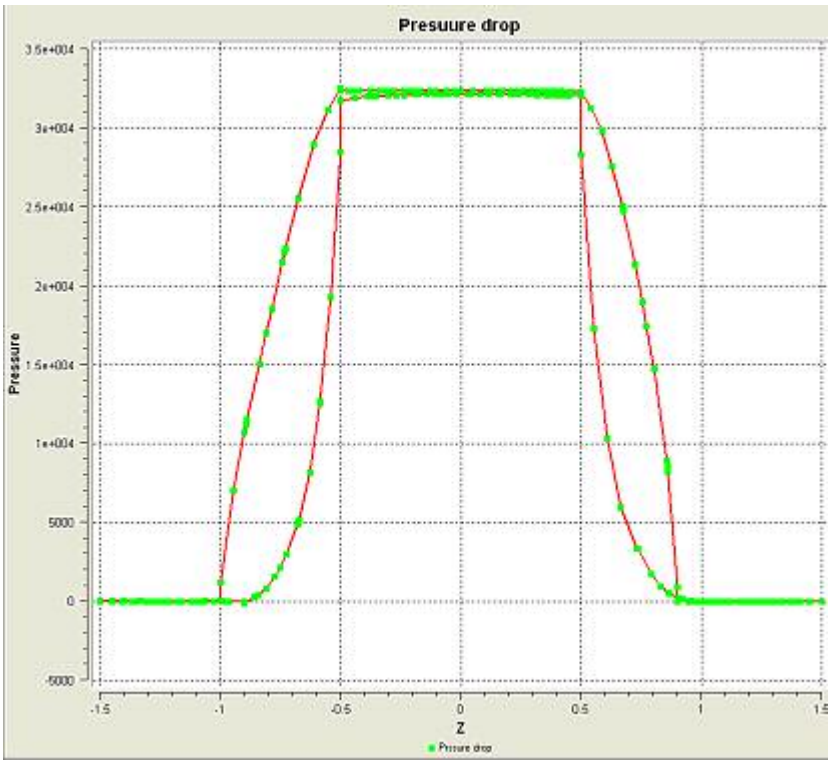

FIGURE C-8: Pressure drop profile for gm2

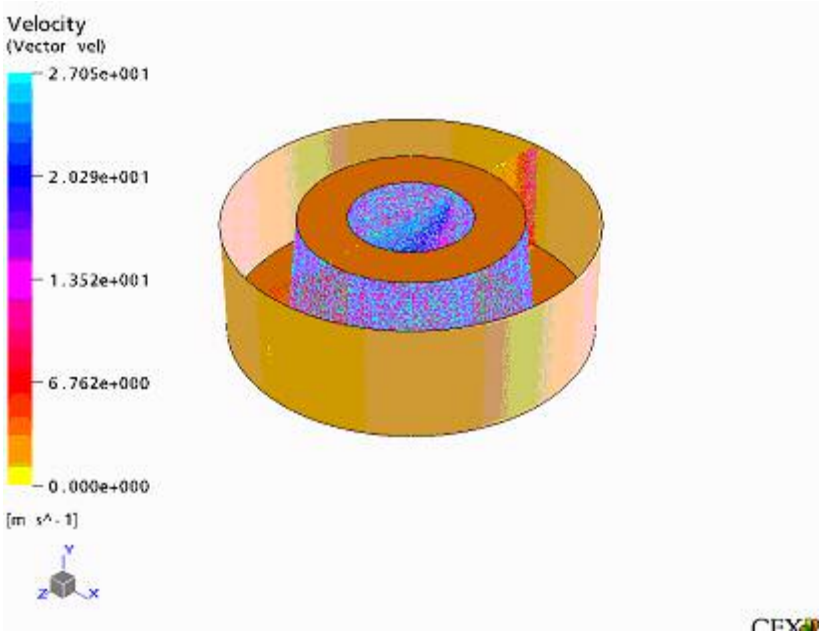

FIGURE C-9: Velocity profile for gm2

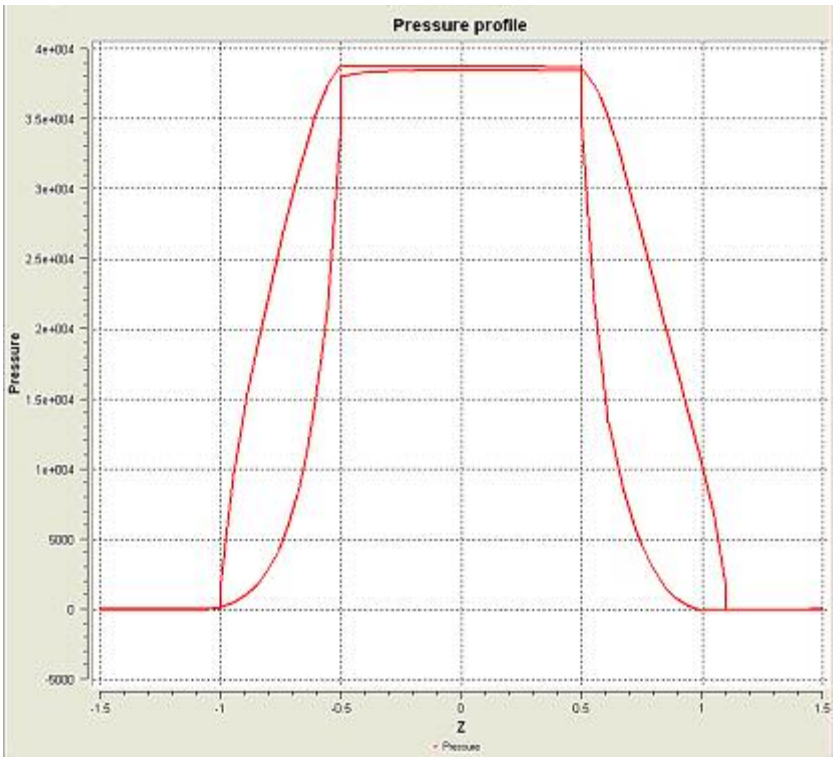

FIGURE C-10: Pressure chart for gm3

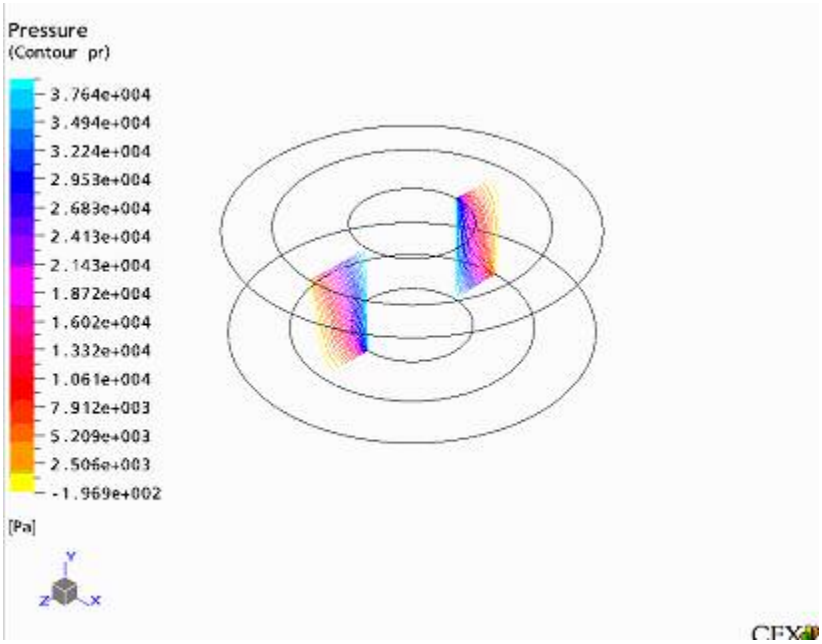

FIGURE C-11: Pressure profile for gm3

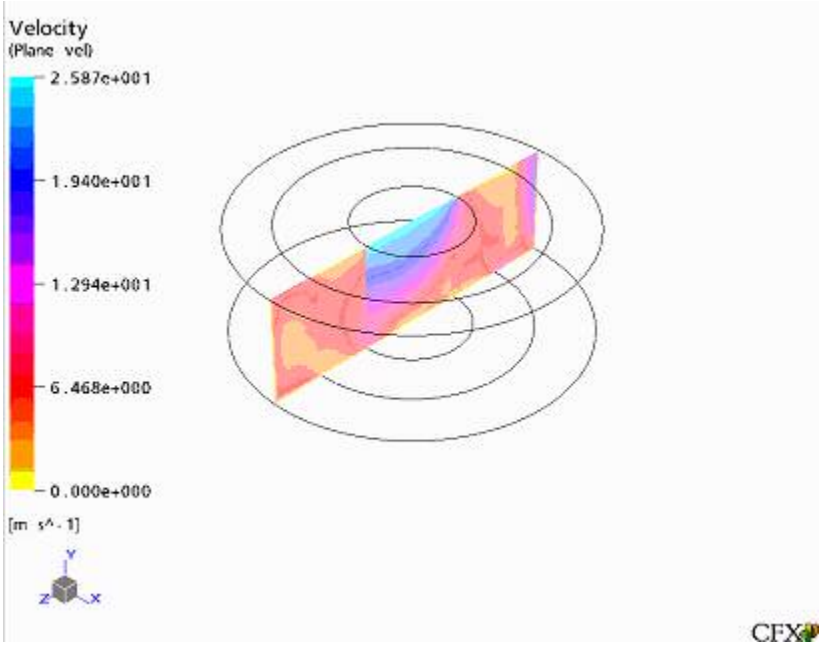

FIGURE C-12: Velocity profile for gm3

APPENDIX D

Additional CFX^{TM} results in table

Table D-1: Radial velocity component for gm1 from CFX simulation, without reaction.

Plane	g1-2	g2-3	g3-4	g4-5	g5-6	g6-7	g7-8	g8-9	g9-10	g10-11
p1	9.46	5.19	4.09	3.90	3.91	3.93	3.25	3.02	3.28	3.36
p2	5.02	5.04	5.01	4.92	4.56	4.48	4.36	4.16	4.05	3.92
p3	4.88	4.94	4.96	5.05	4.88	5.03	5.09	5.11	5.09	5.07
p4	4.35	4.50	4.75	4.91	5.02	5.24	5.19	5.27	5.44	5.46
p5	4.29	4.29	4.71	4.67	5.01	5.31	5.53	5.59	5.71	5.78
p6	3.87	4.14	4.36	4.71	4.61	5.17	5.59	5.75	6.015	6.22
p7	3.37	3.95	4.16	4.44	4.61	5.38	5.48	5.71	6.17	6.37
p8	3.23	3.15	3.50	3.99	4.55	4.87	5.91	6.04	6.59	6.83
p9	2.27	2.69	3.12	3.49	3.73	5.00	5.58	6.11	6.85	7.75
p10	1.80	1.40	1.87	2.17	2.67	2.55	3.89	5.44	7.36	8.36

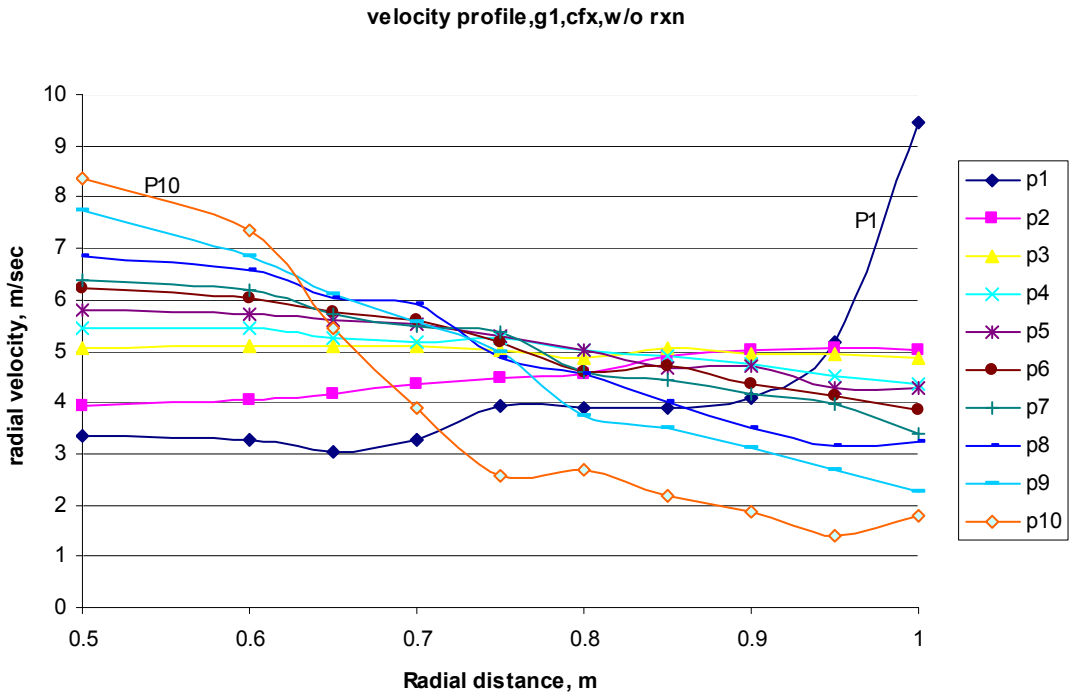

FIGURE D-1: Radial velocity profile for gm1 in CFX™ without reaction

Table D-2: Radial velocity component for gm1 from numerical solution without reaction

Plane	g1-2	g2-3	g3-4	g4-5	g5-6	g6-7	g7-8	g8-9	g9-10	g10-11
p1	9.43	5.23	4.04	3.89	3.91	3.95	3.28	3.00	3.46	3.39
p2	5.01	5.05	5.02	4.93	4.58	4.63	4.39	4.65	4.08	3.89
p3	4.89	4.95	4.98	5.08	4.90	5.05	5.10	4.95	4.98	5.10
p4	4.31	4.49	4.78	4.93	5.05	5.25	5.21	5.28	5.45	5.48
p5	4.28	4.30	4.73	4.68	5.05	5.28	5.50	5.58	5.73	5.81
p6	3.89	4.15	4.38	4.73	4.65	5.18	5.62	5.73	5.99	6.18
p7	3.39	3.97	4.18	4.46	4.58	5.40	5.50	5.73	6.23	6.40
p8	3.24	3.18	3.52	4.03	4.51	4.85	5.95	6.05	6.66	6.90
p9	2.30	2.75	3.15	3.38	3.75	5.02	5.60	6.13	6.81	7.72
p10	1.83	1.39	1.82	2.10	2.68	2.53	3.93	5.48	7.38	8.38

Table D-3: Axial velocity component for gm1 from numerical solution, without reaction

Plane	g1	g2	g3	g4	g5	g6	g7	g8	g9	g10
p1-2	7.25	0.79	-0.65	-0.30	-0.34	0.40	-0.55	-0.48	1.30	1.89
p2-3	3.67	3.15	2.29	2.30	1.28	1.55	1.24	2.48	2.15	2.83
p3-4	3.65	3.35	3.05	2.83	2.42	2.73	2.85	2.79	3.10	3.46
p4-5	3.35	3.10	3.09	3.07	3.13	3.23	2.99	3.29	3.54	3.78
p5-6	3.21	3.02	3.08	3.05	3.17	3.38	3.68	3.71	4.03	4.23
p6-7	2.89	2.88	2.81	2.99	2.62	3.35	3.62	3.71	4.20	4.42
p7-8	2.48	2.63	2.65	2.70	2.60	3.30	3.39	3.68	4.30	4.65
p8-9	2.35	2.02	1.85	1.89	2.28	2.50	3.35	3.74	4.30	4.99
p9-10	1.65	1.55	1.20	1.25	1.38	2.25	2.45	3.00	4.55	5.70
p10-11	1.30	-0.05	-0.36	-0.49	-0.28	-1.58	-0.55	0.69	2.50	5.72

Table D-4: **Radial velocity component for gm1 from numerical solution, with methanol synthesis reaction**

Plane	g1-2	g2-3	g3-4	g4-5	g5-6	g6-7	g7-8	g8-9	g9-10	g10-11
p1	7.58	4.35	3.44	3.40	3.51	3.65	3.06	2.92	3.36	3.48
p2	4.08	4.22	4.30	4.26	4.09	4.21	4.09	4.42	4.01	3.87
p3	3.96	4.14	4.65	4.43	4.30	4.55	4.74	4.61	5.69	5.05
p4	3.40	3.65	4.06	4.20	4.47	4.66	4.82	5.01	5.26	5.41
p5	3.44	3.55	4.03	4.06	4.53	4.77	5.01	5.28	5.52	5.73
p6	3.10	3.49	3.73	4.02	4.18	4.73	5.17	5.41	5.62	6.13
p7	2.72	3.62	3.57	3.87	4.05	4.90	5.11	5.46	6.00	6.31
p8	2.62	2.64	3.02	3.55	4.00	4.41	5.61	5.88	6.39	6.76
p9	1.96	2.30	2.56	2.99	3.74	4.62	5.27	5.92	6.53	7.58
p10	1.42	1.15	1.58	1.92	2.45	2.37	3.70	5.25	7.18	8.31

Table D-5: Axial velocity component for gm1 from numerical solution with methanol synthesis reaction

Plane	g1	g2	g3	g4	g5	g6	g7	g8	g9	g10
p1-2	5.80	0.66	-0.67	-0.52	-0.33	0.44	-0.57	-0.43	1.25	1.86
p2-3	2.96	2.87	2.31	2.02	1.28	1.40	1.19	2.35	2.11	2.68
p3-4	2.98	2.80	2.44	2.43	2.13	2.50	2.69	2.65	3.09	3.59
p4-5	2.66	2.64	2.49	2.62	2.77	2.93	2.85	3.03	3.59	3.85
p5-6	2.63	2.46	2.56	2.63	2.73	2.92	3.17	3.38	3.65	4.14
p6-7	2.08	2.21	2.40	2.58	2.33	2.90	3.40	3.68	4.21	4.39
p7-8	2.04	2.14	2.23	2.31	2.27	2.84	3.17	3.55	4.15	4.61
p8-9	1.82	1.75	1.51	1.63	1.99	2.34	3.02	3.38	4.26	4.93
p9-10	1.38	1.12	0.87	105.78	1.10	2.01	2.21	2.71	4.46	5.34
p10-11	1.10	-0.36	-0.40	-0.31	-0.22	-1.50	-0.39	0.56	2.42	5.59

Table D-6: Radial velocity component for gm2 from CFX simulation without reaction

Plane	g1-2	g2-3	g3-4	g4-5	g5-6	g6-7	g7-8	g8-9	g9-10	g10-11
p1	x	x	6.75	6.13	4.55	4.35	4.26	3.81	3.94	4.17
p2	x	5.68	6.11	5.57	5.57	5.22	5.01	4.81	4.33	4.61
p3	x	5.08	4.94	5.17	5.34	5.44	5.30	5.40	5.16	5.65
p4	x	4.54	4.77	4.84	5.24	5.35	5.48	5.53	5.74	6.02
p5	x	4.33	4.73	4.77	5.13	5.40	5.66	5.81	5.95	6.06
p6	3.64	4.00	4.21	4.52	4.91	5.37	5.50	5.88	6.13	6.38
p7	3.22	3.77	3.86	4.17	4.67	5.36	5.56	5.88	6.12	6.44
p8	2.98	3.07	3.30	3.85	4.16	5.20	5.69	5.81	6.45	6.73
p9	2.54	2.51	2.73	3.68	3.55	4.08	4.91	6.16	6.69	7.23
p10	1.54	1.40	1.66	2.44	3.65	2.67	3.86	5.21	6.62	6.06

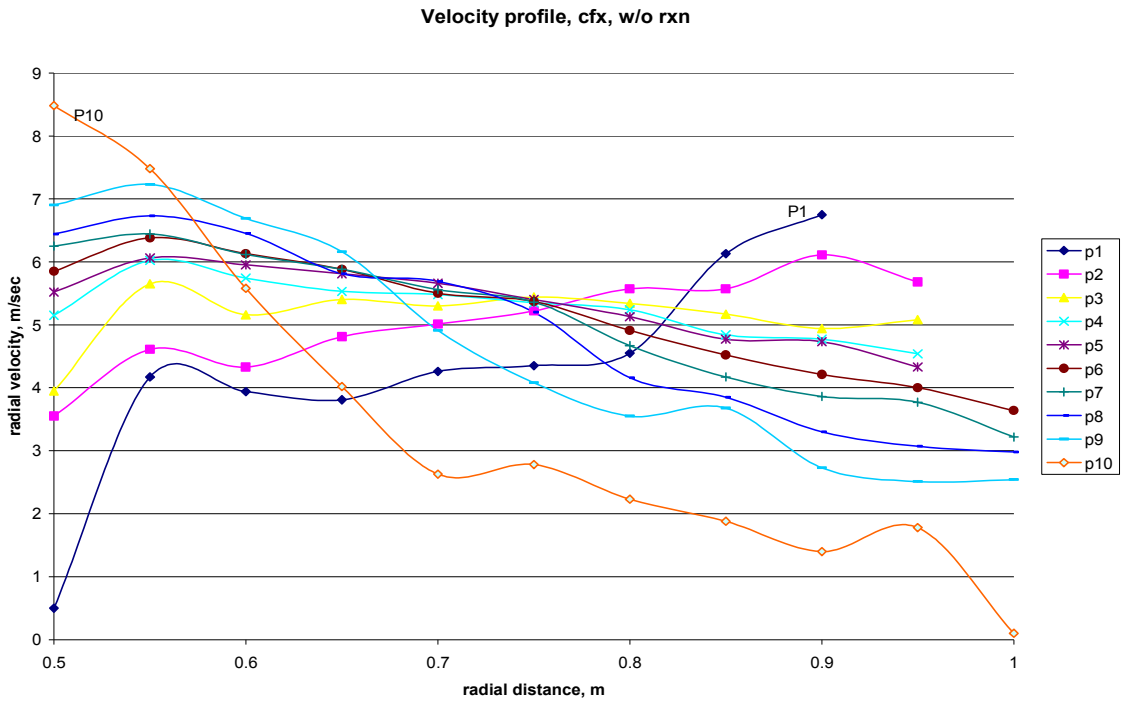

FIGURE D-2: Velocity profile from CFX simulation for gm2 without reaction

Table D-7: Radial velocity component for gm2 from numerical solution without reaction

Plane	g1-2	g2-3	g3-4	g4-5	g5-6	g6-7	g7-8	g8-9	g9-10	g10-11
p1	x	x	6.85	6.15	4.58	4.33	4.28	3.88	3.97	4.27
p2	x	5.77	6.13	5.58	5.67	5.32	4.98	4.83	4.39	4.67
p3	x	5.16	4.96	5.18	5.36	5.45	5.32	5.46	5.06	5.69
p4	x	4.58	4.82	4.88	5.18	5.37	5.49	5.58	5.78	6.12
p5	x	4.23	4.71	4.74	5.18	5.42	5.72	5.83	5.96	6.08
p6	3.62	4.01	4.23	4.55	4.93	5.38	5.48	5.90	6.15	6.40
p7	3.23	3.78	3.88	4.18	4.68	5.38	5.58	5.90	6.13	6.48
p8	3.02	3.15	3.32	3.95	4.18	5.25	5.72	5.83	6.48	6.75
p9	2.58	2.55	2.78	3.69	3.57	4.18	4.93	6.18	6.73	7.30
p10	1.56	1.44	1.67	2.43	3.67	2.68	3.89	5.22	6.68	6.14

Table D-8: Axial velocity component for gm2 from numerical solution, without reaction

Plane	g1	g2	g3	g4	g5	g6	g7	g8	g9	g10
p1-2	x	x	3.65	2.82	0.36	0.08	1.07	0.67	1.68	2.66
p2-3	x	4.46	4.49	3.28	2.88	2.26	2.15	2.56	2.35	3.26
p3-4	x	3.96	3.67	3.65	3.26	3.28	2.97	3.35	3.33	3.42
p4-5	x	3.48	3.55	3.50	3.57	3.59	3.65	3.72	4.02	4.28
p5-6	x	3.49	3.44	3.47	3.55	3.64	3.98	4.10	4.16	4.32
p6-7	2.82	2.95	3.06	3.15	3.35	3.67	3.77	4.11	4.36	4.56
p7-8	2.44	2.78	2.79	2.65	2.78	3.40	3.65	4.02	4.28	4.73
p8-9	2.39	2.25	1.96	2.22	2.26	3.24	3.25	3.33	4.23	4.99
p9-10	1.89	1.68	1.45	1.83	1.45	1.33	2.28	3.14	4.42	5.23
p10-11	1.15	0	0	0.08	1.29	-0.91	0.58	0.59	2.82	4.24

Table D-9: **Radial velocity component for gm2 from numerical solution, with methanol synthesis reaction**

Plane	g1-2	g2-3	g3-4	g4-5	g5-6	g6-7	g7-8	g8-9	g9-10	g10-11
p1	x	x	5.62	5.29	3.95	3.85	3.89	3.74	3.88	4.18
p2	x	4.58	5.15	4.80	4.95	4.75	4.63	4.54	4.15	4.54
p3	x	4.20	4.17	4.46	4.68	4.88	4.89	5.11	4.97	5.57
p4	x	3.71	4.00	4.15	4.60	4.84	5.02	5.22	5.45	5.91
p5	x	3.57	3.96	4.11	4.54	4.88	5.18	5.47	5.66	5.96
p6	2.94	3.32	3.54	3.95	4.34	4.84	5.08	5.49	5.98	6.22
p7	2.54	3.06	3.24	3.60	4.09	4.84	5.12	5.54	5.93	6.35
p8	2.33	2.48	2.80	3.23	3.68	4.73	5.22	5.48	6.20	6.64
p9	2.04	2.10	2.34	3.20	3.16	3.71	4.54	5.81	6.46	7.07
p10	1.26	1.16	1.41	2.12	3.24	2.42	3.57	4.94	6.36	6.04

Table D-10: Axial velocity component for gm2 from numerical solution, with methanol synthesis reaction

Plane	g1	g2	g3	g4	g5	g6	g7	g8	g9	g10
p1-2	x	x	3.02	2.49	0.22	0.03	1.00	0.61	1.61	2.54
p2-3	x	3.64	3.75	2.82	2.53	2.01	1.96	2.41	2.19	3.13
p3-4	x	3.26	3.13	3.16	3.13	2.96	2.73	3.15	3.31	3.47
p4-5	x	2.91	3.00	3.03	3.12	3.22	3.33	3.46	3.86	4.27
p5-6	x	2.80	2.91	3.00	3.12	3.31	3.57	3.87	4.11	4.22
p6-7	2.26	2.44	2.56	2.67	2.90	3.31	3.44	3.87	4.30	4.47
p7-8	1.96	2.35	2.34	2.28	2.53	3.06	3.38	3.69	4.15	4.58
p8-9	1.83	1.82	1.63	1.87	1.90	2.84	2.99	3.16	4.05	4.85
p9-10	1.56	1.42	1.22	1.59	1.27	1.15	2.01	2.81	4.28	4.43
p10-11	1.02	0.00	0.00	0.08	1.06	-0.81	0.44	0.52	2.75	4.29

Table D-11: Radial velocity component for gm3 from CFX simulation, without reaction

	g1-2	g2-3	g3-4	g4-5	g5-6	g6-7	g7-8	g8-9	g9-10	g10 11	g11 12	g12 13
p1	8.68	5.81	3.74	3.66	3.38	3.55	3.55	3.43	3.46	3.64	2.92	2.91
p2	4.82	4.97	4.48	4.25	4.41	4.19	4.20	4.17	4.14	4.10	3.91	4.36
p3	4.64	4.51	4.57	4.60	4.61	4.51	4.68	4.62	4.61	4.87	4.66	4.63
p4	4.19	4.17	4.25	4.50	4.67	4.76	4.89	5.05	5.23	5.14	5.50	5.44
p5	4.13	4.13	4.21	4.27	4.47	4.71	5.10	5.15	5.30	5.42	5.50	5.65
p6	x	3.96	3.94	4.11	4.40	4.64	4.98	5.34	5.71	5.77	6.10	5.93
p7	x	3.63	3.46	3.86	4.10	4.43	4.93	5.45	5.66	5.97	6.19	6.47
p8	x	2.99	3.12	3.60	3.93	4.11	4.68	5.07	5.64	6.07	6.51	6.76
p9	x	2.90	2.24	2.46	3.10	2.60	3.94	4.65	5.62	6.76	7.46	7.65
p10	x	x	1.50	2.25	2.32	2.81	2.84	3.74	4.00	5.35	7.42	8.56

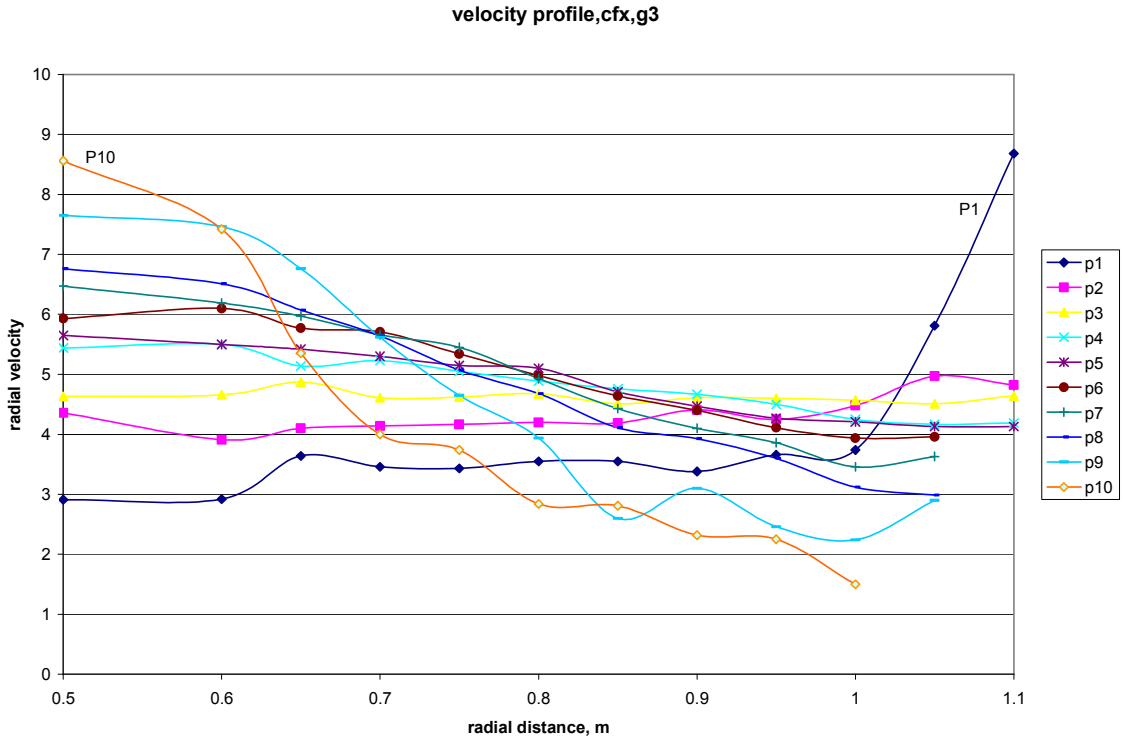

FIGURE D-3: Radial velocity profile for gm3 from CFX simulation

Table D-12: Radial velocity component for gm3 from numerical solution, without reaction

	g1-2	g2-3	g3-4	g4-5	g5-6	g6-7	g7-8	g8-9	g9-10	g11 12	g12 13	g13 14
p1	8.66	5.83	3.76	3.70	3.42	3.56	3.57	3.46	3.49	3.60	2.94	2.96
p2	4.85	5.01	4.52	4.23	4.46	4.23	4.25	4.27	4.19	4.09	3.89	4.38
p3	4.66	4.53	4.58	4.62	4.63	4.55	4.69	4.64	4.63	4.89	4.67	4.64
p4	4.20	4.23	4.21	4.46	4.69	4.74	4.93	5.02	5.20	5.15	5.56	5.48
p5	4.18	4.14	4.23	4.28	4.44	4.73	5.13	5.17	5.32	5.43	5.55	5.60
p6	x	3.98	3.95	4.13	4.42	4.46	5.02	5.36	5.72	5.78	6.12	5.95
p7	x	3.65	3.48	3.88	4.12	4.45	4.95	5.46	5.67	5.98	6.20	6.48
p8	x	3.02	3.16	3.58	3.91	4.15	4.67	5.19	5.62	6.02	6.45	6.66
p9	x	2.92	2.26	2.48	3.12	2.65	3.98	4.66	5.68	6.72	7.49	7.62
p10	x	x	1.55	2.21	2.38	2.87	2.89	3.75	4.02	5.38	7.43	8.58

Table D-13: Radial velocity component for gm3 from CFX simulation with methanol synthesis reaction

	g1-2	g2-3	g3-4	g4-5	g5-6	g6-7	g7-8	g8-9	g9-10	g10 11	g10 11	g10 11
p1	7.05	4.94	3.26	3.26	3.09	3.40	3.36	3.28	3.35	3.61	2.95	2.81
p2	3.90	4.12	3.75	3.74	3.98	3.86	3.97	3.94	3.99	4.10	3.89	4.16
p3	3.79	3.75	3.94	4.02	4.07	4.10	4.30	4.44	4.49	4.79	4.66	4.42
p4	3.38	3.49	3.60	3.74	4.02	4.17	4.45	4.63	5.07	5.14	5.29	5.19
p5	3.34	3.49	3.62	3.77	4.02	4.17	4.74	4.86	5.04	5.21	5.40	5.27
p6	x	3.30	3.34	3.47	3.83	4.16	4.49	4.96	5.53	5.61	5.99	5.68
p7	x	2.98	2.95	3.34	3.56	3.97	4.43	5.13	5.49	5.74	6.07	6.05
p8	x	2.48	2.64	3.05	3.48	3.67	4.22	4.73	5.32	2.97	6.42	6.33
p9	x	2.39	1.97	2.18	2.75	2.36	3.66	4.34	5.31	6.58	7.36	7.31
p10	x	x	1.28	1.94	1.95	2.46	2.60	3.53	3.96	5.15	7.28	8.07

Table D-14: Axial velocity component for gm3 from CFX simulation with methanol synthesis reaction

	g1	g2	g3	g4	g5	g6	g7	g8	g9	g10	g11	g12
p1-2	5.12	2.17	-0.50	-0.41	-0.46	-0.26	-0.29	-0.39	-0.27	0.54	0.10	1.35
p2-3	2.54	2.85	1.22	0.85	1.31	0.79	0.86	0.93	1.27	1.32	1.87	2.71
p3-4	2.58	2.48	2.34	2.14	2.18	1.59	2.01	1.86	2.05	2.60	2.85	3.05
p4-5	2.34	2.36	2.34	2.24	2.21	2.23	2.41	2.71	2.96	3.06	3.74	3.71
p5-6	2.28	2.35	2.28	2.28	2.35	2.42	2.66	2.74	3.03	3.20	3.58	3.84
p6-7	x	2.20	2.12	2.13	2.28	2.41	2.65	3.01	3.47	3.65	4.19	4.04
p7-8	x	2.03	2.07	1.97	2.05	2.12	2.26	2.72	3.00	3.50	4.00	4.40
p8-9	x	1.75	1.81	1.85	1.75	1.77	1.98	2.24	2.62	3.42	4.04	4.49
p-10	x	1.62	1.20	1.12	0.99	-0.30	1.11	1.67	2.39	3.51	4.73	5.22
p10-11	x	1.03	0.33	0.06	0.08	0.81	-0.39	-0.24	-0.57	-0.55	2.02	5.38

Table D-15: Axial velocity component for gm3 from CFX simulation without reaction

	g1	g2	g3	g4	g5	g6	g7	g8	g9	g10	g11	g12
p1-2	6.55	2.63	-0.44	-0.35	-0.52	-0.26	-0.29	-0.38	-0.29	0.65	0.10	1.35
p2-3	3.25	3.53	1.42	0.92	1.46	0.89	0.93	0.96	1.35	1.34	1.95	2.95
p3-4	3.22	3.02	2.76	2.55	2.30	1.72	2.19	1.96	2.15	2.65	2.88	3.22
p4-5	2.89	2.88	2.76	2.60	2.55	2.49	2.59	2.76	3.15	3.12	3.75	3.88
p5-6	2.85	2.86	2.72	2.69	2.67	2.75	2.93	2.98	3.19	3.35	3.73	4.08
p6-7	x	2.78	2.62	2.49	2.55	2.61	2.79	3.15	3.53	3.79	4.30	4.28
p7-8	x	2.46	2.25	2.15	2.25	2.39	2.51	3.08	3.28	4.01	4.25	4.69
p8-9	x	2.05	2.08	2.15	1.98	1.96	2.15	2.38	2.85	3.49	4.11	4.85
p9-10	x	1.96	1.40	1.25	1.15	-0.25	1.15	1.76	2.46	3.57	4.79	5.49
p10-11	x	1.25	028	0.08	0.04	0.51	-0.39	-0.46	-0.57	-0.51	1.97	5.42

VITA

Anjani K. Singh

Candidate for the Degree of

Master of Science

Thesis: MODELING OF RADIAL FLOW DYNAMICS FOR FIXED BED REACTOR

Major Field: Chemical Engineering

Biographical:

Education: Received Bachelor of Technology degree in Chemical Engineering from Indian Institute of Technology, Kharagpur, India in May 1996. Completed the requirements for Masters of Science degree with major in Chemical Engineering at Oklahoma State University in December 2005.

Experience: Worked as Deputy Manager (Process) at Indian Petrochemical Corporation Limited from July 2001 to July 2004, as Process engineer from July 1997 to June 2001 and as trainee from June 1996 to June 1997. Worked as a Research Assistant in Unit Operations lab in Oklahoma State University from Jan 2005 to May 2005 and as a Teaching Assistant in Chemical Engineering Modeling. Joined Aspentech Inc. as a customer support consultant.

Name: Anjani K Singh Date of Degree: December, 2005

Institution: Oklahoma State University Location: Stillwater, Oklahoma

Title of Study: MODELING OF RADIAL FLOW DYNAMICS FOR FIXED BED REACTOR

Pages in Study: 128 Candidate for the Degree of Master of Science

Major Field: Chemical Engineering

Scope and Method of Study: The purpose of this research was to study the flow distribution in the radial fixed bed reactors (RFBR) and suggest ways to improve the flow distribution. Three different geometries were created to study the flow distribution in RFBRs. The flow distribution was also studied for reaction in the RFBR. The bed length was varied with height. The simulation was done in CFX^{TM}.

Findings and Conclusions: The RFBR with increasing bed length with height improved the flow distribution (improved the flow distribution by 40%). The flow distribution in the RFBR with reduced bed length with height, improved by 20%. The radial velocity component for increased bed length RFBR reduced by 6% as compared to that of uniform bed length RFBR. The RFBR with increasing bed length with height is the most promising configuration for improving flow distribution.

ADVISER'S APPROVAL: Dr. Karen A High